Chapter 6: SCREENING TESTS FOR CANDIDATE FIRE SUPPRESSANTS

Richard G. Gann, Ph.D.
National Institute of Standards and Technology

J. Douglas Mather, Ph.D.
Chemical Development Studies, Inc.

TABLE OF CONTENTS

6.1 THE NEED FOR SCREENING TESTS

A primary component of the Next Generation Fire Suppression Technology Program (NGP) was the survey of the "world" of chemistry, seeking to identify chemicals that merited examination under practical fire suppression conditions or to enable a finding that no previously unidentified such chemicals existed. This entailed consideration of thousands of compounds, a task detailed in the next chapter of this book. While full-scale testing of chemicals is eventually necessary to demonstrate acceptability, it is impractical to use such tests to narrow the large list of candidates. Full-scale tests are strongly influenced by the initial and boundary conditions surrounding the fire and suppression event. Complex, non-linear relationships among the agent, the flow field, and the fire cannot be unraveled from these full-scale suppression tests because critical parameters cannot be controlled tightly enough, and the number of tests is constrained by cost, time, safety and environmental considerations. Rather, performing this survey required a protocol for rapid and inexpensive screening of this large number of chemicals to identify those relatively few agents worthy of further examination as alternative fire suppressants.

There are multiple, critical chemical properties whose beneficial values promoted the widespread use of halon 1301 (CF_3Br) and which would contribute to the consideration of alternative fire suppressants. These properties were listed in Chapter 1 and will be discussed further below. A testing hierarchy was needed to ensure that the most important properties were considered first. Estimation of values of these properties, for comparison with appropriately selected target values, needed to be obtained using minimal mass of the chemicals since:

- The purchase of testing quantities of this many chemicals would be prohibitively expensive,
- Many compounds would need to be custom synthesized, at significant cost, and
- Some compounds would be of unknown toxicity.

Prior to the NGP, various methods had been used to screen chemicals. Some of these were explicit, others were informal or ill-defined. Shortly before the start of the NGP, a pilot effort had arrived at preliminary screening procedures and criteria for alternatives to both halon 1301 and halon 1211 (CF_2ClBr).[1] These screening procedures were able to distinguish between gases and liquids of varying degrees of performance. The authors noted the importance of the purity of the chemical being examined. They also developed classes of performance for new chemicals, related to the values for halons 1211 and 1301.

The NGP development of a screening protocol built on this and other formal and informal procedures. The first item of business was to review the existing protocols. In this pursuit, the NGP conducted a Workshop on Agent Compatibility with People, Materials and the Environment on November 14 and 15, 1997.[2] Approximately 40 experts from government, academia, and industry participated in the evaluation and revision of current test methods for application to screening candidates for the next generation of fire suppressants. A distinction was made between screening and evaluation/analysis tests. Screening tests are meant to provide guidance in the identification of suitable compounds (and the elimination of unsuitable

compounds) from a long list of candidates, whereas evaluation/analysis tests are performed as part of the risk assessment process that is required for qualifying all halon replacement chemicals. This chapter describes the set of screening tests used by the NGP research team.

6.2 GENERAL APPROACH

For a single candidate suppressant, performing a full battery of screening tests for the 12 properties listed in Chapter 1 could require about 4 moles of chemical, about 8 days, and $15,000 (in 1990 dollars).[1] This was beyond the resources of the NGP. Thus, the first order of business was to identify which of the 12 properties should be the subjects for initial screening. This decision was based on the properties deemed most important for a successful chemical, most likely to disqualify a chemical, and easiest to determine. A second task was to identify or develop efficient and reasonably accurate screening tests, recognizing that these would not necessarily be the tests used in the final acceptance of an agent. The selection was based on ease of operation for these types of chemicals, the extent of prior data available, the amount of chemical required, and the relevance of the figure(s) of merit to the NGP applications. Existing methods were adapted or new methods were developed to meet anticipated needs. The third task was to set an order of screening tests to perform. As will be seen in Section 6.9, not all of the screening tests were routinely used.

For each property to be screened, a three-step process was followed:

1. Determine whether there was a value in the published literature.
2. Estimate the value of the property from the values for analogous compounds. If available, make use of quantitative structure-activity relationships (QSARs).
3. Perform the selected screening test.

The expanse of organic and inorganic chemistry was sorted into chemical families. Each family was characterized by one or more chemical features, e.g., the presence of a carbon-carbon double bond or a bromine atom. Since a family might include hundreds of individual chemicals, a small number of most likely prospects were identified that had desirable values of the screening properties, estimated using the first two of the steps above. For instance, chemicals with low boiling points were preferred, since they would be most likely to disperse rapidly (see below). If commercially available, small quantities of these chemicals were purchased. Otherwise, source(s) for custom synthesis were identified. (This is detailed in Chapter 7.) The laboratory tests were then performed as described in the remainder of this chapter.

6.3 AGENT PROPERTIES TO BE SCREENED

In reviewing the 12 properties identified as affecting the desirability of a chemical compound as a halon 1301 alternative, the following evaluation emerged:

- Fire suppression efficiency. This was a property that needed to be screened. Halon 1301 quenches most flames at a concentration of about 3 volume % in air. HCF-125 (C_2HF_5), noted in Chapter 1 as the best commercially available alternative under the DoD Technology Development program, has acceptable values of other key chemical properties, but typically quenches flames at about 8 volume % in air, with some modest variation depending on the fuel.[3] It was dissatisfaction with the additional required mass and storage volume that led to the formulation of the NGP. The target for the screen results of candidate chemicals was a

fire suppression efficiency better than HFC-125 and preferably comparable to that of halon 1301.

- Effective quenching of flame re-ignition. It was presumed that a chemically active suppressant (see Chapter 3) would require little agent mass beyond that needed for open flame quenching. A physical flame suppressant would need an increase similar to that for HFC-125. Thus, no screen testing was deemed necessary.
- Atmospheric lifetime. Environmental effects were the problem that provoked the search for halon alternatives. Since the focus of the NGP was on identifying volatile candidate fire suppressants that would disperse well, compounds were screened for atmospheric effects only. Atmospheric lifetime became the key environmental figure of merit, since chemicals with short residence times in the troposphere would make minimal contributions to ozone depletion, global warming, and other, as yet unknown, types of environmental pollution. The Environmental Protection Agency (EPA) required a low value for approval under its Significant New Alternatives Policy (SNAP) Program.[4,i] Manufacturers could expect a continuing market in a chemical with a low value (assuming desirable values of the other chemical properties). Similarly, fire suppression systems owners did not want to be required to replace their systems yet another time. For screening purposes, the NGP aimed for lifetime estimates of the order of one month. Halon 1301 has an estimated atmospheric lifetime of 65 years.[5]
- Effectiveness of low-temperature dispersion. Because in-flight fires often occur at operational altitudes where temperatures are low, a successful agent must have high volatility.[ii] NGP experiments established that excellent dispersion was achieved for chemicals whose boiling points were below the ambient temperature in the engine nacelle or dry bay (Chapter 8). The military specification for this minimum operating temperature is -40 °C, although operating temperatures in actual halon 1301 releases have generally been significantly higher (Chapter 2). Halon 1301 and HFC-125 have boiling points below -50 °C, and flashing does occur. Thermodynamic calculations showed that a typical suppressant chemical will have an equilibrium concentration of at least 5 volume % at -40 °C if its boiling point is below 20 °C. However, at these temperatures, the evaporation rate may be too slow for effective dispersion to all parts of the engine nacelle or dry bay before the agent is flushed from the space. Nonetheless, the NGP used a maximum boiling point criterion of 20 °C for screening purposes. As a peripheral benefit, a low boiling point generally means that an agent would eventually evaporate with little or no residue. Thus, no additional screen for agent residue was used.

---

[i] The EPA is responsible for assuring that no halon replacement presents an unacceptable risk to human health or the environment. For toxicity, the primary focus has been to assure the potential for timely egress from the immediate environment generated by the discharge of a fire suppressant. Although the EPA has no requirements on screening candidates, the EPA does characterize the risks associated with halon replacement agents. As part of this process, information on the toxic properties of chemical agents is compiled and combined with the exposure assessment results to estimate risk. The EPA requests toxicity data on a case-by-case basis for the risk characterization. Because many of the current halon replacement agents have been halogenated hydrocarbons, information related to acute toxicity, cardiac sensitization, subchronic toxicity, developmental toxicity and genetic toxicity have been required. Inert gas agents have had a different set of requirements, such as the concentration that produces hypoxia. The EPA, however, does not state specific methods to use for these tests. Ideally, the methods used to screen chemicals advanced as fire suppressants will address the endpoints which the EPA will use to regulate them.

[ii] Halon 1301 is referred to as a total flooding agent. When discharged, it rapidly fills the space it is protecting, becoming able to quench flames in virtually any location. This is contrasted with streaming agents, which are (as the name implies) squirted at a fire. For these fluids, low volatility generally enhances performance by allowing a greater focus of the stream without loss by evaporation.

- Low toxicity of the chemical and its combustion and decomposition products. Most engine nacelle and dry bay fires occur during flight and no people are exposed to the released agent or its by-products. The same is true for in-flight accidental discharges (of which there are very few) in unoccupied spaces. However, there is the potential for a fire or an accidental discharge when the aircraft is on the ground, e.g., during maintenance operations or fire suppression system re-charging. Then, there is the possibility of exposure of people. For halogenated compounds, the primary risk from exposure to low concentrations is cardiac irregularity. The NGP screening criterion was the suppressing concentration should be lower than the lowest observed acute exposure level (LOAEL) for inducing cardiac arrhythmia.

These properties are not entirely independent. For example, the molecules in fluids with low boiling points are generally small, i.e., composed of relatively few atoms. Some of the molecular features that lead to short atmospheric lifetime, such as a carbon-carbon double bond, increase the number of atoms over the simplest single-carbon compounds, which generally increases the boiling point. The presence of atoms that provide efficient flame extinguishment, such as a bromine atom, may increase toxicity.

The following properties were not included in the initial screening. However, preferred measurement methods were identified.[2]

- Low electrical conductivity
- Low corrosivity to metals
- High compatibility with polymeric materials
- Stability under long-term storage

6.4 FIRE SUPPRESSION EFFICIENCY SCREENING

6.4.1 Estimation of Values

The first step in obtaining an approximate value for the concentration of a chemical compound needed to extinguish a flame was based on prior measurement of the compound itself or the known efficiency of analogous compounds. In general, candidate compounds belonged to one of three categories:

- Physically active molecules. These compounds absorb heat into their vibration-rotational modes. In some cases, the breakage of chemical bonds (without immediate recombination) may result in additional endothermicity. The heat absorption removes enthalpy from the flame and its environment, cooling the flame. The effectiveness of such compounds typically increases with an increasing number of atoms, and the more effective compounds tend to have higher boiling points. (See below.) Pitts[6] had performed a thorough study of these chemicals (Chapter 7), and his compilation became the basis for assessing any further candidates of this type.
- Reactive molecules. There are some atoms, such as fluorine, that can be extracted from the suppressant molecule by a hydrogen atom from the flame. The resulting HF bond is sufficiently strong that the fluorine atoms play no further role in the quenching of the flame. There were flame extinguishment data for some fluorocarbons and hydrofluorocarbons, and these values provided a reference for considering additional such compounds.

- Catalytic molecules. Certain atoms were known to participate in chain reactions that lead to the recombination of flame-propagating free radicals. The bromine atom, present in CF_3Br, is one of these. Iodine and phosphorus atoms were known to be of high effectiveness, as were some metal atoms. Chlorine atoms are also known to be catalytic, but with a shorter chain length and thus lower effectiveness than bromine atoms. The presence of one or more of these atoms in a candidate chemical suggested the potential for flame suppression efficiency near that of halon 1301. NGP research and testing refined this list as the Program evolved.

6.4.2 Cup Burner

The most commonly used apparatus for examining fire suppressant chemicals is the cup burner, and it was the workhorse of this Program. In 1961, Creitz published a bench-scale apparatus that could be used to measure the effectiveness of chemicals at extinguishing a small, gaseous diffusion flame that was housed in a vertical glass chimney.[7] His apparatus was the predecessor of the cup burners that were to follow. By 1973, workers at ICI had adapted this to enable the use of a burning liquid pool.[8] Today, there are numerous cup burners in use around the world, not all of which are identical. There is a project underway to create an NFPA standard for the cup burner design and procedure for its use. A schematic is shown in Figure 6–1; close-up photographs appear in Figure 6–2.

A similar burner was used at the Factory Mutual Research Corporation (FMRC).[9] Researchers at the National Institute of Standards and Technology (NIST) replaced the liquid pool with a stick of polymethylmethacrylate[1], and Tapscott and co-workers at the New Mexico Engineering Research Institute (NMERI) developed a liquid cup burner of smaller diameter that would use less agent.[10] In this apparatus, the cup diameter was 13 mm and the chimney diameter was 50 mm.

For gaseous or volatile liquid flame suppressants, the NGP used the NMERI cup burner with n-heptane as the fuel. The operation was straightforward.[10] The pure chemical was placed in a Tedlar bag, which was placed in a pressure chamber. To force the agent from the bag, a known flow of air was introduced into the chamber, compressing the bag and causing a known flow of agent vapor to the base of the cup burner. Dilution air, monitored with a mass flowmeter, was also introduced into the burner base.

The level of the burning liquid fuel was set to be flush with the lip of the cup. The air stream was established flowing upward past the cup, typically at about 0.17 L/s (flow velocity about 0.08 m/s) in the NMERI device. After a short pre-burn period, the candidate suppressant was introduced into the air stream at a concentration below the expected value for flame extinguishment. After determining that this concentration did not quench the flame (within about 10 s), the suppressant flow was increased, and the flame was observed for about 10 s again. This stepwise increase was continued until the concentration was sufficient to extinguish the flame. Further tests were sometimes performed to refine the extinguishing value, generally to within about 0.5 volume %. The process typically consumed 0.03 moles of the chemical if the extinguishing concentration was about 5 volume %.

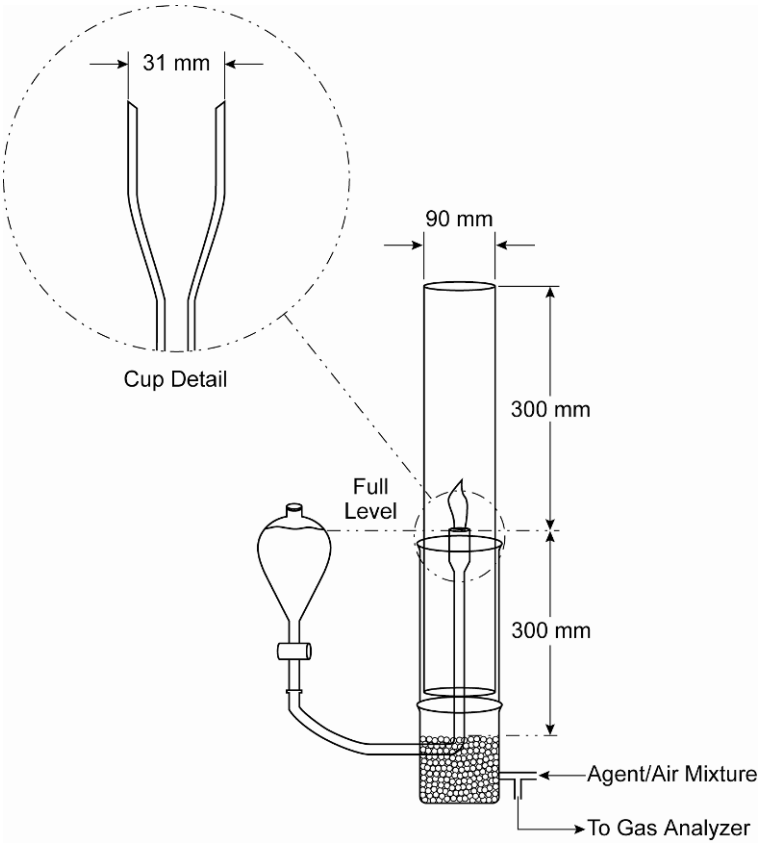

Figure 6–1. Schematic of the Cup Burner Apparatus.
(Adapted from Kidde-Fenwal drawing, used with permission)

Figure 6–2. Photographs of a Standard Cup Burner.
(Kidde-Fenwal photographs, used with permission)

A different injection mode was used if the candidate suppressant was of lower volatility, i.e., the boiling point was such that the equilibrium concentration in ambient air was near or below the extinguishing concentration.[10] The liquid sample was discharged by a syringe pump at a measured rate into a nebulizer. The sample reservoir and syringe pump were cooled to depress vaporization and minimize bubble formation within the pump and connective tubing. The nebulized mist was carried by a metered flow of heated air (Figure 6–3) into a heated glass column and fully evaporated. The air-agent mixture entered the cup burner at a temperature between 40 °C and 50 °C. The cup burner chimney was heated to eliminate condensation of the agent on the glass surface. (See Figure 6–4.)

Using these approaches, the apparatus was usable to address compounds with boiling points from at least -58 °C (halon 1301) to 130 °C. In some cases, when it was not possible to obtain a sufficient mass of the chemical for a determination of the extinguishing concentration, the value was estimated, and a single test was performed to establish an upper bound.

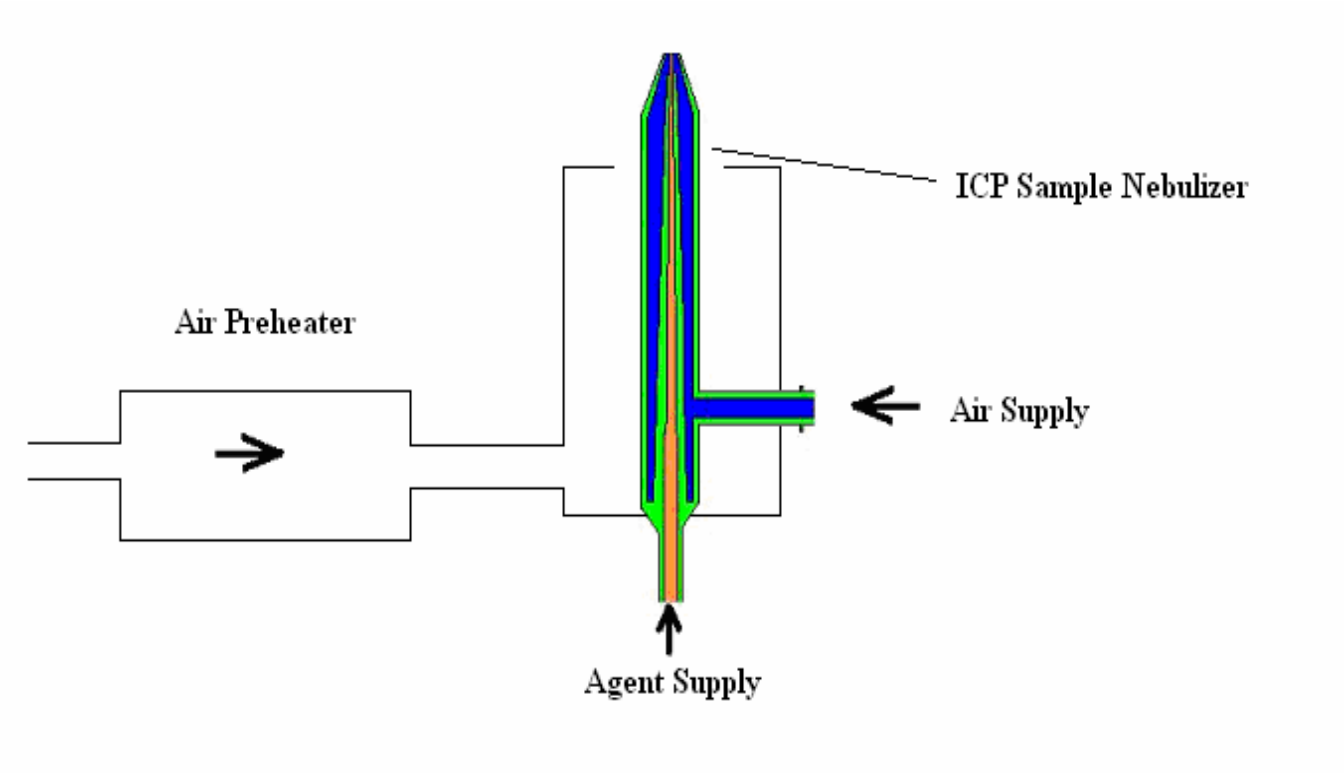

Figure 6–3. Schematic of Sample Nebulizer.
(Chemical Development Studies, Inc. drawing, used with permission)

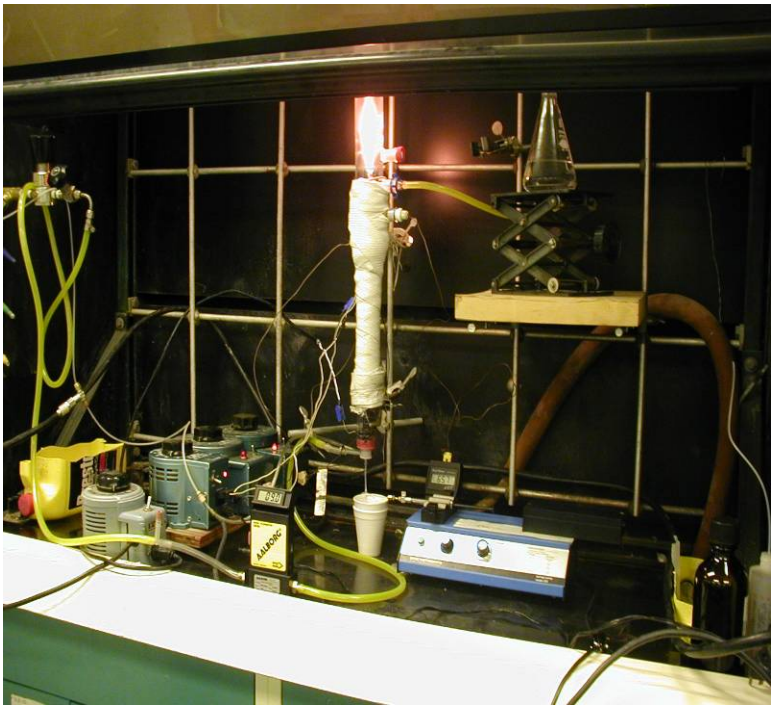

Figure 6–4. Heated Cup Burner for Appraising High-boiling Flame Suppressants. (Chemical Development Studies, Inc. photograph, used with permission)

6.4.3 Dispersed Liquid Agent Fire Suppression Screen (DLAFSS)

Need for a Liquid Agent Screen

In practice, fluid suppressants are stored as liquids under pressure. This enables storing more than 100 times the agent mass in a given volume, compared to storage as a compressed gas. Upon release, the fluid partially vaporizes, with the remaining fraction emerging as droplets of varying size. When they reach the flame zone, the droplets absorb additional heat, cooling the flame as they vaporize. This heat of vaporization can be a significant contribution to the agent's flame suppression efficiency, especially for water or other polar compounds. It was anticipated that some such compounds, with other desirable properties, would merit screening for their fire suppression effectiveness. The cup burner, dispensing only gases, does not capture this additional benefit.

For the NGP, Yang and co-workers designed, constructed, and demonstrated a laboratory-scale apparatus that could perform the screening of liquid agents in a well-controlled experimental setting.[11] The following describes the design and the operational procedure of the Dispersed Liquid Agent Fire Suppression Screen (DLAFSS). Detailed component drawings are documented in the appendices to a more detailed report.[12]

General Description

As shown in Figure 6–5 and Figure 6–6, the apparatus consisted of:

- a burner that generated a flame whose properties made it appropriate for examining liquid aerosol suppressants and whose extinguishment was readily observed,

- a wind tunnel that produced a flow field in which the droplets were transported to the flame in a well characterized manner, and
- a liquid droplet generator that generated small amounts of liquid aerosol agent of controlled and known dimension.

The device could also be used to screen gaseous fire suppressants. In principle, the apparatus could be employed to screen powders by incorporating a powder delivery system in lieu of a liquid droplet generator; however, that was not pursued.

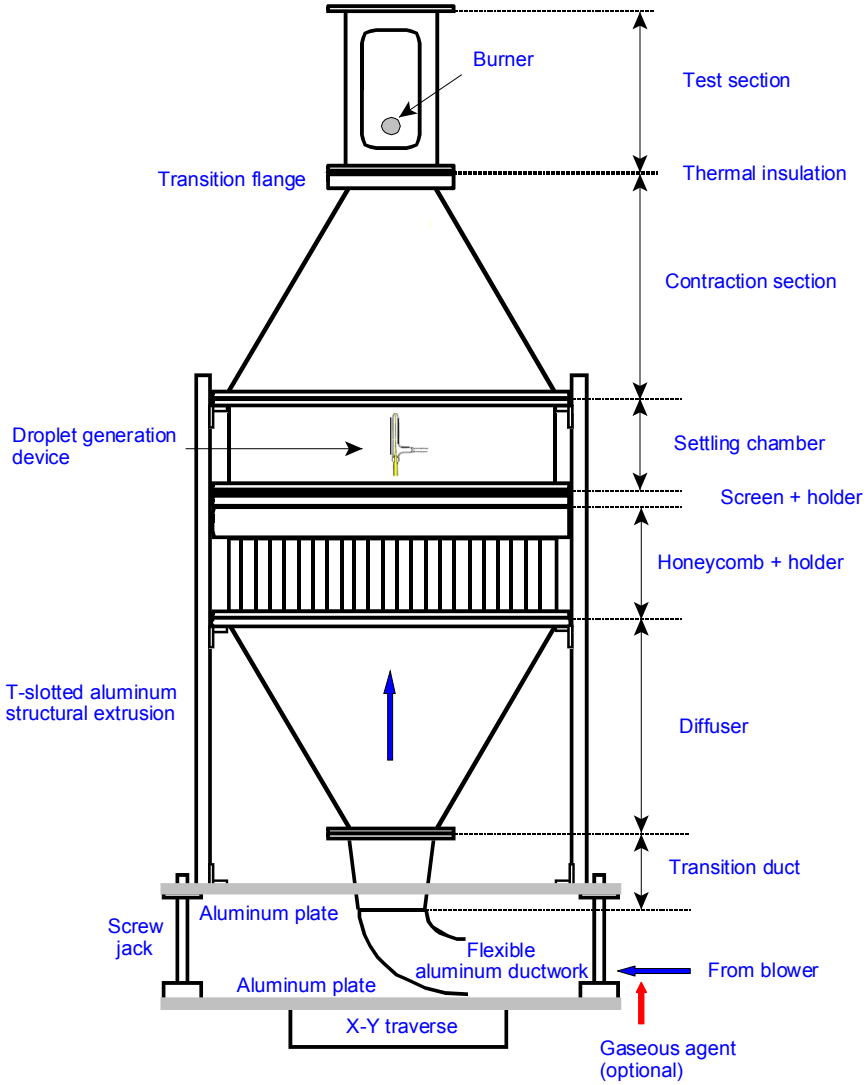

Figure 6–5. Schematic of the DLAFSS Wind Tunnel.[12]

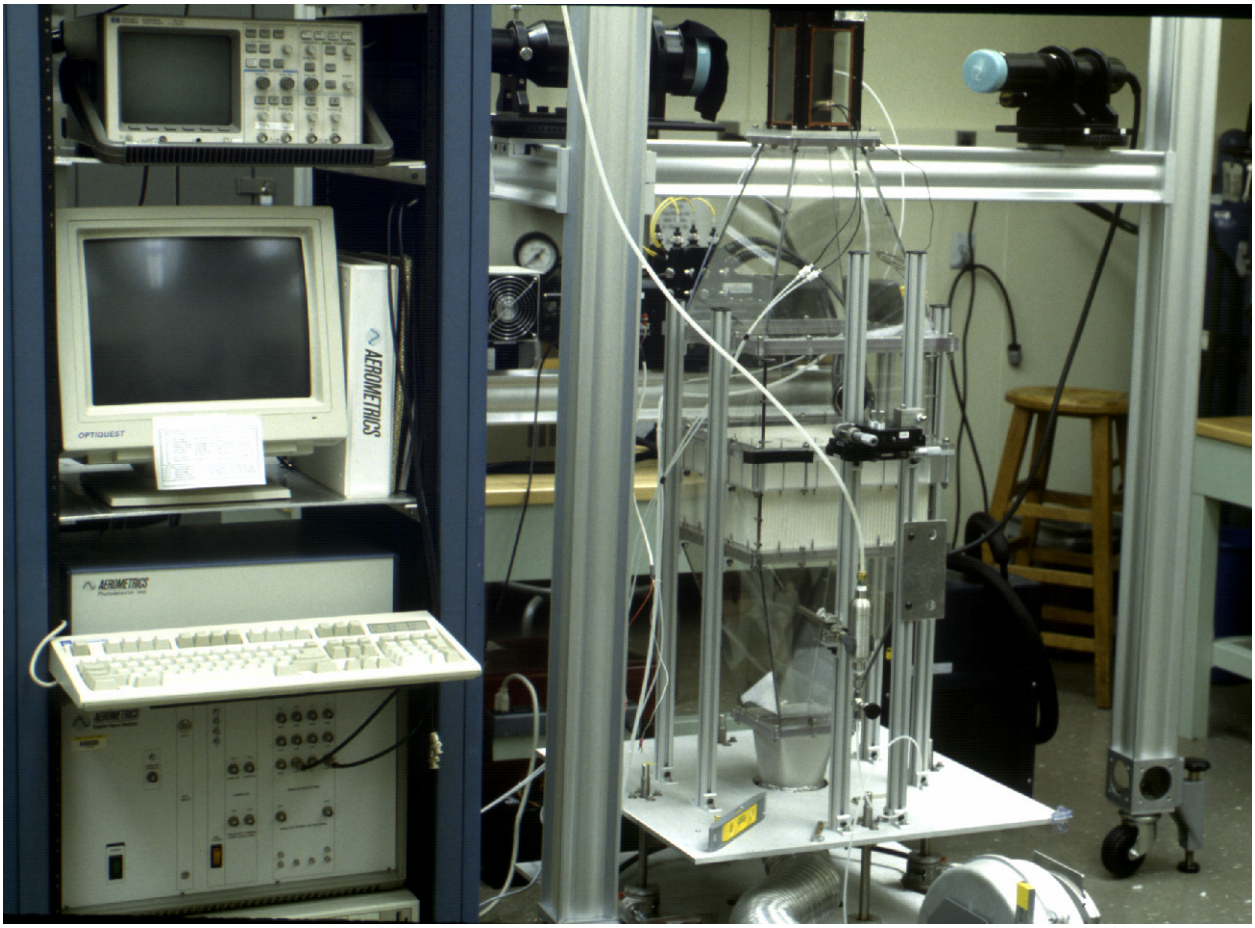

Figure 6–6. Photograph of the DLAFSS Wind Tunnel.[12]

The burner was designed to be durable, easily built, installed, operated, and able to generate reliable screen test data. It is shown schematically in Figure 6–7 and photographically in Figure 6–8. The burner was a replaceable, porous (20 μm typical pore diameter) sintered stainless steel, standard ½" UNF-threaded cup filter, with a length of 3.18 cm, an inner diameter of 1.12 cm, and an outer diameter of 1.58 cm. The burner was screwed onto an extended water-cooled insert through which fuel was injected. The water was used to cool the burner (to prevent damage to the porous surface structure) and the fuel (to prevent fuel pyrolysis prior to its ejection through the porous surface). A water-cooled, cylindrical brass rod, of the same diameter as the burner, extended the burner cylinder across the test section. The downstream hemicylinder of the burner surface was coated with a thin layer of high-temperature-resistant black paint in order to prevent fuel ejection into the wake region. The high pressure drop across the porous sintered surface assured a very uniform fuel flow over the burner surface.

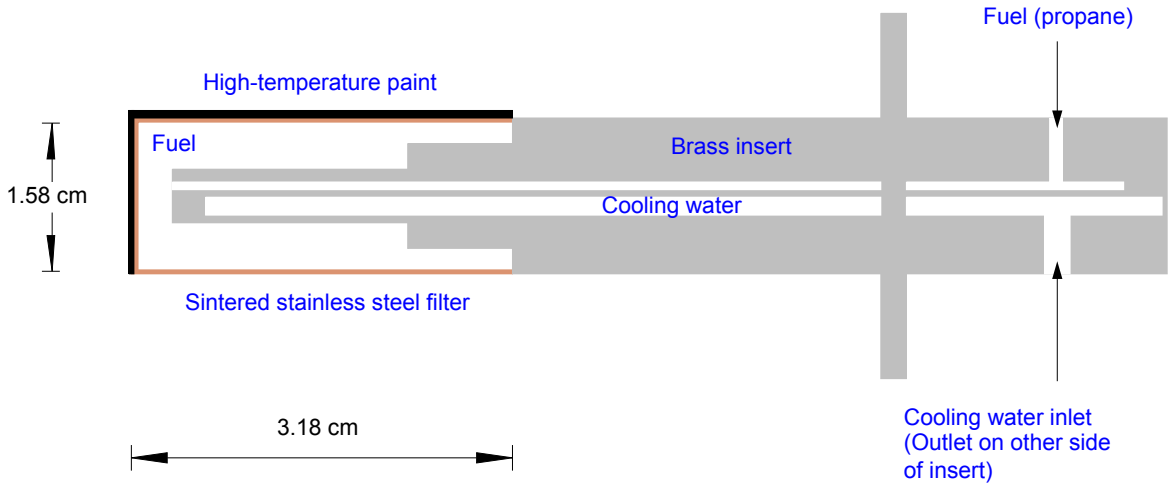

Figure 6–7. Cut-away View of the DLAFSS Burner Insert.[12]

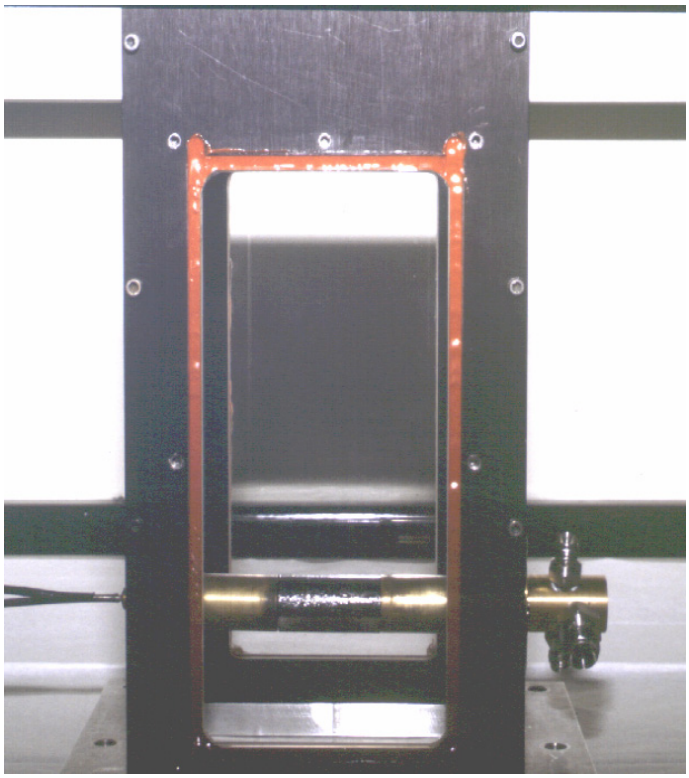

Figure 6–8. Photograph of the DLAFSS Burner Assembly.[12]

Propane, which is moderately sooting, was used as the fuel. Its flow was regulated by a mass-flow controller (with a range of 0 L/min to 4 L/min), which was controlled by a personal computer using a data acquisition board and software. A bubble flow meter was used to calibrate the mass-flow controller. The fuel was ejected uniformly from the cylinder surface, and a counterflow diffusion flame was formed in the forward stagnation region of the burner (Figure 6–9a).

This type of burner, devised by Tsuji[13,14,15,16] and commonly referred to as a "Tsuji burner," has been extensively used to study flame structure and flame extinction using inert gases,[17] halons,[18] and powders.[18] There are many advantages to the use of a counterflow cylindrical burner. The fuel and the oxidizer flows can be independently adjusted. The flame is laminar, two-dimensional, and very stable in the forward stagnation region. The geometry of the burner and the flow field allow for relatively simple analysis of the forward stagnation region.[19,20,21,22,23,24,25] Both enveloped (Figure 6–9a) and wake (Figure 6–9b) flames can be easily maintained over a wide range of fuel and oxidizer flows. The flame is easily observed, and critical stages such as the blow-off limit (abrupt transition from an enveloped flame to a wake flame) can be ascertained with ease and high reproducibility. The flame front can be easily accessed by intrusive[14, 15] or non-intrusive[20, 25] probing techniques, thus enabling detailed studies of flame structure, if desired.

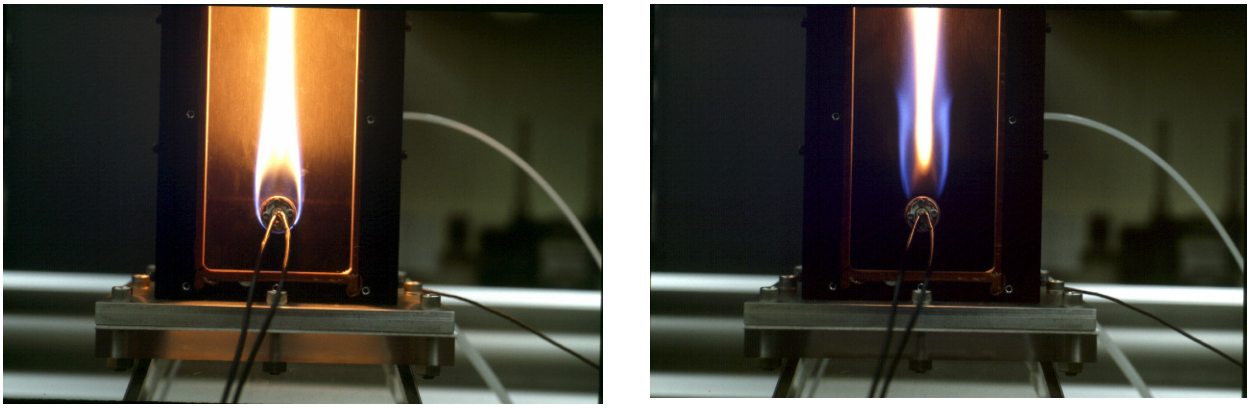

(a) (b)

Figure 6–9. An Enveloped Flame (a) and a Wake Flame (b).[12]

The advantage of the current burner design over those used in the past was that burner replacement could be easily performed when clogging of the porous burner surface occurred due to the deposition of soot particles or residue from liquid agents containing dissolved solids. [18]

The wind tunnel provided a uniform, low turbulence intensity oxidizer flow to the porous cylindrical burner. As shown in Figure 6–5, the air flow in the wind tunnel was oriented vertically upwards. There were five major components in the wind tunnel. The tunnel, except the test section, was made of clear polycarbonate and polymethylmethacrylate for visual observation of droplet transport toward the burner.

- The variable speed blower introduced the air flow into the tunnel through an expandable, flexible 10 cm diameter aluminum ductwork. A coupling converted this circular cross section to the square shape of the remainder of the tunnel. A slide gate damper at the blower inlet enabled control of the air intake.

- The 30 cm long diffuser had a 10 cm x 10 cm inlet cross section and an expansion ratio (based on area) of 1:9.
- The flow straightener section, which served to insure that the flow to the test section is laminar and uniform over the entire cross-section, consisted of a polycarbonate honeycomb and a screen. The honeycomb cells had a nominal diameter of 3.2 mm. A 50-mesh center-to-center stainless steel screen with 30 % open area and with wire diameter of 0.23 mm was used.
- The 30 cm long contraction section had a contraction ratio (based on area) of 9:1, with an inlet cross sectional area of 30 cm x 30 cm. A smooth-surfaced transition flange was placed between the outlet of the contraction section and the inlet of the test section, along with a thermal insulation gasket.
- The test section had a cross sectional area of 10 cm x 10 cm and a length of 20 cm. It was made of black-anodized aluminum with three Pyrex observation windows (12 cm x 7 cm x 0.64 cm) mounted flush against the three walls and sealed using high-temperature silicone. The burner was inserted through the fourth wall. The combustion products from the burner were vented to an exhaust hood.

A three-dimensional traverse mechanism was used to position the entire wind tunnel with respect to stationary optical instrumentation for droplet characterization at various locations near the burner. The wind tunnel was mounted on an aluminum base plate, which was placed on four worm-gear screw jacks coupled together via flexible shafts. The jacks were mounted on a second aluminum plate and were driven by a stepping motor and a computer-controlled microstepping indexer drive to raise and lower the tunnel. The horizontal movement of the wind tunnel was provided by mounting the whole wind tunnel assembly on a milling machine index table.

Two droplet generation techniques were developed:

- A piezoelectric droplet generator that created uniform liquid droplets of diameter near 100 μm.[26] The operating principle of the droplet generator is based on the break-up of a nitrogen-pressurized jet ejecting from an orifice as a result of controlled vibration from a piezoelectric transducer driven at a fixed frequency. The droplet generator consisted of a liquid chamber which was connected to a 40 mL stainless steel reservoir, a bleed port (for eliminating any air bubbles trapped inside the chamber during priming), an orifice plate containing a sapphire orifice, and a piezoelectric transducer. The transducer was bonded with conductive epoxy to a circular disc stamped from flat stainless steel shim stock (0.38 mm thick).

  Although distilled and de-ionized water and a few very dilute aqueous solutions have been successfully tested with this droplet generator,[27] clogging of the orifice opening constantly plagued the continuous operation of the piezoelectric droplet generator, aggravated by liquids with high loading of dissolved salts. This approach was subsequently not considered for further development.
- A small glass nebulizer was of the type used in inductively-coupled plasma atomic emission spectroscopy and was commercially available. The nebulizer was mounted at the same location (in the settling chamber of the wind tunnel) as the piezoelectric droplet generator. A schematic of the nebulizer is shown in Figure 6–10.

The aerodynamic break-up of a liquid stream issued from the capillary by high-velocity air caused the formation of a fine mist of droplets. Because of the differences in the droplet formation mechanisms, a relatively large opening (diameter ≈ 100 μm) of the capillary in the nebulizer, compared to the sapphire orifice (diameter ≈ 30 μm) above, could be used with a wide range of liquids, including those with a relatively high salt concentration. The large capillary opening made the nebulizer less prone to clogging. Fluid was fed to the nebulizer by a small, programmable syringe pump. Air was supplied to the shell of the nebulizer by a mass-flow controller. The resulting mist was entrained upwards toward the flame by the air flowing in the tunnel. The atomizing air flow was set at 0.25 L/min, which was the highest flow that could be used without disturbing the flame at the burner. Because of this limit, the atomization efficiency of the nebulizer dropped when the liquid delivery rate was increased beyond 1.3 mL/min; that is, larger droplets were generated that may not be entrained upward by the air flow in the tunnel.

The droplet generator was located in the settling chamber and was approximately 42 cm upstream of the burner. The presence of the droplet generator in the wind tunnel did not create any significant perturbation or blockage effect on the oxidizer flow field near the burner because the flame characteristics did not change with or without the presence of the droplet generator in the flow stream. By adjusting the location of the droplet generator with respect to the burner, droplet loss to the wind tunnel walls was minimized because the resulting dispersed droplet cloud was confined to a very narrow region near the burner.

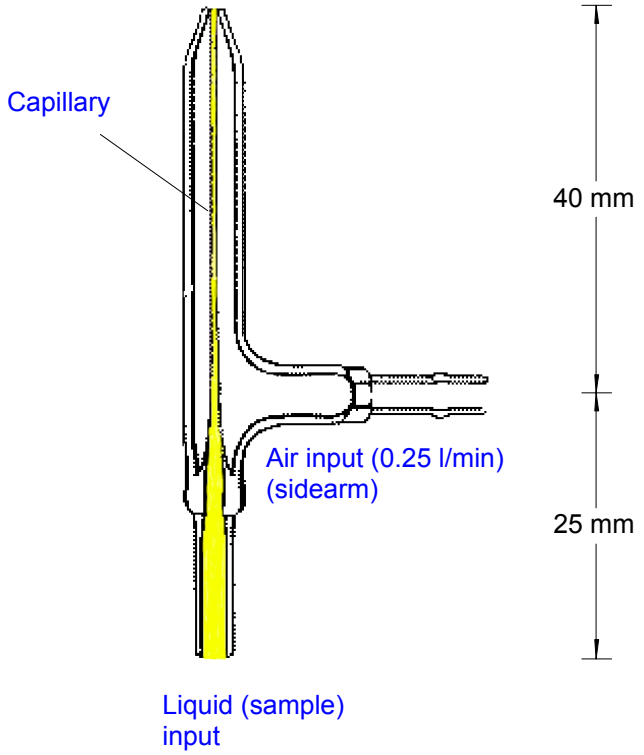

Figure 6–10. Schematic of the DLAFSS Nebulizer.[26]

Measurements of droplet size using a two-component Phase Doppler Particle Analyzer with a Doppler Signal Analyzer showed that the Sauter mean diameter is 20 μm to 30 μm for fluids having a range of colligative properties. About 90 % of the droplets fell within ± 5 μm of the mean value.

Operation

There were two ways to perform the screen experiments: (1) increasing the air flow at a fixed liquid agent application rate until blow-off occurs, and (2) increasing liquid agent application rate at a fixed air flow until blow-off occurs. The former was selected because the procedure requires less agent, and there was no need to correct for the lag time from changing the syringe pump setting (to increase the liquid flow) to attaining a steady liquid delivery rate.

For the rapid, *relative* indicator of the performance of candidate liquid suppressants, the fuel flow was fixed at 2 L/min, which corresponds to an ejection velocity of 4.2 cm/s. This value virtually eliminated an effect of fuel flow on blow-off velocity. Once a stable flame has been established, a fixed concentration of agent aerosol was added to the air stream; the concentration was low enough that the stable enveloped flame was maintained. The air velocity was then increased until there was a transition from a stable enveloped flame to a wake flame. This was generally a sharp change. The "figure of merit" for the agent, at that mass fraction in the air stream, was the value of the air velocity at blow-off: the higher the air blow-off velocity, the less effective the fire suppressant.

The following procedure was then used to determine a "standard" mass fraction of agent at flame extinction. Since there were many liquid agent delivery rates that one can use in the screening procedure, a reference delivery rate was needed to compare and interpret the fire suppression effectiveness of various liquid agents in a consistent and meaningful way.

Nitrogen was selected as a reference gas due to the availability of suppression data for both the cylindrical and cup burners. The mass fraction of nitrogen to extinguish a propane cup burner flame is 0.32.[28] DLAFSS experiments[12] have shown that the nitrogen mass fraction at blow-off, equivalent to the cup burner value, corresponded to a reference blow-off velocity of ≈ 30 cm/s.[iii] At this velocity and a propane flow of 2 L/min, an enveloped flame could not be stabilized. Therefore, to compare the results obtained from the cylindrical burner to conditions commensurate with cup-burner results, extrapolation to a lower air velocity was required. The procedure was as follows:

- A blow-off air velocity without fluid application (but with air flowing in the nebulizer) was obtained, followed by a blow-off experiment with a fixed fluid application rate.
- The fluid delivery rate at an air velocity of 30 cm/s was then deduced by linear extrapolation. Based on experience, an application rate between 0.6 mL/min and 1 mL/min appeared to be appropriate, which was a compromise between minimizing the fluid consumption for a test and attaining a blow-off velocity close to the reference blow-off velocity of 30 cm/s.

Once the application rate corresponding to the reference blow-off velocity was deduced, the reference mass flow of the liquid agent, $\dot{m}_{agent,ref}$, was calculated using the liquid density. The reference mass fraction of the liquid agent in the air stream was then

[iii] It is expected that similar reference blow-off velocities will be obtained when the cup burner results for other gases are used because at the *same* low global strain rate in a counterflow flat-flame burner, the agent extinction concentrations agree well with the measurements obtained from a cup burner.

$$Y_{agent,ref} = \dot{m}_{agent,ref} / (\dot{m}_{agent,ref} + \dot{m}_{air,ref}) \quad (6\text{-}1)$$

where $\dot{m}_{air,ref}$ is the mass flow of air, calculated from the cross-sectional area of the test section and an air velocity of 30 cm/s.

Sample Results with Aqueous Suppressants

Several test fluids (water, skim milk, 30 % sodium iodide, and 30 % and 60 % potassium lactate) were used to evaluate the performance of the screening apparatus.[11,29] Milk is known to be a fire suppressant,[30] sodium iodide was selected because it may be more effective than sodium bromide[31], and potassium lactate has been demonstrated to be more effective than water.[31] Figure 6–11 shows the screening results for these test fluids. In each case, only 10 mL of sample was needed to perform a rapid screen with one repeat. For a given fluid, increasing the liquid application rate decreased the blow-off velocity. As expected, a mass fraction of 60 % potassium lactate was more effective than 30 % potassium lactate. Water was the least effective when compared to skim milk, 30 % sodium iodide, and 60 % potassium acetate. Based on this set of data, the coefficient of variation from run-to-run using the liquid screening apparatus was estimated to be better than 20 %.

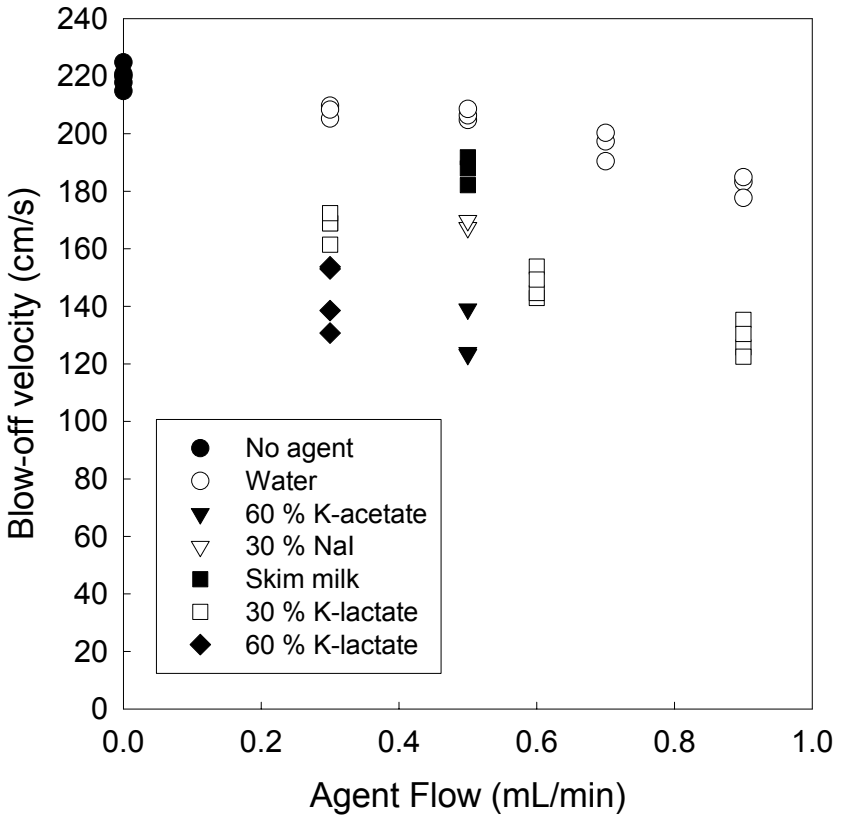

Figure 6–11. Screening Results for Various Aqueous Fluids.[12]

Table 6–1 summarizes the calculations of the reference agent mass fraction in air using the screening results from Figure 6–11 and the approach described above. Average values of the blow-off velocities were used in the extrapolation. For cases where blow-off velocities at more than one liquid application rate were available, linear regressions were used to extrapolate the reference blow-off velocities.

Table 6–1. Calculated Nominal Agent Mass Fractions at Reference Blow-off Air Velocity of 30 cm/s. [12]

Agent	$V_{agent,ref}$ (mL/min)	Agent density (g/ mL) @ 20 °C	$M_{agent,ref}$ (g/s)	*Nominal* agent mass % (%)	$m_{water,ref}/m_{agent,ref}$
Water	4.62	1.00	0.08	2.6	1.0
60 % K-acetate	0.99	1.34	0.02	0.8	4.0
30 % NaI	1.76	1.29	0.04	1.3	2.0
Skim milk	2.78	1.01	0.05	1.6	1.6
30 % K-lactate	1.74	1.15	0.04	1.2	2.0
60 % K-lactate	0.71	1.33	0.02	0.6	4.0

The last column of Table 6–1 lists the ranking indices relative to water. For example, the 60 % K-acetate and 60 % K-lactate solutions were considered to be four times more effective than water at the reference blow-off velocity. If the droplets were not homogeneously dispersed across the total cross-sectional area, the calculated agent mass fraction would be underestimated. The effective area was considered as the effective coverage area of the mist in the test section. Depending on the effective coverage area, a difference of a factor of two to three in the calculated liquid mass fraction resulted. By placing a sheet of filter paper over the exit of the test section for a short duration with the wind tunnel operating (without the burner) and the nebulizer atomizing water with a dye added, the droplet-impact (color) pattern on the filter paper was used as an indicator to determine the mist coverage area in the test section. The color pattern, which was approximately circular, indicated that the mist from the nebulizer completely covered the burner and its vicinity. The mist coverage area was estimated to be about 40 % of the total cross-sectional area of the test section for all the conditions encountered in these screening tests.

Water and the aqueous agents studied were found to be more effective than CF_3Br, compared to the propane cup burner value (mass fraction of 0.17 for CF_3Br).[28] The computational study by Lentati and Chelliah[32] also demonstrated that 20 μm water droplets were more effective at extinguishing an opposed-flow methane diffusion flame than CF_3Br (mass fraction of 4.24 % vs. 5.9 %) at an extinction strain rate of 176 s^{-1}. Although the ratio of the DLAFSS nominal water mass fraction to the cup burner value for CF_3Br using propane was smaller, the two studies were in qualitative agreement in terms of the suppression effectiveness of water droplets.

Care should be exercised when extrapolating the screening results in Table 6–1. These were obtained using an idealized laboratory flame and a droplet delivery system such that the transport of fine liquid droplets *to* the flames was not a factor in determining the suppression effectiveness. In real fires, droplet entrainment and transport to the fire can significantly affect the liquid agent mass concentration required to suppress a fire, especially in highly obstructed enclosure fires.

6.4.4 Transient Application, Recirculating Pool Fire Apparatus (TARPF)

Need for the Apparatus

Both the cup burner and the DLAFSS determine the minimum concentration of agent needed to suppress a flame by increasing the agent flow slowly until a critical volume fraction is achieved in the oxidizer stream and flame extinction is observed. In practice, however, agents designed to replace CF_3Br are discharged rapidly, not steadily. Solid propellant gas generators (SPGGs), for example, typically discharge their effluent in 10 ms to 500 ms. A robust and repeatable means to evaluate the effectiveness of different formulations at these fast application rates requires a non-conventional screening device.

NIST research staff developed a Transient Application, Recirculating Pool Fire (TARPF) suppression facility to screen different agents and prototype systems as an indicator of full-scale performance.[33] The TARPF agent suppression screen was designed to reproduce the most difficult fire situation and to allow control of critical agent discharge parameters, including agent discharge rate and duration, air flow, and obstacle geometry. The performance of gaseous agents, aerosols and SPGGs was examined.

The apparatus derived from prior work by Hirst and Sutton,[34] who developed a wind tunnel to explore the impact of step height, air flow, and pressure on the blow-out of a jet fuel pool fire stabilized behind a backward facing step. Hirst et al.[35] studied the suppression of these types of fires using various halons, and concluded that a liquid pool burning in a flow behind an obstacle is the most difficult fire to extinguish. This was borne out in full-scale tests done later.[36] Experiments by Hamins et al.,[37] in cooperation with Walter Kidde Aerospace, were conducted in a wind tunnel scaled down from the earlier work by Hirst to examine the performance of HFC-125 and HFC-227ea. Investigations at the Air Force Research Laboratory[38] as part of the NGP sought to determine the detailed structure during suppression of a non-premixed methane/air flame stabilized behind a step. The changing character of the flame with step height and air velocity was examined, along with the amount of halon 1301 required to suppress the flame as a function of the flow parameters and injection interval.

A turbulent spray burner had been designed in earlier work at NIST[39] to simulate an engine nacelle spray fire resulting from a ruptured fuel or hydraulic fluid line. Flames were suppressed using gaseous and powdered agents. Hamins et al. [37] redesigned the burner to include a heated disk in the center of the flow downstream of the fuel nozzle. They showed that the concentration of nitrogen necessary to extinguish a turbulent propane flame increased substantially with surface temperature. The same trend, but to a lesser degree, was observed with hydrofluorocarbons.

Previous studies had demonstrated the effectiveness of SPGGs and their hybrids in full-scale fire suppression experiments.[40,41] Solid propellant gas generators undergo rapid solid-phase reactions producing inert gases, principally carbon dioxide, water vapor, and nitrogen, as well as particulates composed of inorganic salts. Each component individually behaves as a fire suppressant. Hybrid generators are particularly attractive for some special situations such as inhabited spaces or cold temperature applications.[42] The hybrids use the hot inert SPGG exhaust to vaporize and expel a secondary suppressant, typically a liquid, such as water or a low boiling point halocarbon, through a nozzle.[43]

Experimental Facility

Hardware

As shown in Figure 6–12 and Figure 6–13, the TARPF was a small wind tunnel consisting of a number of sections. The main portion of the tunnel was 2.5 m long with a square cross section 92 mm on a side. (Detailed mechanical drawings of key components of the facility can be found in reference 44.) Air, supplied by a compressor rated for a maximum flow of 180 g/s at 1.0 MPa, could be delivered to the tunnel at speeds, averaged over the 92 mm square cross section, up to 17 m/s. Flow was monitored using a calibrated sonic orifice and a piezoelectric pressure transducer. The inlet air temperature could be heated to above 200 °C. A honeycomb flow straightener and mixing screens were located 1 m upstream of the test section. The burner consisted of a sintered bronze plate, 92 mm wide by 190 mm long. Propane, the primary fuel, could be supplemented with a JP-8 spray. The expanded relative uncertainty[iv,45] in the flows of fuel and air were ± 5 % of the measured value, based upon the manufacturers' specifications for the metering orifice and mass flow controllers. Stainless steel baffles between 10 mm and 55 mm high were located upstream of the burner. A ramp could also be inserted to form a 25 mm high backward-facing step.

To investigate different re-ignition scenarios, a hot surface obstruction was set up immediately downstream of the propane porous burner. (See Figure 6–12.) The v-shaped obstruction was 25 mm in height, the base was 25 mm wide, and was centered across 50 mm of the wind tunnel passage. An S-type thermocouple was place on the external upstream surface of the obstruction. A high-resistance, high temperature ceramic adhesive was used to adhere the thermocouple to the Inconel surface, 15.5 mm thick. An ethane torch was supported underneath the obstruction to heat the inner surface to over 1100 °C. A mass flow controller was used to regulate the obstruction surface temperature. The fire was initiated by a spark across two electrodes protruding from the side wall of the test section 20 mm above the surface of the burner and 20 mm downstream of the step. Heat release rates were up to 10 kW. A 30 Hz video camera could view the flame and the suppression process from above and the side through 6 mm thick Pyrex windows. For some experiments, a 1000 Hz digital camera was used to investigate the flame dynamics. A photograph of a typical flame taken through the window is shown in Figure 6–14. The inclined mirror above the apparatus reflects a top view of the flame.

A stream of JP-8 droplets provided a source of re-ignition for the propane flame as they were directed directly onto the heated obstruction after flame suppression. The droplet array was generated from a 0.14 mm sapphire orifice that was pressure fit into a 3.1 mm tube. The tube was inserted into the wind tunnel passage from the top wall at a position 25 mm upstream of the flame stabilizing obstacle. The end 3.8 mm of the tube was bent 90° into the direction of the air stream, and was centered between the passage top wall and face of the ramp. The JP-8 was forced through the injector with nitrogen back pressure at 170 kPa. The low back pressure and several sintered filters (with a pore size of 7 μm and 2 μm) were used to help prevent clogging of the injector. Initially, piezo-electric crystals were used to initiate droplet breakup, but impingement of the fuel on the heated obstruction was difficult due to entrainment of the individual droplets into the high-velocity air flow. Impingement was achieved successfully by directing the non-atomized fuel stream on the heated obstruction.

[iv] The expanded relative uncertainty on all dimensions and independent parameters described in this chapter is ± 50 % of the highest significant place reported, with a coverage factor of 2, unless otherwise stated.

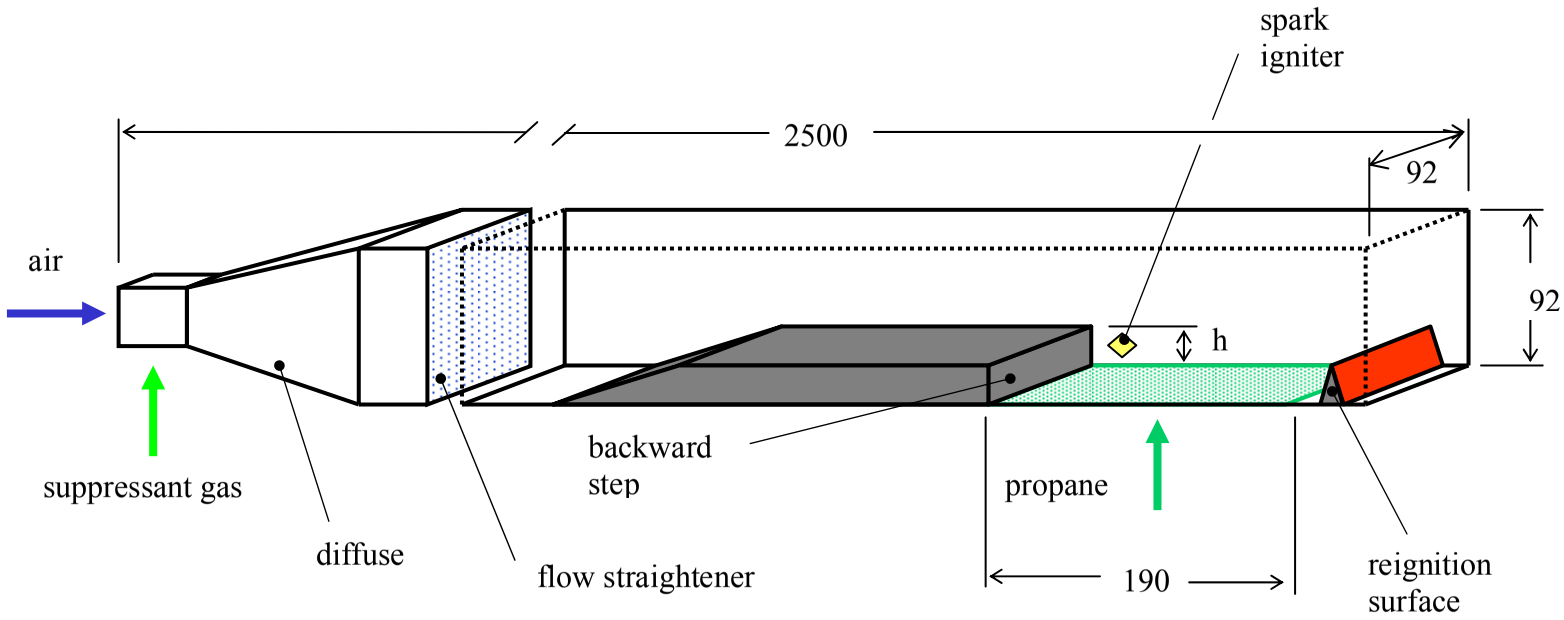

Figure 6–12. Schematic of Step-stabilized Pool Fire Apparatus. [44] Dimensions are in millimeters.

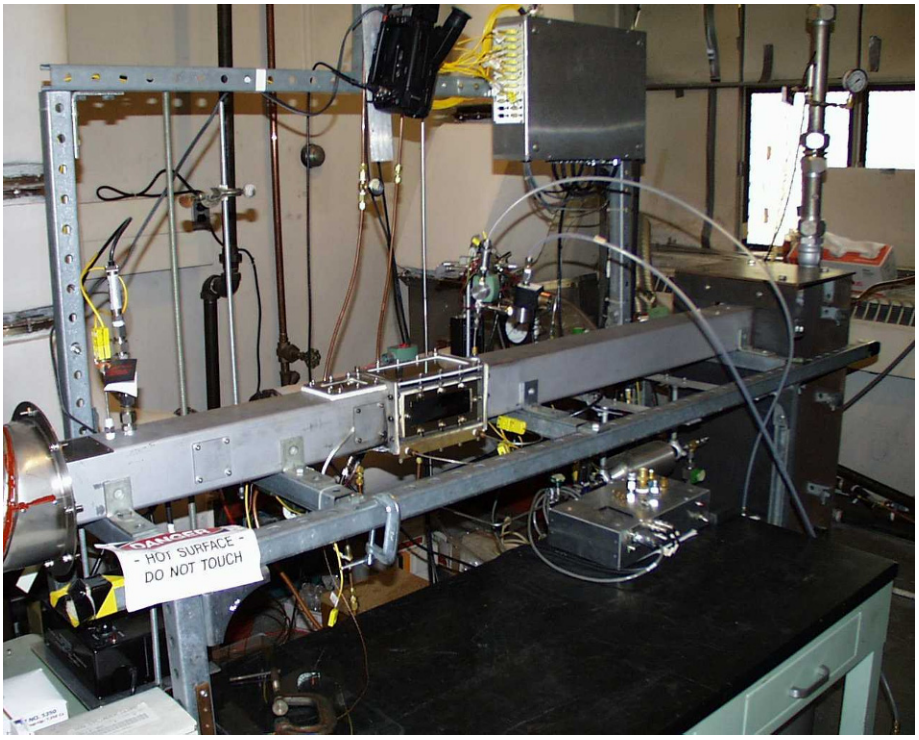

Figure 6–13. Photograph of the TARPF. (NIST photo)

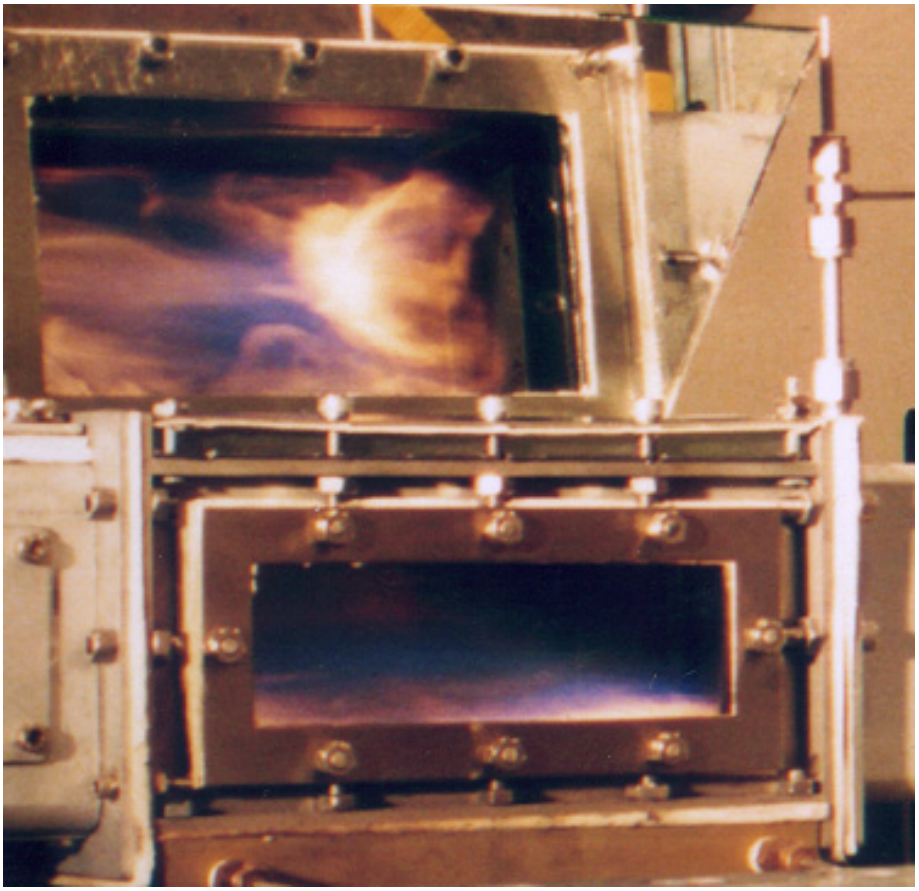

Figure 6–14. Photograph of a Baffle-stabilized Propane Flame in the TARPF. (NIST photo)

The JP-8 injection time (controlled by a solenoid valve), and flow were varied in order to optimize the impingement process. The impingement of the fuel onto the obstruction surface resulted in a significant decrease in the surface temperature, and care was taken to compensate for this effect during experiments.

The fire suppressing agent was injected downstream of the air metering orifice. Since the air flow was choked by the metering orifice, the introduction of the agent was accomplished without altering the total air flow.

Volatile Agents

Gaseous agents (nitrogen, CF_3Br, and HFC-125) were stored in 1 L and 2 L stainless steel vessels with the pressure monitored by a 1 ms response piezoelectric transducer, and the temperature measured with a chromel-alumel thermocouple. An electronic timer controlled the interval (10 ms to 1000 ms) that a solenoid valve on the agent vessel remains open. The agent passed through a 6 mm diameter orifice before it was injected through two opposed radial ports into the air passage upstream of the diffuser. A computer monitored the flow controllers, pressure transducers, and thermocouples, and sent a signal to the electronic timer to open and close the solenoid valve while releasing the flow of suppressant. The mass of the gaseous agent released was determined from the change in pressure and temperature in the storage vessels. The expanded uncertainty in the calculated mass was ± 2 %, with a minimum absolute uncertainty of 0.12 g attributable to the resolution of the pressure transducer. The discharge rate and duration were controlled by the initial agent pressure and an electronically actuated solenoid valve. The piezoelectric pressure transducer was able to follow the change within about 5 kPa, but the thermocouple response was too slow. To determine the instantaneous mass discharge, the nitrogen was assumed to be an ideal gas with the expansion inside the bottle occurring isentropically. The uncertainty in dm/dt was estimated to be ± 2 g/s.

Aerosol Agents

Aerosol agents required a totally different injection system than what has been described above or used previously. The flows and injection durations of commercial fuel injectors were not adjustable over the range and with the precision necessary for the current application.

The liquid dispensing system (Figure 6–15) consisted of a liquid reservoir, a compressed air cylinder, two computer-controlled solenoids, and a hollow-cone atomizer. The atomizer was positioned equidistant vertically between the ramp and the upper wall of the wind tunnel, and at discrete locations along the air passage from 65.5 cm upstream of the propane porous burner to a location downstream near the ramp. Several different atomizers were used while trying to obtain a well-dispersed spray of droplets in the air passage. The atomizers were commercially manufactured to the following: (1) a nominal spray angle of 70° when operated at 1.03 MPa with a flow of 1.9 mL/s, and (2) a nominal spray angle of 60° when operated at 0.69 MPa with a flow of 1.1 mL/s. Operating these atomizers at nominal pressures normally resulted in a fully developed spray, and thus an increase above the nominal condition had a small effect on reducing droplet size. When positioned at upstream locations, the spray appeared to fill the entire air passage cross section. To initiate a mist for a fixed duration, the data acquisition system activated the solenoid that was connected to the reservoir. At the end of the discharge, the solenoid was deactivated to terminate the flow to the atomizer. The second solenoid leading to a drain was simultaneously activated to prevent any residual flow to the nozzle and dripping from the nozzle.

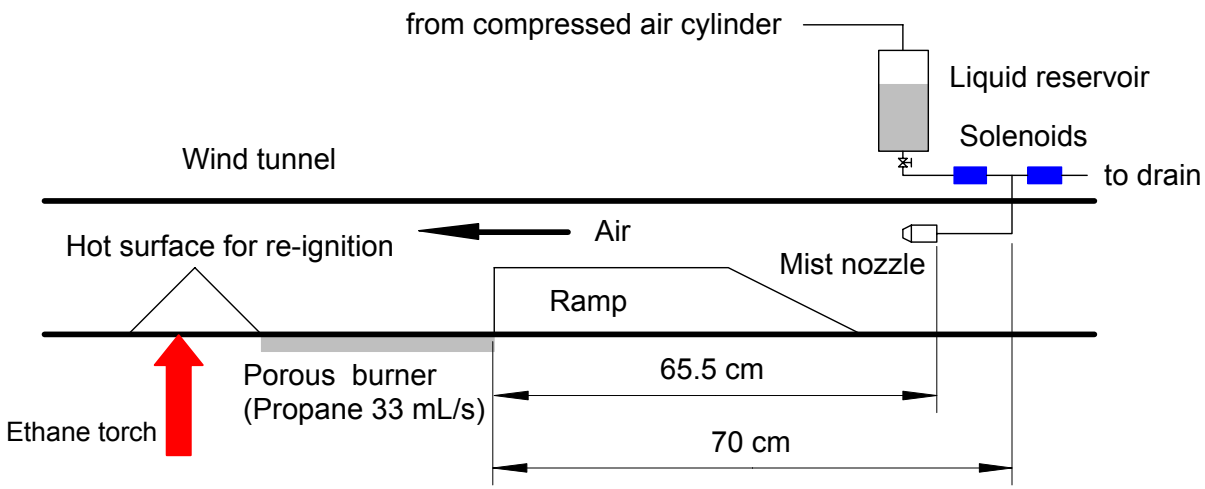

Figure 6–15. Liquid Aerosol Agent Injection System. [12]

SPGG Facility and Operation

Gas generators are manufactured in discrete units using specific chemical formulations and orifice sizes that are designed based on the particular application. The TARPF operator can control neither the total mass discharged nor the injection time interval of the SPGG. To accommodate this limitation, a custom discharge chamber was designed to allow the operator to select the fraction of the SPGG discharge that is injected into the flame zone. The hardware was designed to allow standard size gas generators (which contain significantly more material than is required for suppression in the TARPF) to be evaluated by repeating the test sequence with identical gas generators and incrementally increasing the fraction of SPGG effluent allowed to flow into the TARPF air stream. The SPGG effluent passed through a metering orifice and was injected into the air stream using the same manifold as for the compressed gaseous agents. The flow through the bypass port was discarded into a laboratory exhaust hood. The pressure in the discharge chamber was monitored by a 1 ms response piezoelectric transducer and the temperature was measured with a 76 μm type K thermocouple. Figure 6–16 is a schematic diagram of the SPGG injection system; and Figure 6–17 is a close-up photograph.

The housing, enclosing the entire injection system, was made of 6 mm thick stainless steel as a precaution against a premature or explosive discharge. The internal volume was approximately 200 mL. There were four main ports on the discharge chamber as seen in Figure 6–17:

A ¾ NPT female thread connecting to the gas generator cartridge holder,

A variable area metering orifice (1.6 mm to 6.4 mm diameter) to limit the flow into the TARPF,

A bypass port tapped for a 2 NPT nipple, and

A 19 mm port for mounting a pressure relief blow-out diaphragm.

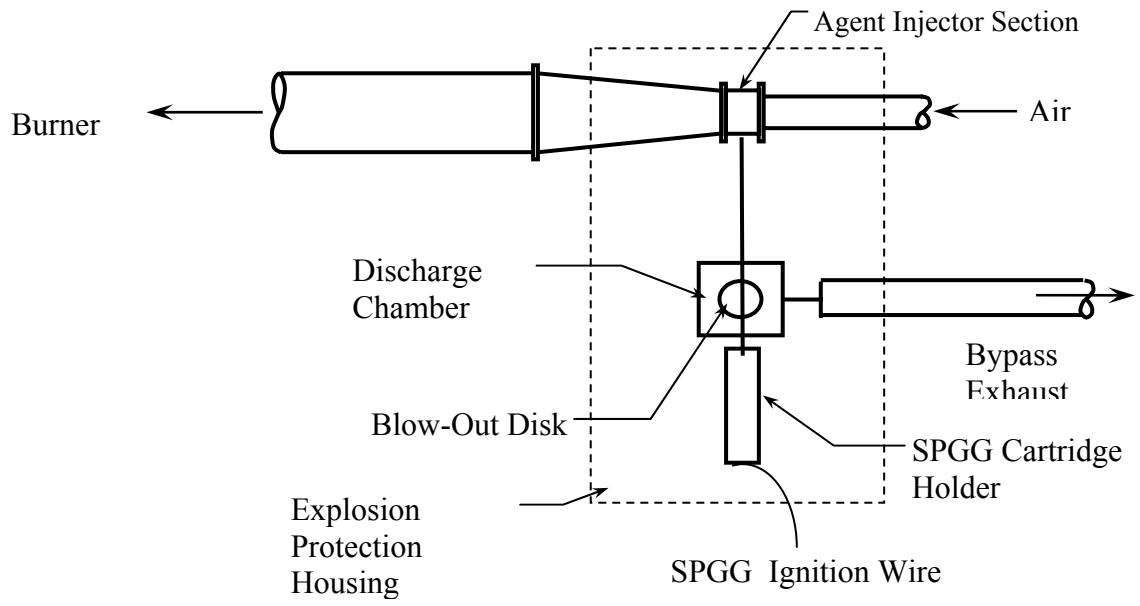

Figure 6–16. Schematic Diagram of the SPGG Injection System. [44]

The fraction of the SPGG effluent injected into the TARPF was varied by selecting the size of Ports 3 and 4. In many of the experiments, Port 4 was left open to maximize the bypass area.

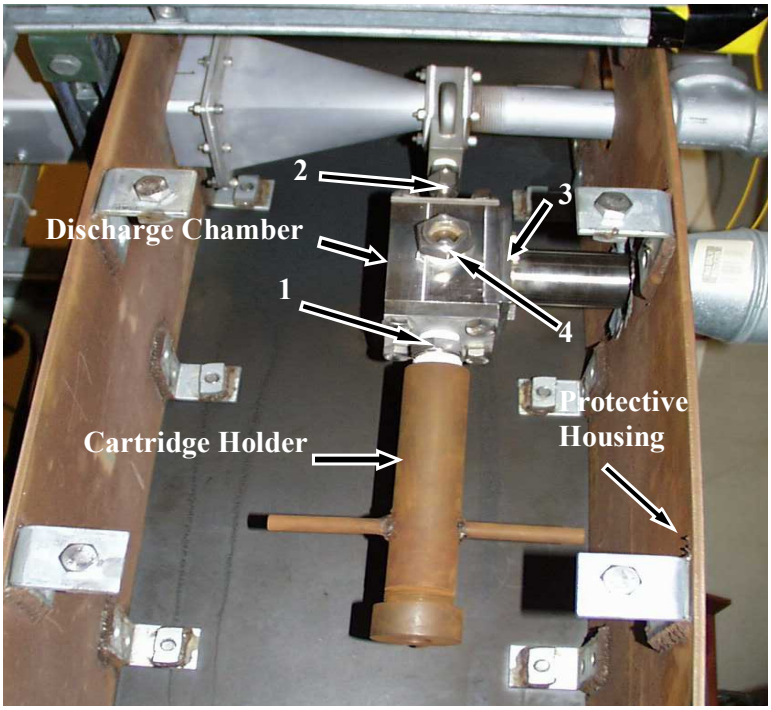

Figure 6–17. Photograph of TARPF Injection System with Housing Cover Removed. The four ports in the discharge chamber are: (1) SPGG outlet, (2) metering orifice, (3) bypass, and (4) blow-out.

The mass of the SPGG injected into the TARPF was determined from the total mass discharged and the ratio of the area of the metering orifice to the combined area of the metering orifice and the bypass area. The expanded uncertainty in the calculated mass was ± 2 %, with a minimum absolute uncertainty of 0.12 g attributable to the resolution of the pressure transducer. From the temperature and pressure measurements, the rate of suppressant addition to the incoming air, *dm/dt*, was estimated within an expanded uncertainty of ± 2 g/s. The concentration of the SPGG in the air flow was determined from the rate of suppressant addition (*dm/dt*) and the mass flow of air. As in the gaseous agent experiments, the air flow was invariant during the agent discharge due to the use of a sonic orifice.

For the tests performed under the NGP, identical commercial air-bag hybrid gas generators were used, one in each of fifty experiments. Each generator released 20.7 g ± 0.1 g. The discharged mass was specified by the manufacturer and confirmed experimentally by weighing the generators before and after each discharge. The agent was composed of 20 g of compressed argon gas and 0.7 g of a solid propellant, which at equilibrium converts to KCl (s), H_2O, N_2 and a small amount of gaseous CO_2.[46]

The gas generator was discharged after steady-state fire conditions were achieved in the TARPF. The discharge was controlled by engaging an electronic switch on a control box that completed a circuit leading from a 12 V battery to the electrical connector located on the gas generator. One ampere was required to fire the 40 mg squib, which was an intrinsic part of the gas generator. The squib ignites the solid propellant, which rapidly discharges. The combustion products of the solid propellant propelled the gaseous argon from the generator casing, located within the cartridge holder, into the discharge chamber. SPGG cartridges were changed and prepared for the next run in less than 4 min.

Numerical Modeling and Analysis

To better understand the fluid dynamics of the suppression event, the first publicly released version of the Fire Dynamics Simulator (FDS)[47], a computational fluid dynamics model, was used to simulate the baffle or step-stabilized flame in the TARPF facility. The sub-grid scale turbulence model was not used, but rather the coefficients of viscosity, thermal conductivity and mass diffusivity were derived from kinetic theory and empirical extrapolation.[48] Thus, the calculations directly simulated the fluid motion, but not the combustion. Both two-dimensional (higher resolution) and three-dimensional (with turbulent flame structure) simulations were performed. Details of the calculations are presented in References 33 and 44.

Presented in Figure 6–18 are sequences of images separated in time by 0.01 s that are taken from simulations that illustrate the dynamics of the suppression event. Figure 6–18a is a 3-D simulation of a flame stabilized on a 25 mm baffle that is undergoing a successful suppression. Figure 6–18b is a 2-D simulation of flow (moving left to right) over a 25 mm step. The darkness of the image reflects the extent of local heat release. In both Figures, the top images show the flame just prior to discharge of nitrogen into the air stream. Upon injection, the flame was disturbed by a large vortex generated by the pressure pulse. Due to the low Mach number approximation, the gas upstream of the step was essentially incompressible, and the velocity jump from 2.1 m/s to 5.7 m/s was conveyed to all points in the flow domain in 0.02 s, the time of the ramp-up from the base velocity to the injection velocity. Thus, even before the agent arrived at the step, the flame had already been dramatically transformed from its original state. The generation of the large vortex at the step produced a pathway by which the agent could penetrate the region just behind the step, mixing with the gases, cooling and diluting the fuel and oxygen.

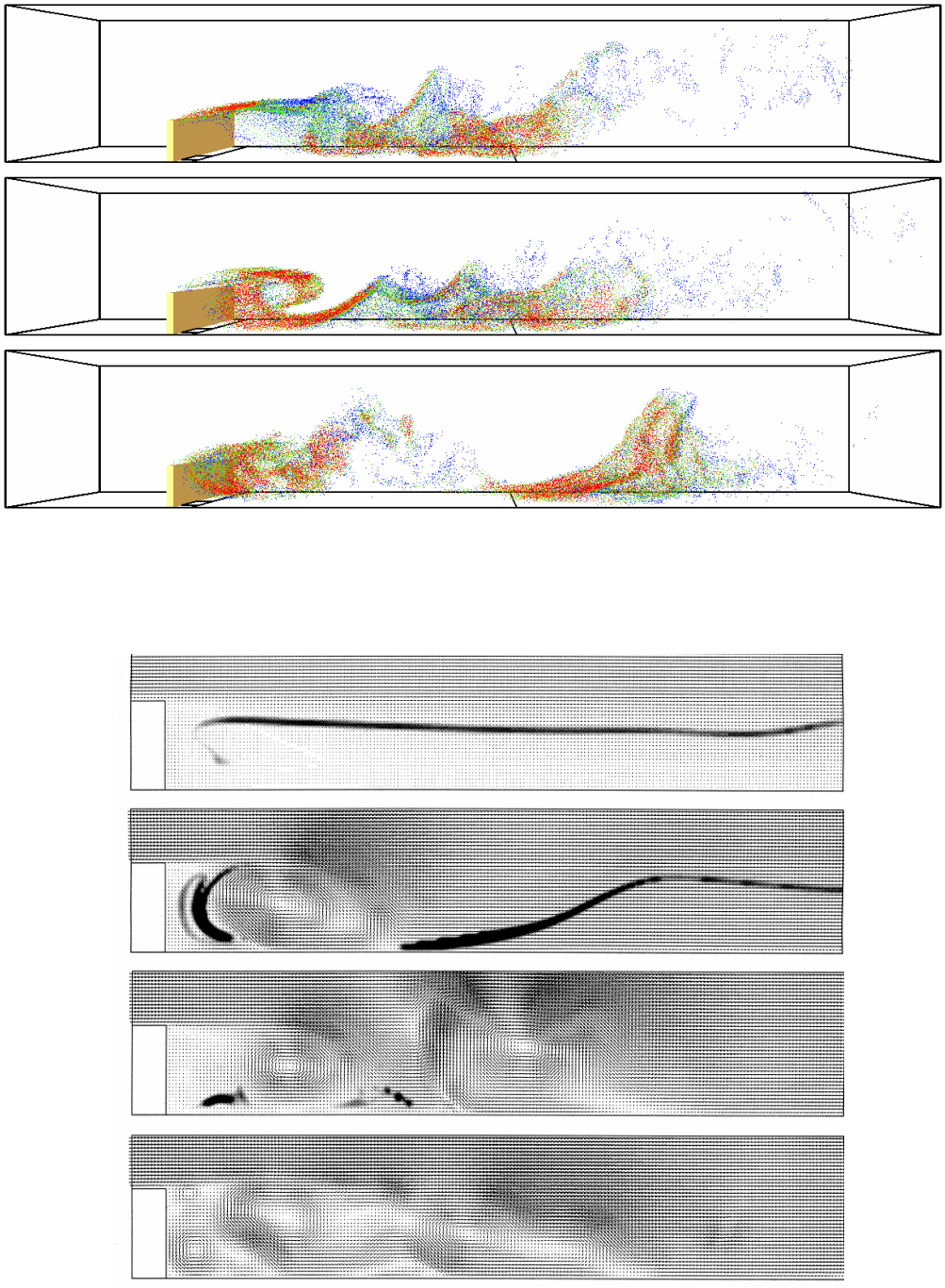

Figure 6–18. Disruption of a Stabilized Flame by the Injection of Nitrogen Upstream of 25 mm High Obstacle.
(a) 3-D Simulation of Flow over Baffle; (b) 2-D Simulation of Flow over Step.
The frames are separated by 0.01 s. [12]

Flow Characterization

The TARPF facility was operated over a range of propane and air flows to examine the flame behavior. Flame blowout, with no added fire extinguishing agent, was achieved either by increasing the air flow or decreasing the propane flow. At low air velocities, a fluctuating laminar flame was anchored on the top downstream edge of the step or baffle and extended well downstream of the porous plate. As the velocity increases, the flame became turbulent and less luminous. Near blowout, the orange color disappeared and the visible blue flame shrunk. With the backward-facing step installed, an average air velocity above the step of over 23 m/s was necessary to blow out the flame if the propane flow was greater than 33 mL/s, corresponding to a velocity of 1.9 mm/s.

Two air flows were chosen to evaluate the ability of the agents to suppress the propane pool fire stabilized by the backward-facing step:

Mean Air Velocity	Propane Flow	Regime[38]
2.1 m/s ± 0.2 m/s	33 mL/s ± 2 mL/s	Regime I (rim-stabilized flame)
5.4 m/s ± 0.2 m/s	85 mL/s ± 2 mL/s	Between Regime I and II (intermittent turbulent flame)

The velocity distribution of the air 76 mm upstream of the burner was measured with a 3 mm diameter pitot tube at seven locations across the duct. The velocity profiles were flat within 5 % over the central three-fourths of the duct. The boundary layer above the step appeared to be less than 7 mm thick. The presence of the flame tended to increase the pitot probe signal, which was likely due to a combination of preheating the air upstream by the flame, acceleration in the flow due to partial blockage of the duct caused by the expanding combustion gas, and a possible shift in electrical output due to heating of the pitot probe and transducer.

The mass of suppressant necessary to extinguish a fire in the TARPF depends upon the fuel and air flows chosen to challenge the suppressant. Figure 6–19 shows how the mass of nitrogen necessary to extinguish a 25 mm baffle-stabilized flame varied with the flow of air and fuel. The uncertainty in any given value was estimated to be ± 0.2 g. When the air speed was less than 5 m/s and the fuel flow was fixed at 45 mL/s ± 2 mL/s, decreasing the speed reduced the amount of nitrogen necessary to extinguish the flame. No flame extinction occurred between 5 m/s and 15 m/s because the mass of nitrogen necessary exceeded the maximum amount contained in the storage vessel. Above 16 m/s, the strain on the flame was sufficient at times to extinguish the flame without the need for any nitrogen. (The dashed lines are included in the figure to assist the eye in identifying the extinction boundaries.)

The propane flow had less than a 5 % effect on the mass of N_2 needed to extinguish the flame, at fixed injection interval and air flow. There was a lower limit for the propane flow (< 12 mL/s) that led to extinction due to heat loss to the burner, even with no N_2 dilution. The upper flow limit (120 mL/s) was dictated by the maximum safe operating temperature of the burner. Since the mass of N_2 needed to suppress the flame did not appear to increase, there was no need to operate the burner at higher fuel flows.

The total mass of N_2 required for suppression also depended on the injection interval. This relationship is plotted in Figure 6–20 for a 3.9 m/s ± 0.2 m/s air flow, 45 mL/s ± 2 mL/s propane flow flame stabilized on the 25 mm baffle. The total number of experiments was more than ten times the number of data points

plotted in this and the following curves; for clarity, only those conditions close to the extinction boundary are included. (For all these figures, the open circles represent the largest mass of N_2 that did not result in extinction; the filled circles are the minimum mass of agent that successfully extinguished the flames.) As the injection interval was increased from 100 ms to 500 ms, the minimum mass required increased over three-fold. The rate of mass addition (total mass/estimated injection interval) decreased with increasing injection interval, as shown in the right-hand figure.

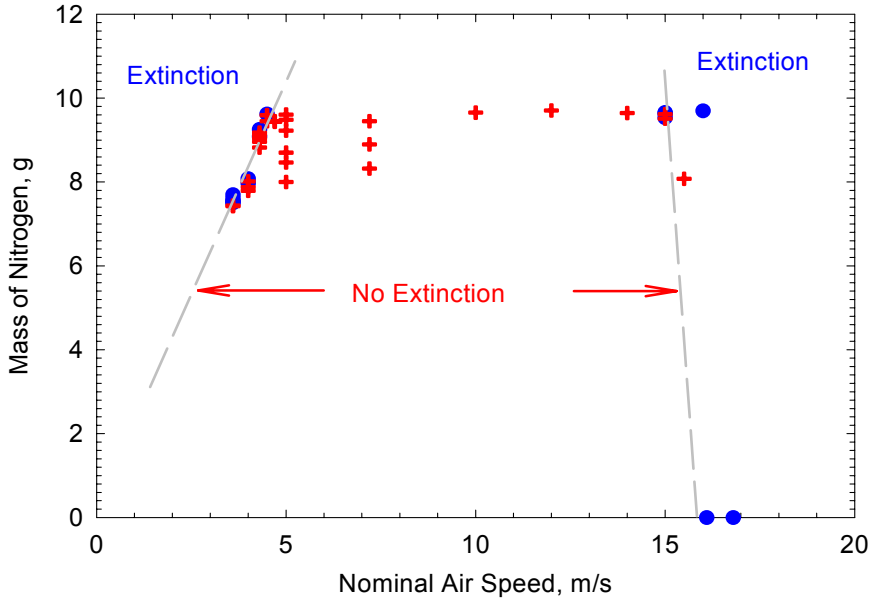

Figure 6–19. Impact of Air Speed on Extinction of a 25 mm Baffle-stabilized Flame.[44] Propane Flow: 45 mL/s; N_2 Injection Time: 312 ms. Circles: Flame Extinction; Crosses: No Extinction

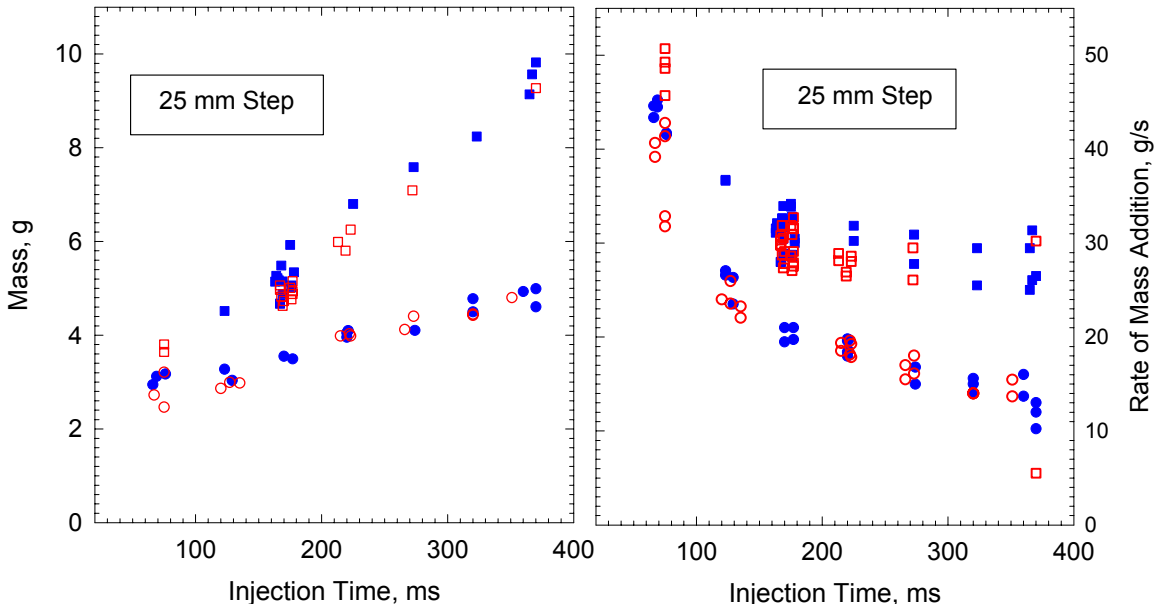

Figure 6–20. Mass and Rate of Nitrogen Addition to Extinguish a 45 mL/s Propane Flame in 3.9 m/s Air Flow.[44]

Next, there was an effect of the geometry of the obstruction on the mass of N_2 needed for flame suppression. The data plotted with squares in Figure 6–21 were taken with the ramp placed in front of the 25 mm baffle to form a backward step-stabilized flame, rather than the simple baffle-stabilized flame represented in Figure 6–20. The air flow was the same in these two cases but the propane flow was higher, 85 mL/s, in Figure 6–21. The addition of the ramp and increase in propane flow did not have much influence on the mass of N_2 required for suppression. For both the baffle and backward step, just under 6 g of N_2 are required when the injection interval is 200 ms ± 10 ms. The data plotted as circles in Figure 6–21 were taken with the nominal air speed reduced to about 1.5 m/s and the propane flow proportionately to 33 mL/s. The squares represent experiments conducted at the high air and propane flows, and circles represent experiments conducted at the lower flows. Less than 4 g ± 0.2 g of N_2 were needed to extinguish this flame if injected over a 200 ms ± 10 ms interval. The differences in rates of mass addition to suppress the high flow and low flow flames can also be seen at the right in Figure 6–21.

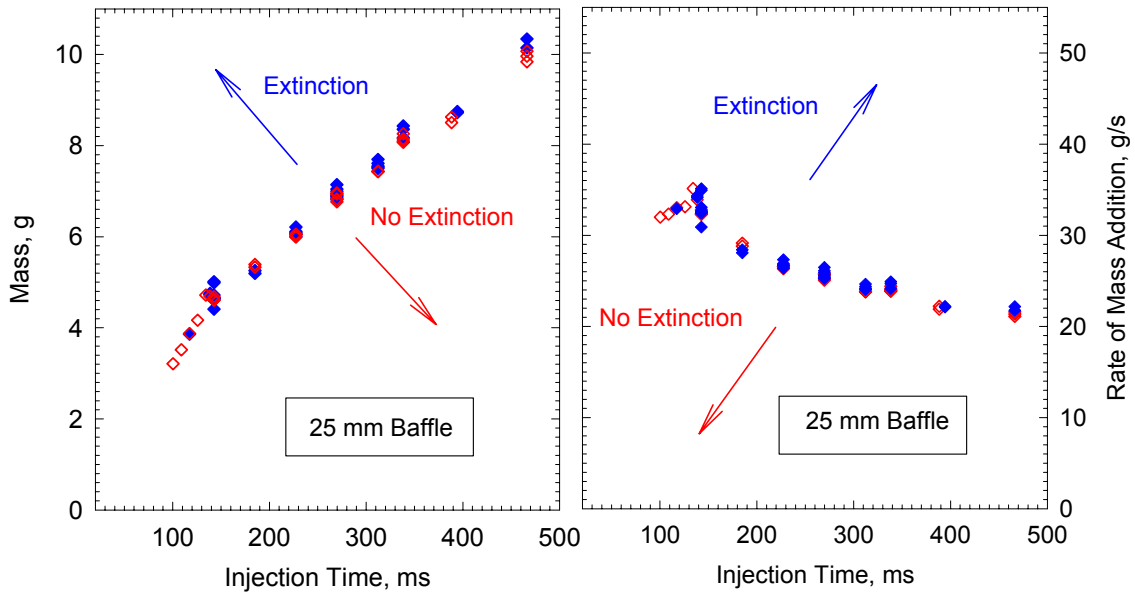

Figure 6–21. Mass and Rate of Nitrogen Addition Required to Extinguish High Flow (squares) and Low Flow (circles) Propane/Air Flames Stabilized Behind a 25 mm Step. [44]

Figure 6–22 and Figure 6–23 show what happens to the required nitrogen mass and addition rate if the baffle height is decreased to 10 mm or increased to 55 mm (blockage from 11 % to 60 %), respectively. The symbols have the same meaning as in Figure 6–21. The short baffle produced a fire which was the easiest to extinguish, and the high baffle the most difficult in terms of the amount and rate of N_2 addition.

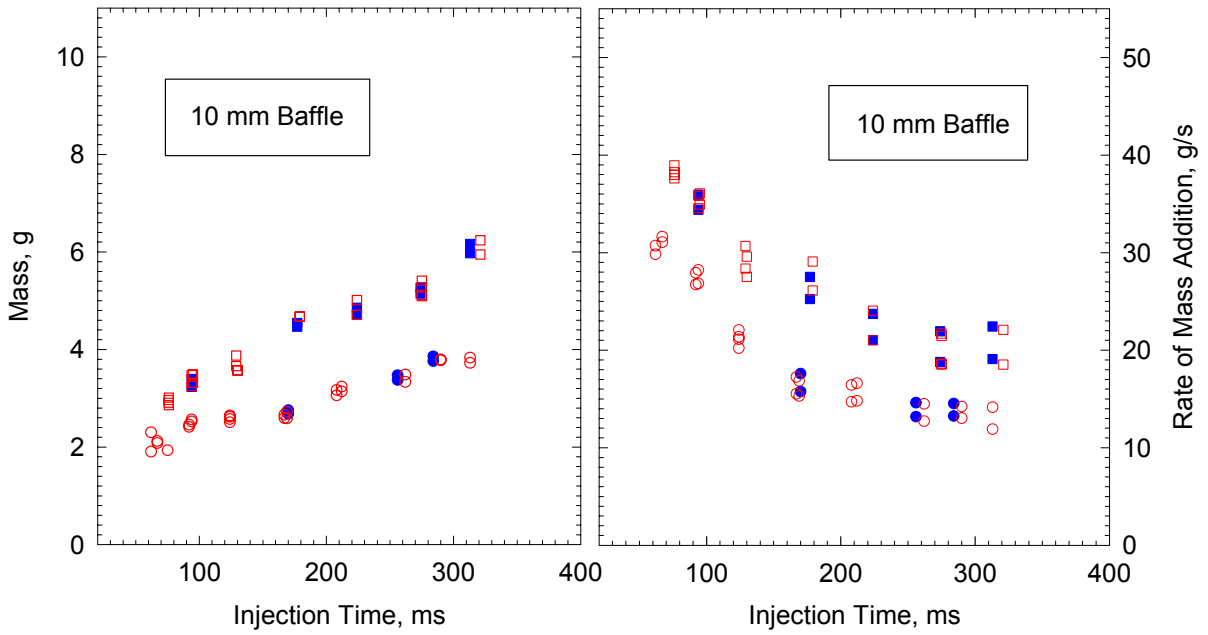

Figure 6–22. Mass and Rate of Nitrogen Addition Required to Extinguish High Flow (squares) and Low Flow (circles) Propane/Air Flames Stabilized Behind a 10 mm Baffle. [44]

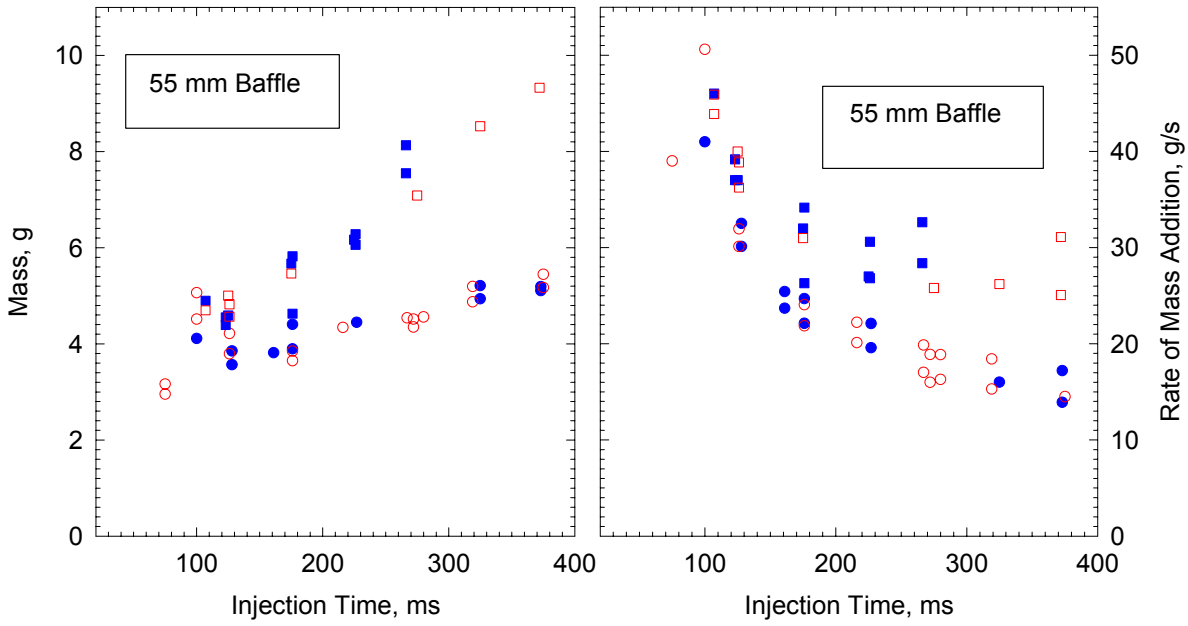

Figure 6–23. Mass and Rate of Nitrogen Addition Required to Extinguish High Flow (squares) and Low Flow (circles) Propane/Air Flames Stabilized Behind a 55 mm Baffle. [44]

The effect of baffle height was not large if the injection interval was at least 150 ms, as can be seen more clearly in Figure 6–24. (Note that 6 mm has been added to the height of each obstacle to account for the distance between the floor of the tunnel and the recessed top surface of the burner.) The bottom curve delineates the minimum amount of nitrogen for suppression when the air flow was fixed at its high value and the agent injection interval was maintained at 175 ms ± 10 ms. The open circles represent the largest mass of N_2 that did not result in extinction for flames stabilized on the different sized baffles; the filled circles are the minimum mass of agent that successfully extinguished the flames. The diamonds are the results for the 25 mm baffle with the ramp in place (backward-facing step). Experiments were also conducted with and without the reignition obstruction shown in Figure 6–12. The amount of N_2 necessary for suppression was unchanged.

The rate of mass addition is plotted in the upper curve of Figure 6–24 (the triangles are the backward-facing step, and the squares are for the baffles). The data are plotted two ways: the higher value is the rate of nitrogen addition computed during the first 50 ms that the solenoid valve is open; the lower value is the average over the entire open interval measured from the pressure trace. The estimated rate of mass addition varied substantially, especially for the 55 mm baffle, depending upon whether the averaging period was the first 50 ms or the entire time that the solenoid remains open.

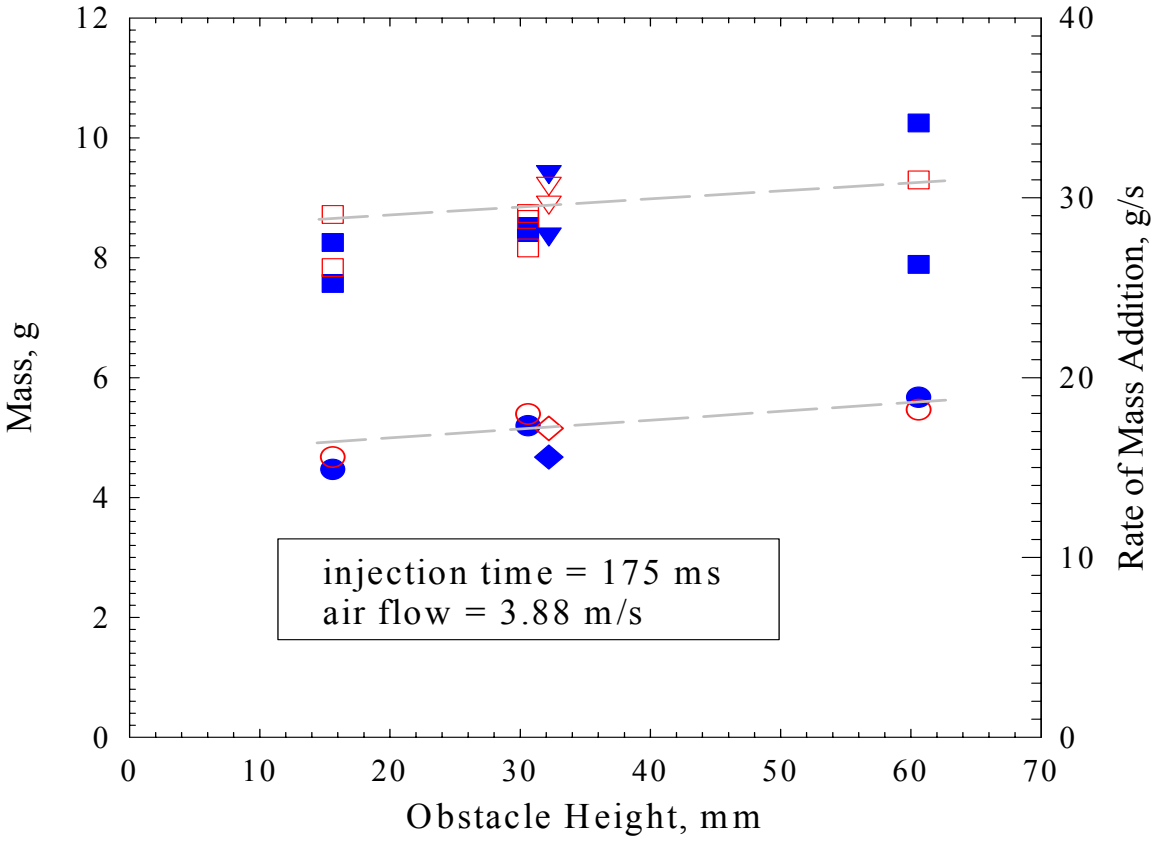

Figure 6–24. Impact of Obstacle Height on the Total Mass and Rate of Addition of Nitrogen Required to Suppress an Obstacle-stabilized Pool Fire. [44]

Effect of Type of Gaseous Suppressant

Figure 6–25 is a plot of the minimum agent volume fraction that extinguished the fires (X) as a function of the agent injection time interval (Δt) for both N_2 and CF_3Br. The parameter X is defined as the average volume flow of agent during the injection interval divided by the sum of the agent and bulk air flows.

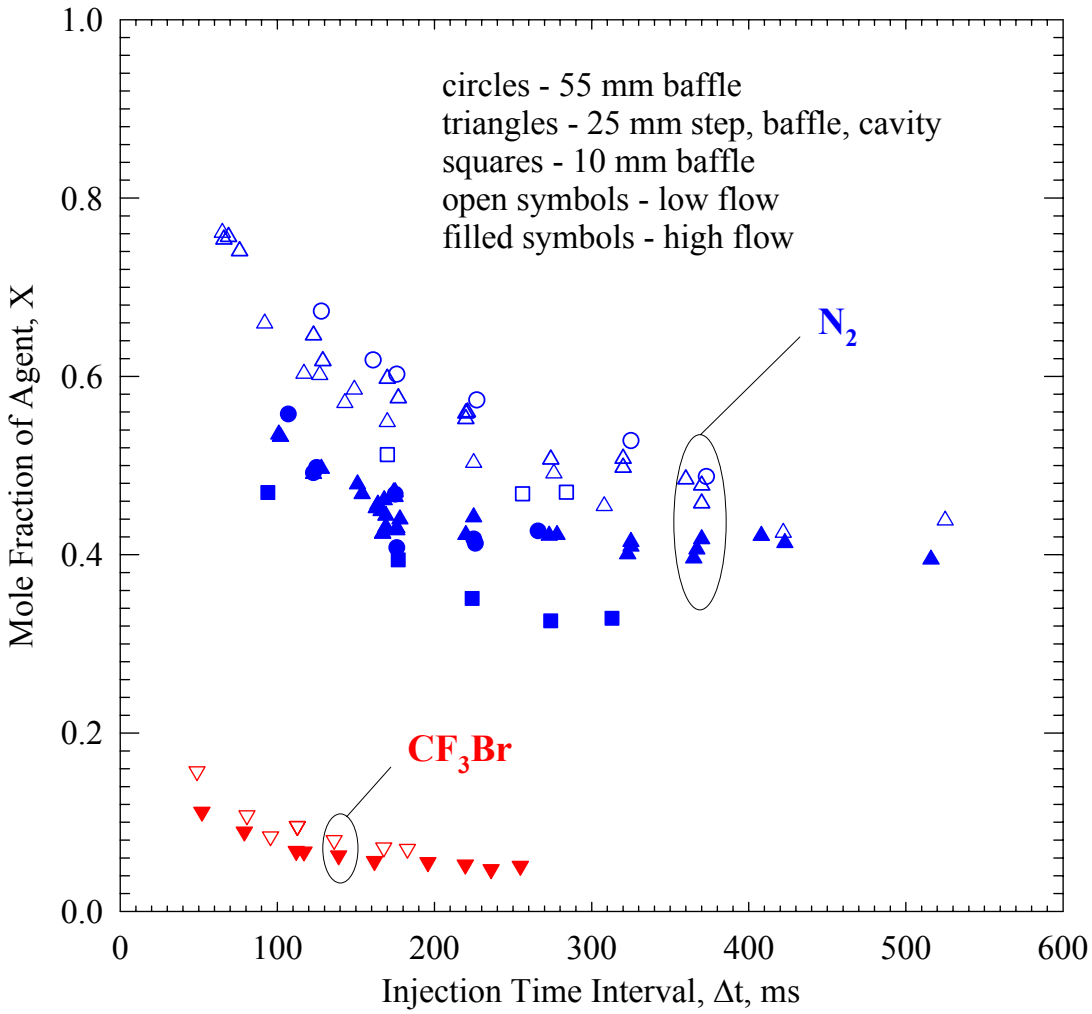

Figure 6–25. Mole Fraction of Suppressants (N_2 and CF_3Br) Added to Air at Extinction Boundary for High and Low Flow Conditions, as a Function of Injection Time Interval and Obstacle Geometry.[44]

The data represent experiments conducted over a range of conditions including air velocities that varied from 2 m/s to 9 m/s, propane flows from 33 mL/s to 85 mL/s, and baffle heights between 10 mm and 55 mm, in addition to the 25 mm backward step. The open and closed symbols represent the low and high air flow conditions, respectively. Figure 6–25 shows that X decreased with increasing injection time interval for all obstacle types and both agents. The highest volume fraction requirements were consistently for the low air flow conditions. For some experiments, the value of X was nearly 0.8 for short injection intervals. The most challenging geometric configuration was the 55 mm baffle, followed by the 25 mm obstacles, and the 10 mm baffles. There was little difference in X between the 25 mm step, 25 mm

cavity and the 25 mm baffle and those data are presented as one group in Figure 6–25. The effectiveness of CF_3Br was compared to that of N_2 using the 25 mm high backward step. The 1 L storage vessel was used to accentuate the pressure change associated with the small quantities of CF_3Br required for suppression. Only 1.6 g ± 0.2 g of CF_3Br injected for 100 ms was needed to extinguish the flame under the high air flow conditions (corresponding to $X \approx 0.075$), as compared to 3.9 g ± 0.2 g for N_2 as agent ($X \approx 0.5$) under similar conditions. These results were consistent with numerous studies that showed that CF_3Br is a more effective suppressant than N_2 for both free standing and baffle stabilized flames.

Effect of Hot Surface

Experiments were conducted to assess the importance of a nearby hot surface (Figure 6–12) on the effectiveness of a fire suppressant. An ethane-fueled torch was used to preheat the upstream surface of the obstacle to produce temperatures in excess of 1000 °C as measured on the exterior face. Pyrometer readings of the interior (i.e., fire-side) surface indicated temperatures were about 50 °C cooler. Experiments determined that hot surface temperatures close to 1000 °C were needed to ignite the propane pool when the air and propane were set to the low flow conditions.

A spray nozzle was located upstream of the stabilizing step that allowed liquid JP-8 to be sprayed over the propane pool and onto the heated inverted-vee surface. The fuel acted to cool the surface approximately 150 °C below the temperature that had been obtained when only the gaseous propane fuel was flowing. The JP-8 was ignited and formed a flame that stabilized behind the vee when the temperature of the surface exceeded 900 °C.

To test for re-ignition of the propane fire, the propane fire was initiated under the operating conditions of an air flow velocity of 1.5 m/s and a propane flow of 33 mL/s, and the obstruction was heated to the temperature desired. The flame was observed to extend past the obstruction. The agent (N_2, HFC-125, or CF_3Br) was introduced to the system for three different injection times of 75 ms, 100 ms, and 150 ms, and the occurrence of flame suppression was observed. (The agent injection time was varied to observe its effect on re-ignition of the propane fuel.) The agent storage cylinder pressure was increased if suppression did not occur, and the process repeated. In order to determine the efficacy of the JP-8 stream in the re-ignition process, experiments were conducted with the JP-8 stream directed against the heated obstruction while the unignited propane was still flowing into the wind tunnel. If re-ignition did not occur after 10 s, then the propane flow was terminated. A variety of re-ignition results were observed which depended on the injection time interval of the agent and JP-8 stream. Re-ignition was found to occur when the obstruction was above 900 °C (bright red), and was affected by the cooling provided by the agent and JP-8 liquid stream.

The influence of the surface temperature was found to be bi-modal: when the temperature of the hot surface (with the JP-8 and propane flowing) was below about 880 °C ± 10 °C, the amount of agent necessary for suppression was the same as when the surface was unheated; and when the temperature was above 890 °C ± 10 °C, reignition always occurred within about 10 s independent of higher temperatures or the amount of N_2 added. A similar finding resulted when nitrogen was replaced by CF_3Br, although the measured dividing temperature was about 50 °C higher. This difference may have been associated with a build-up of carbon on the hot surface that insulated the fire-side surface from the ethane torch, making an accurate determination of the surface temperature more difficult.

A few experiments were conducted with the temperature reduced to the Leidenfrost point (290 °C for JP-8) to determine if an increase in contact time would compensate for the lower temperature. Ignition of the JP-8 and propane did not occur. Satcunanathan and Zaczek[49] measured the ignition delay of kerosene and diesel fuels on a hot metal surface and found that ignition could occur in less than 1 s for a 2 mm diameter droplet, but that the ignition time increased for temperatures between about 500 °C and 550 °C due to surface boiling. No ignition of the JP-8 droplets was observed in the TARPF when the vee-surface temperature was maintained in the range between 360 °C and 440 °C. However, Jomaas et al.[50] found that ignition of a JP-8 pool fire occurred in their step-stabilized burner for temperatures in the same range.

SPGG Results

For the SPGG experiments, the nominal velocity of the air above the backward-facing step was maintained constant at 5.4 m/s; the propane flow was 85 mL/s (at standard temperature and pressure). The high pressures (typically 1000 kPa to 3000 kPa) produced in the SPGG discharge chamber and the known area of the metering orifice allowed the mass flow of agent added to the air stream of the TARPF to be estimated by assuming that the flow through the orifice is choked. Five replicate tests produced virtually indistinguishable mass flow and thermocouple temperature traces.

The SPGG discharge time was consistently 20 ms ± 1 ms, which is over three times faster than the shortest N_2 or CF_3Br injection interval, and was not much affected by the bypass port area. The bypass ratio (A_{in}/A_{tot}) is the area of the inlet metering orifice (port 2) divided by the total open area available for flow to exit the discharge chamber (ports 2, 3, and 4) The time interval, Δt, is shown in Figure 6–26 as a function of the estimated discharge mass. The total mass delivered to the air stream during the discharge process was found by integrating dm/dt over Δt. Excluding the highest and lowest area ratios, the estimated mass delivered can be seen in Figure 6–26 to be linearly proportional to the area ratio; however, almost 50 % more mass was estimated than one would expect. The dashed line in Figure 6–26 indicates that a 1-to-1 relation would exist if the mass were directly proportional to the area ratio.

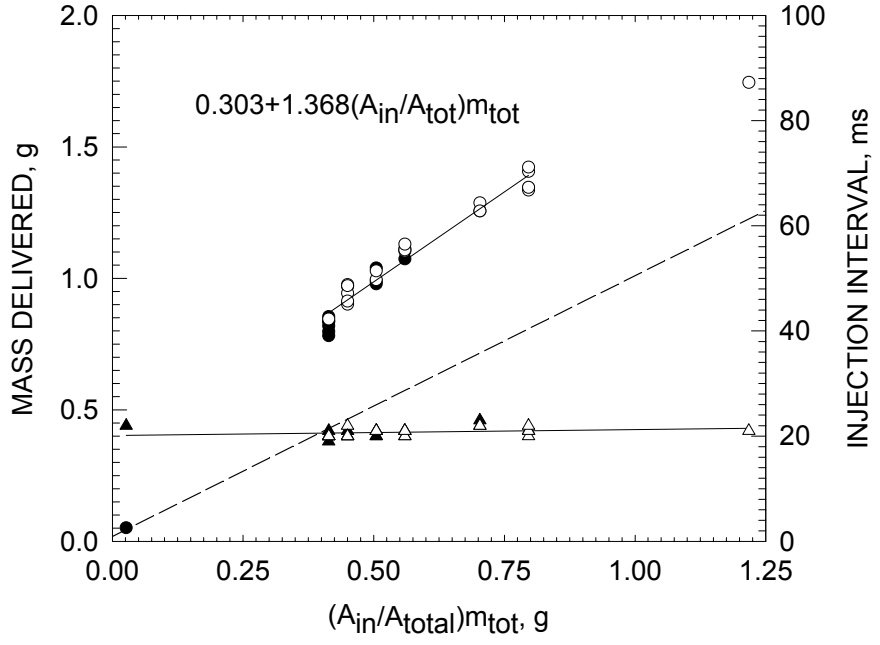

Figure 6–26. Injection interval (triangles) and Calculated Mass Delivered to Flame (circles) as a Function of Area Ratio Times Total Mass of Gas Generated (20.7 g).[44]

There are several factors that contributed to an uncertainty in the estimate of the deployed mass of agent. First, uncertainties in the gas composition and temperature upstream of the metering orifice affected the estimate since the mass was proportional to the square root of the molecular weight divided by the temperature. A factor of two underestimate in this parameter would cause a 40 % over-estimate in mass, which, if corrected for, would cause the data plotted in Figure 6–26 to more closely align with the dotted line. A second source of uncertainty was the complexity of the flow within the discharge chamber created by the jet emanating from the SPGG. The calculation assumed that the upstream flow was steady and parallel to the axis of the metering orifice, but the flow was highly transient and more perpendicular.

Suppression of the propane pool fire with the hybrid gas generators occurred when at least 1.5 g of agent was injected into the fire; conversely, extinction never occurred when less than 0.7 g was added. The % of the fires suppressed varied when the agent mass was between these limits, as shown in Figure 6–27. The suppression statistics were generated by lumping the mass from thirty-three discharges into bins 0.2 g wide, centered about the data plotted. The solid line is a fit to the data assuming that the shape is sigmoidal. It is apparent from the curve that there was a 50 % chance that suppression would be successful if the amount of agent were 0.9 g ± 0.1 g, and there was a 90 % success rate for 1.3 g ± 0.1 g of agent.

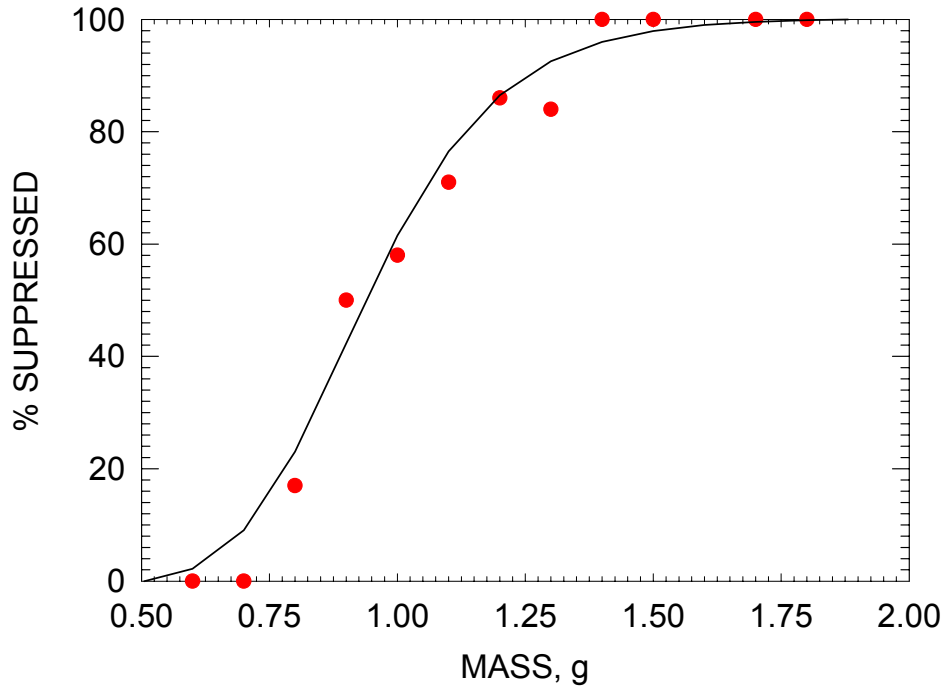

Figure 6–27. Percentage of Flames Extinguished as a Function of Mass Delivered to Flame by an SPGG. [44]

Figure 6–28 is a plot of the mass of agent required for suppression versus the injection time interval. All of the SPGG data are lumped around 20 ms since the injection time was fixed. Linear fits to the nitrogen and halon 1301 data yielded intercepts of 1.6 g for nitrogen and 1.2 g for halon 1301. The SPGG data fall close to the halon results. The significance of the linear shape and the value of the intercept was unclear; however, the superior performance of the gas generator was undeniable.

The mass fraction of agent, β, is defined as the total mass injected divided by the injection duration, Δt, over the sum of the mass flow of air plus the mass flow of agent. The percentage of occasions that the flame was extinguished is plotted in Figure 6–29 as a function of β.

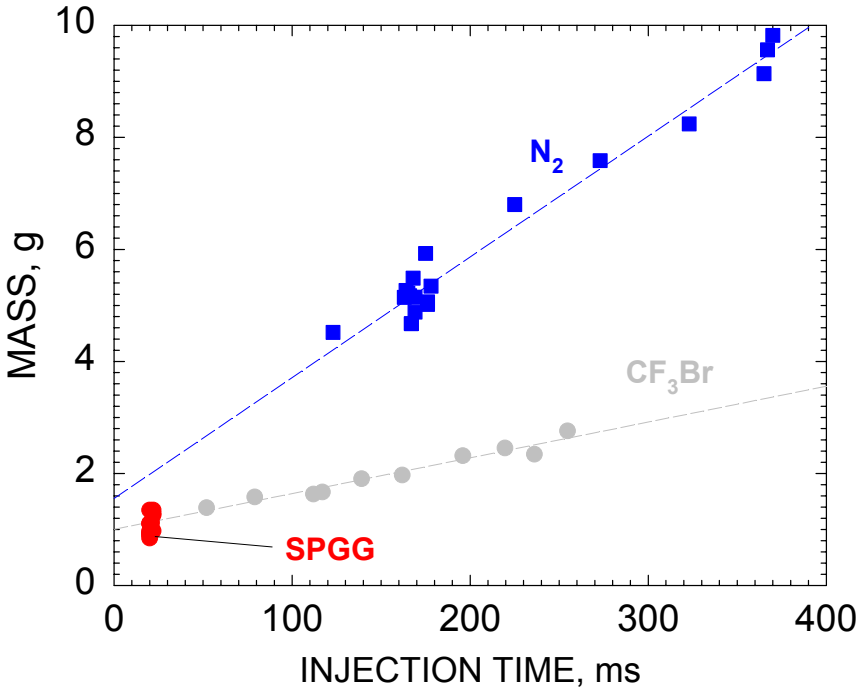

Figure 6–28. Impact of Injection Time Interval on the Mass of Agent Required to Suppress a Step-stabilized Propane Pool Fire. [44]

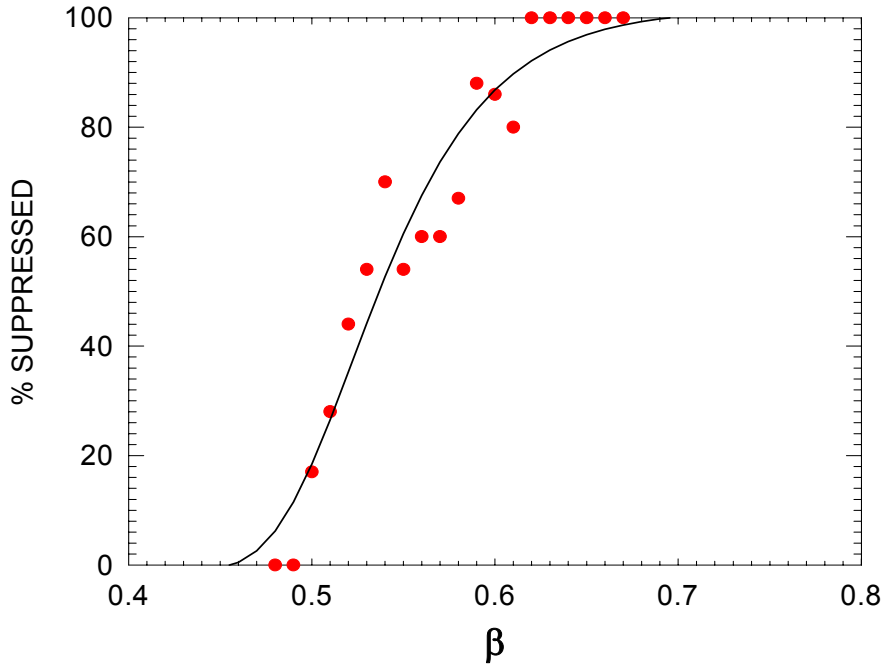

Figure 6–29. Percentage of Flames Extinguished as a Function of Estimated Mass Fraction of Agent. [44]

All of the fires were extinguished when β was greater than 0.62; none for a mass fraction below 0.49. The definition of β for the SPGG differs somewhat from the definition as applied to the gaseous agents because the mass discharge profiles for SPGG and the gaseous agents were different. Whereas the mass

injection rate of the gaseous agents was controllable through selection of the injection hardware, the SPGG mass injection rate was practically dependent on the propellant effluent generation rate (i.e., the propellant burning rate). For the same mass, variation of the discharge profile led to variation in agent effectiveness. Optimization of the rate of agent discharge is an area that would benefit from further study, which could be approached from analytic, numerical, and experimental perspectives.

Data Correlation

The effectiveness of the gaseous agents was compared to that of the SPGG through use of a simple agent mixing model to describe the suppression phenomena. A more detailed description of the model can be found in Grosshandler et al.[51] and Hamins et al. [37] A characteristic time, τ, for mixing of the agent into the flame zone was defined in terms of the air and agent volume flows, ($V'_{air}+ V'_{agent}$), and the step height, h, as

$$\tau = \gamma h /\{(V'_{air}+ V'_{agent})/[(L-h)L]\} \quad (6\text{-}2)$$

where L is the width of the tunnel and γ is an empirical non-dimensional parameter that relates the ratio of the distance that a fluid element travels within the recirculation zone to the obstacle height. Takahashi et al. [38] measured the characteristic mixing time in a similar facility and found γ to be around 40. Evaluating Equation 6-2 for the range of flows and baffle heights examined in the current study and using a value of 40 for γ, τ was found to vary between 0.04 s and 0.40 s.

Hamins et al. [37] found that for a specified injection duration it is possible to relate the volume fraction of agent required to achieve extinction, X, to the characteristic mixing time, τ, according to the following relation:

$$X/X^* = [1-\exp(-\Delta t/\tau)]^{-1} \quad (6\text{-}3)$$

where X^* can be found experimentally by flowing agent continuously into the air stream at increasing rates until extinction occurs. If the air flow is low enough, the value of X^* is expected to be similar to the cup burner extinction requirements. For propane in a cup burner, Trees et al.[52] found the value of X^* to be 0.32 for N_2, 0.41 for Ar, and 0.039 for CF_3Br. Others have found similar results.[53]

Figure 6−30 compares the suppression results for N_2, CF_3Br, and SPGG through use of Equation 6-3, where the normalized volume fraction is plotted as a function of the non-dimensional injection interval. For the SPGG results, X^* is assumed to equal the X^* value for argon. While the data do not fall exactly on the model, the trend of the results are well represented by the single curve when one considers run-to-run variations due to the statistics associated with suppression of a turbulent flame. The results show that the effectiveness of the SPGG hybrid significantly exceeds the model predictions.

For laminar diffusion flames strained at intermediate rates, Trees et al. [52] showed that the minimum extinction volume fraction of agent in a counterflow flame decreases from the cup burner value when the strain rate is 50 s^{-1} to much smaller values for a strain rate of 400 s^{-1}. Although the flow in the recirculating region behind a step is much more complicated than in a counterflow flame, the strain rate in the current study should scale with $1/\tau$. When the flow of air is increased sufficiently, the flame becomes strained to the point that agent is not needed for extinguishment and the flame blows out. In other words,

as the air flow in the TARPF increases, the model represented by Equation 6-3 in Figure 6–30 must be adjusted not only for changes in τ, but also for changes in the value of X^*.

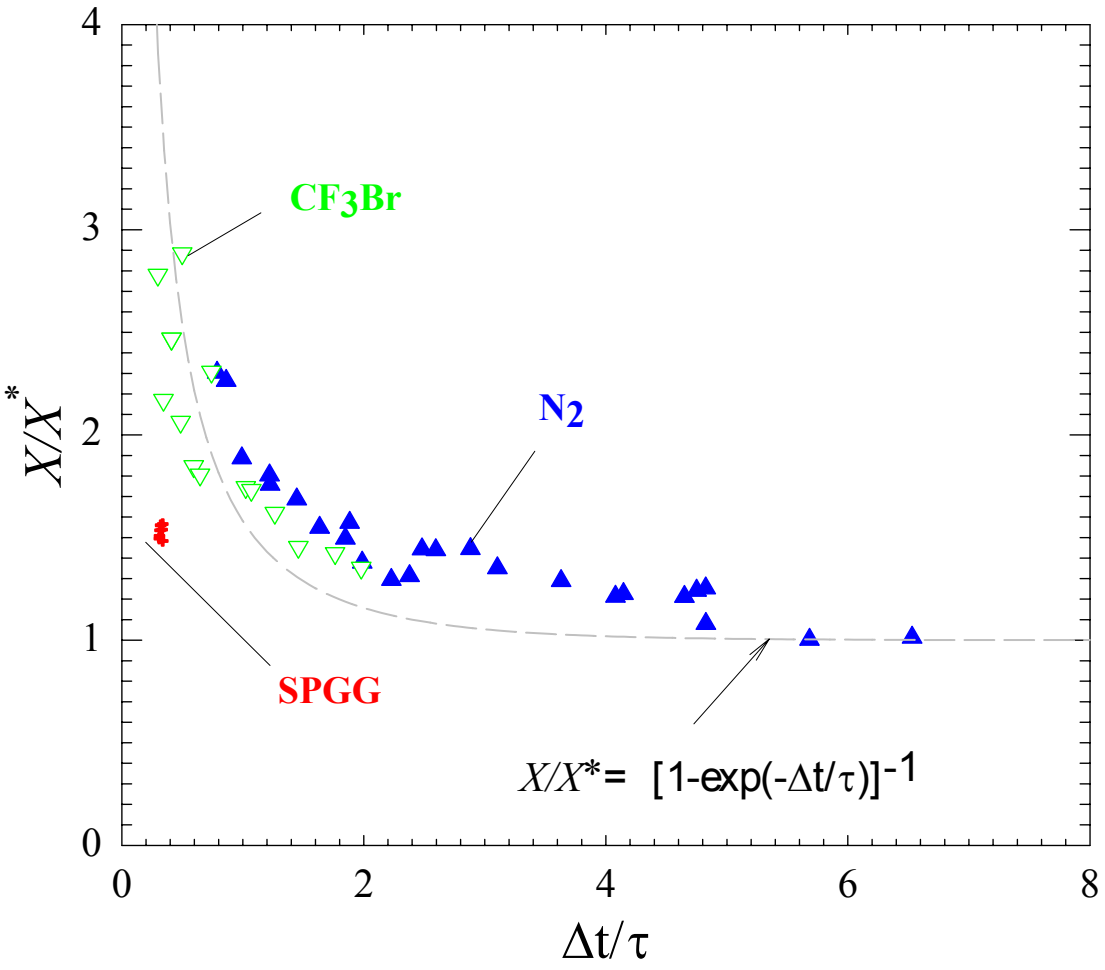

Figure 6–30. Normalized Volume Fraction as a Function of Non-dimensional Injection Interval, Comparing N_2, CF_3Br, and SPGG. [44]

A number of direct numerical simulations of N_2 suppressing the step-stabilized flame were conducted assuming a finite reaction rate with one step chemistry. The injection interval and volume fraction of nitrogen were varied, and the flame structure was followed through the transient period. Either the flame was extinguished, or it was reestablished following the passage of the N_2 pulse. Figure 6–31 summarizes the results. Open diamonds indicate that no suppression occurred; solid diamonds imply that suppression was successful. The gray symbols refer to the experimental N_2 and CF_3Br data for all geometries examined. The dotted line is from Equation 6-3.

The computations were able to distinguish regimes of extinction and non-extinction in the case of nitrogen as an agent. The numerical model could not predict what would happen when a chemically active agent like CF_3Br is introduced into the flame. The cooling and dilution of the flame by the agent

could be predicted, and hopefully, simplified combustion mechanisms for various chemically-active agents can be developed that will lead to a better understanding of the dynamics of fire suppression.

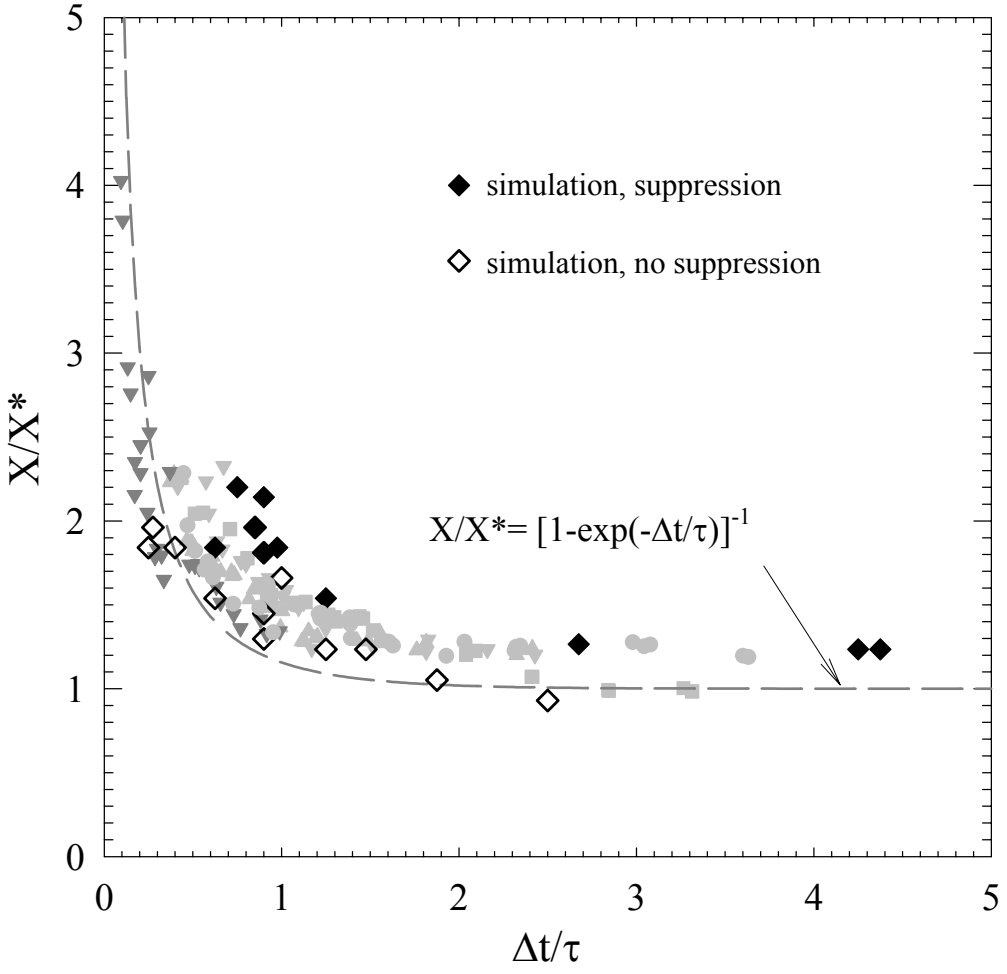

Figure 6–31. Suppression Volume Fraction of Agent (N_2 or CF_3Br) Normalized by Cup Burner Values (X*) as a Function of Injection Time Interval Normalized by Characteristic Residence Time (τ). Gray symbols: experimental results keyed to Figure 6–25; black diamonds: direct numerical simulations with N_2. [44]

Important Findings

- The minimum volume fraction of agent for suppression, normalized by the cup burner value, correlated with $[1 - \exp(-\Delta t/\tau)]^{-1}$, where Δt is the injection time interval and τ characterizes the mixing time behind the obstacle in the flow.
- The general character of the flame and its extinction by a thermal gaseous agent was captured by a direct numerical simulation of the flow based upon single-step chemistry, and numerical experiments have corroborated the simple correlation of the experimental data for N_2.

- The measured difference between the decrease in agent storage bottle pressure and the arrival of the agent at the fire highlighted the importance of determining the agent concentration locally and the difficulty in relating changes in bottle pressure to actual mixing conditions.
- For the first time, both compressed and solid-propellant generated gases could be compared side by side, and the effect on performance of different formulations, particle loadings and burning rates for various SPGG designs could be unambiguously discriminated.
- When the temperature of a hot surface downstream of the pool was above 800 °C, the flame, following suppression, reignited and stabilized on the hot surface. At a temperature below 800 °C, the number of reignitions approached zero. This result was in contrast to when the hot surface was located between the stabilizing step and the fuel pool, in which a delayed reignition was observed at temperatures as low as 400 °C.

6.4.5 Summation

Because of the expected diversity of physical and chemical properties of candidate fire suppressants, the NGP developed three apparatus for screening fire suppression efficiency. The cup burner was the workhorse for examination of the chemicals, as discussed further in Chapter 7. The DLAFSS was available for assessing those chemicals with high boiling points and high heats of vaporization. The TARPF was available for appraising those chemicals and delivery systems for which it was expected that burst delivery would significant modify the interpretation of data obtained using the cup burner.

6.5 ATMOSPHERIC LIFETIME SCREEN

6.5.1 Factors Affecting Atmospheric Harm

The NGP screening protocol had its roots in the 1990 development of screening procedures for ozone depletion potential (ODP)[v] and global warming potential (GWP).[vi, 1] It was updated and refined as the result of a 1997 NGP workshop[2] and constraints on the agent chemistry resulting from the other properties being screened.

A comprehensive discussion of atmospheric chemistry and the effects of pollutants can be found in reference [54]. The principles that determined the NGP screening protocol were:

- Both ODP and GWP are directly related to the lifetime of a test substance in the atmosphere. The greater the persistence of a chemical, particularly within the troposphere, the greater the potential for adverse effects on the global environment. It was assumed that other, as yet undetermined effects would also be directly related to atmospheric lifetime.
- The tropospheric lifetime of a chemical is determined by the rates of physical and chemical removal processes. The most important of these are the reactivity with respect to OH radicals and absorption of solar radiation in the VIS-UV region of the solar spectrum. For each such process, it must be established that the products are rapidly removed from the atmosphere, e.g., by rainout. In general, OH reactions are important if there are abstractable H atoms

[v] The ozone depletion potential of a gas is defined as the change in total ozone per unit mass emission of the gas, relative to the change in total ozone per unit emission of CFC-11 ($CFCl_3$).

[vi] The global warming potential of a gas is defined as the change in irradiance at the tropopause (the boundary between the stratosphere and the troposphere) per mass of the gas emitted relative to the change in irradiance per mass of carbon dioxide.

available or if the test compound has unsaturated C-C bonds (aromatic or aliphatic). Fully halogenated alkanes are unreactive with respect to OH radicals. The mechanism whereby most CFCs and halons are destroyed in the atmosphere is by absorption of solar radiation in the 170 nm to 300 nm region. For a replacement chemical, photolysis in the troposphere could also be important if the chemical absorbs solar radiation in the VIS-UV part of the spectrum. For example, photolysis efficiently removes organic iodine compounds within the troposphere. Other removal processes, including physical removal (*i.e.*, rainout, aerosol scavenging and solvation) are significantly slower. Methods for estimating lifetimes due to these physical processes are discussed in Reference 55.

- Ozone depletion potential is also directly related to the numbers and kinds of certain atoms in a compound's chemical formula. If a test substance does not contain chlorine, bromine, iodine, or nitrogen, the current knowledge of stratospheric chemistry indicates that the ozone depletion potential is zero. Each of these four atoms can have a deleterious effect on stratospheric ozone, and many molecules containing them will have a positive ODP value. The calculation of ODP requires the use of an atmospheric model with a complete input of chemistry, solar irradiation, and transport. Comparison of the results of various models, ranging from the most elaborate three dimensional models to the much simpler one dimensional models, indicates that in the case of the halocarbons, simple models give results adequate for use in developing screening tests.[56] Halon 1301 has an estimated ODP value of about 13.
- Global warming potential is directly related to the capability of a test compound to absorb radiation in the region of the "atmospheric window" between 7 μm and 13 μm. Test compounds which are weak absorbers in this region are unimportant with regard to global warming.

6.5.2 Prior Estimation Methods

Stratospheric Ozone Depletion

Skaggs and Nimitz[57] proposed a method for estimating ODP values for halocarbons of containing one or two carbon atoms and no bromine atoms. The method related the ODP to two factors: a reactivity factor, related to the number of chlorine atoms in the molecule, and a survival factor, i.e., the fraction of molecules reaching the stratosphere. The relationship is shown in Equation 6-4.

$$\text{ODP} = c_1 n^{c_2} e^{-(c_3/t)} \tag{6-4}$$

where:

n is the number of chlorine atoms

t is the atmospheric lifetime

n^{c_2} is the reactivity factor

c_2, and c_3 are parameters to be fit

$e^{-(c_3/t)}$ is the survival factor

c_1 is a normalizing constant

This equation gave values that were relatively close to the rigorously calculated ODPs used in fitting the parameters. Since the rigorously calculated ODP values and atmospheric lifetimes used in the parameter fitting have changed since the equation was originally proposed, the reported parameters are not given here.

Iikubo and Robin[58] extended this formulation to include estimation of ODP values for bromine-containing compounds.

$$ODP = A\ E\ P\ [(\#Cl)^B + C(\#Br)]\ D^{(\#C-1)} \qquad (6\text{-}5)$$

Here, P is the photolysis factor, which was set equal to 1.0 if there were no special structural features that made the molecule subject to tropospheric photolysis. Otherwise, P = 0.180 for a bromine geminal to a chlorine (e.g., Br-C-Cl), P = 0.015 for geminal bromine atoms (Br-C-Br), or P = 0.370 for vicinal bromine atoms (Br-C-C-Br). The fitting parameter values were: A = 0.446, B = 0.740, C = 32.000, and D = 1.120. The hydrogen factor, E, was set equal to 1.000 if there were no hydrogen atoms; otherwise it was set equal to 0.0625. #C, #Br, and #Cl are the numbers of carbon, bromine, and chlorine atoms, respectively.

Use of Equation 6-5 gave, at best, rough approximations, even if the equation was restricted to simple saturated halocarbons (Table 6–2). The trends, however, were preserved. It may be that a better fit of parameters could be obtained with a larger set of more recent data as a basis.

Table 6–2. Estimated and Reported ODP Values (Relative to CFC-11) for Selected Halocarbons.

Compound	Formula	Calculated ODP	Reported ODP	Reference
Halon 1301	$CBrF_3$	14.3	12	59
Halon 1211	$CBrClF_2$	2.6	5.1	59
Halon 2402	$CBrF_2CBrF_2$	17.4	6.6	60
HBFC-22B1	$CHBrF_2$	0.89	0.74	61
HBC-30B2	CH_2Br_2	0.03	0.17	62
HBC-40B1	CH_3Br	0.89	0.64	59
HCFC-123	$CHCl_2CF_3$	0.050	0.014	59

Atmospheric Lifetime

To a great extent, values of ODP and GWP are determined by the tropospheric lifetimes of the compounds. Regardless of the chemical, the ODP and GWP values will be negligible if tropospheric removal is efficient. Tropospheric removal reactions can be either bimolecular or unimolecular. Bimolecular reactions involve reaction with atmospheric species such as hydroxyl free radicals (•OH), tropospheric ozone (O_3), oxygen atoms (•O in ^3P, ^1D electronic states), etc. Unimolecular reactions include photolysis, thermal dissociation, and heterogeneous absorption (aqueous or particulate aerosols).

The rate of disappearance of a species, *C*, due to a bimolecular reaction with an atmospheric species A can be expressed as shown in Equation 6-6, where [*C*] and [*A*] are the concentrations of species *C* and *A*,

and k_2 is a second-order reaction rate constant. Similarly, the rate of removal through unimolecular reactions is expressed by a first-order differential equation with the first-order reaction rate constant k_1 as shown in Equation 6-7. Typical units for k_2 and k_1 are, respectively, cm^3/molec-s and s^{-1}, with concentrations in molec/cm^3. The rate constants k_1 and k_2 are constant only under a given set of conditions. For example, for photolysis, k_1 depends on the radiation flux and wavelength; for reaction with atmospheric particulate, k_1 depends on the concentration (and composition and other characteristics) of the particulate.

$$\frac{d[C]}{dt} = -k_2[C][A] \tag{6-6}$$

$$\frac{d[C]}{dt} = -k_1[C] \tag{6-7}$$

Careful consideration shows that all reactions can actually be considered "bimolecular" in form since the concentration of particulate, for example, is incorporated into k_1 for particulate removal, and the "concentration" (actually, the flux) of photons is incorporated into k_1 for photolysis.

The concentration of a species undergoing reaction, as shown in Equation 6-6 or Equation 6-7, decays exponentially as given by Equation 6-8. Here $[C]_o$ is the initial concentration, $[C]_t$ is the concentration at any time t, and $t_{1/e}$ is the "e-folding" atmospheric lifetime, i.e., the time required for the concentration of an atmospheric species to decay to 1/e (approximately 0.369) of its initial value. The e-folding lifetime is related to the reaction rate constant by or depending on whether the reaction is bimolecular (Equation 6-9) or unimolecular (Equation 6-10).

$$[C]_t = [C]_o e^{t/t_{1/e}} \tag{6-8}$$

$$t_{1/e} = 1/k_2[A] \tag{6-9}$$

$$t_{1/e} = 1/k_1 \tag{6-10}$$

Using these equations, one can estimate the atmospheric lifetime due to various removal processes by using globally averaged values for concentrations of reactant species.

A globally averaged tropospheric hydroxyl free radical concentration of 9.7×10^5 molecules/cm^3 and a globally averaged tropospheric ozone concentration of 5.0×10^{11} molecules/cm^3 have been used for such estimations.[63,64] In the global averaging approximation, one uses reaction rate constants for a mean tropospheric temperature. Values around 298 K are often used[65] and were used in the NGP estimations.

In the global average approximation, atmospheric lifetime is directly proportional to the second-order rate constant (k_{OH}) for reaction with •OH, when this is the primary tropospheric removal process. Thus, an alternative way to estimate the atmospheric lifetime for a compound *B* removed only by reaction with •OH was to use Equation 6-11 to relate the lifetime of *B* ($t^B_{1/e}$) to that ($t^C_{1/e}$) of a reference compound *C*.[66] Here, k^B_{OH} and k^C_{OH} are the second-order hydroxyl reaction rate constants for the two materials. Methyl chloroform (CH_3CCl_3) is usually the reference compound. This method is equivalent to using the globally averaged •OH concentration when this concentration has been determined from measurements of

atmospheric removal of methyl chloroform, as in the case of the value used in this report. [63] Note that with the appropriate rate constants, one could use an equation similar to Equation 6-11 when a removal mechanism other than reaction with a hydroxyl free radical predominates, as long as the removal mechanism for the compound of interest (B) is the same as that for the reference compound (C).

$$t_{1/e}^{B} = t_{1/e}^{C}(k_{OH}^{C} / k_{OH}^{B}) \tag{6-11}$$

Attempts to use Quantitative Structure-activity Relationships (QSARs) to predict k_{OH} values have not been highly successful.[67] A procedure based on the C-H bond energy (and, thus, related to the activation energy for hydrogen atom abstraction by •OH) gave disappointing fits to rigorously calculated atmospheric lifetimes, though re-parameterization with more recent data might help. [57] Since many of the compounds of interest as halon replacements contain fluorine atoms, there was one trend of interest. Examination of rate constants for a variety of fluorinated compounds indicated that fluorine substitution activated hydrogen atoms on the same carbon atom toward •OH abstraction, but deactivated hydrogen atoms on carbon atoms immediately adjacent. The reaction of •OH with CH_3CH_2F, for example, proceeds primarily (85 %) with hydrogen atom abstraction from the CH_2F group.[68]

Better results may be available through quantum mechanical calculations. There was strong evidence that k_{OH} values vary linearly with the calculated values for the highest occupied molecular orbital in hydrofluorocarbons.[69]

6.5.3 The Screening Protocol

Estimation of the atmospheric impact of candidate fire suppressant considered several properties. The following is the sequence that was typically followed:

- A small molecule that did not contain chlorine, bromine, iodine, or nitrogen was generally "passed."
- For a larger molecule or one that contained one or more of the four atoms, but contained a feature that bespoke a high rate of reactivity in the troposphere (see below), its reaction rate with OH was estimated. The potential of the molecule to absorb VIS-UV radiation was also estimated.
- The reaction rate was measured for a molecule that fared well in the prior step and in the screens for fire suppression effectiveness and volatility.

The following sections relate the methods to be used in such appraisals.

6.5.4 Removal by Hydroxyl Radical Reaction

Hydroxyl radicals can transform and remove trace atmospheric substances from the troposphere by abstracting hydrogen atoms or by addition/displacement reactions at unsaturated sites in the molecule. The reaction of any substance, X, with OH can be written as

$$X + OH \rightarrow PRODUCTS \tag{6-12}$$

and the rate of one of these reactions is given by:

$$\frac{-d(X)}{dt} = k_{OH}(OH)(X), \quad (6\text{-}13)$$

where k_{OH} is the rate constant for reaction, (X) the concentration of species X, and (OH) is the average tropospheric OH concentration. Since (OH) is essentially constant (concentration independent of the presence of the trace substance X in the atmosphere), the expression can be written as:

$$\frac{-d(X)}{(X)} = k_{OH}(OH)(dt) \quad (6\text{-}14)$$

or:

$$ln\left(\frac{X_O}{X_t}\right) = k_{OH}(OH)\,t, \quad (6\text{-}15)$$

where X_0 is the concentration at some zero of time, and X_t the concentration at time t. The time for the concentration to decay from X_0 to X_t is thus given by:

$$t = \frac{\ln\left(\frac{X_O}{X_t}\right)}{k_{OH}(OH)}. \quad (6\text{-}16)$$

The atmospheric half-life (where X_0/X_t has been set equal to 2.718, the base of natural logarithms), or atmospheric lifetime, can be defined as:

$$t = \frac{\ln(2.718)}{k_{OH}(OH)} \text{ or } t = \frac{1}{k_{OH}(OH)}. \quad (6\text{-}17)$$

Using an average atmospheric hydroxyl radical concentration of 10^6 molec cm^{-3} [70], the tropospheric lifetime becomes:

$$t_{OH}(trop) = \frac{3 \times 10^{-14}}{k_{OH}}, \quad (6\text{-}18)$$

where the units of t_{OH}(trop) are years (1 year = 3 x 10^7 s) and of k_{OH} are cm^3 $molec^{-1}$ s^{-1}. For the identification of compounds with tropospheric lifetimes of the order of a month or less, desirable values of k_{OH} are 3 x 10^{-13} cm^3 $molec^{-1}$ s^{-1} or higher.

Values of k_{OH} may be determined by direct laboratory measurement of the rate constant of reaction, or may be estimated using structure-activity relationships. The latter is preferred for screening those compounds for which appropriate data are available, since the measurements are quite labor intensive and the calculation is faster and less expensive and uses none of the compound.

Experimental Measurement of OH Rate Constants

The method of choice for this determination was the flash-photolysis resonance fluorescence technique.[71,72,73] It is a precise, reliable, and commonly used method for the measurement of OH rate constants over the range of rate constants of about 10^{-14} to 10^{-9} cm^3 $molec^{-1}$ s^{-1}. This method measures the loss of OH under conditions of excess test compound and yields an absolute measurement of the OH rate constant. It is mandatory that the sample of the test compound be free of impurities that are significantly more reactive than the test substrate, e.g., unsaturated compounds or compounds with many easily abstracted hydrogen atoms. The method requires the participation of senior scientific staff. A schematic of a typical apparatus is shown in Figure 6–32.

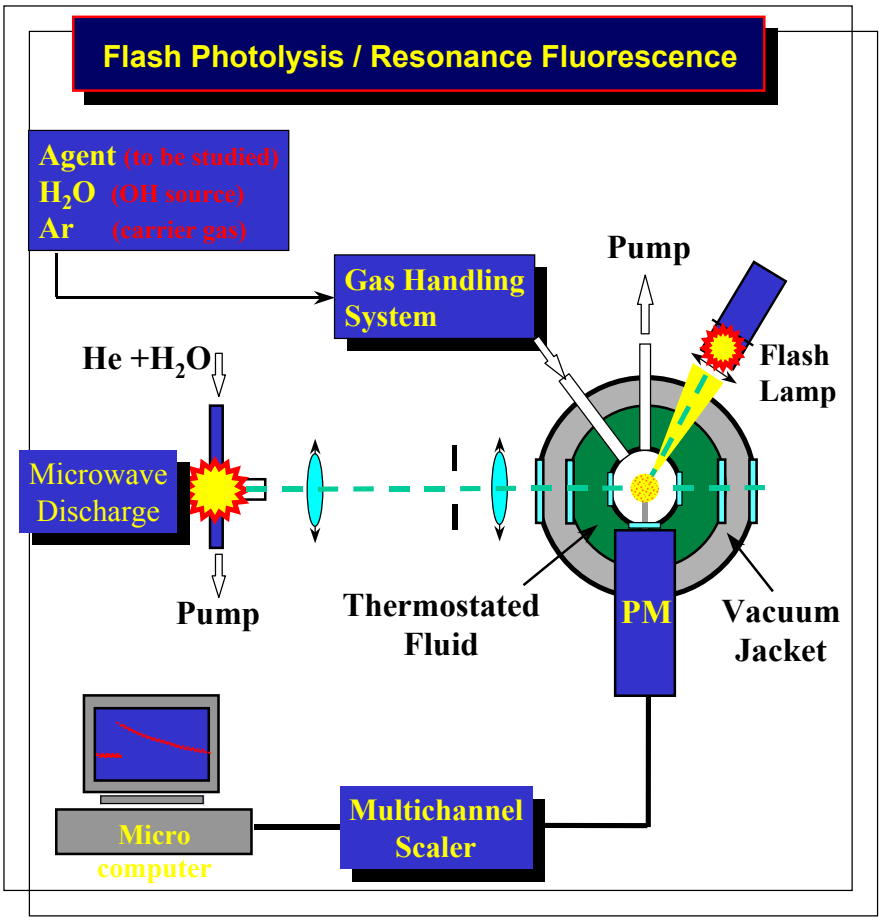

Figure 6–32. Schematic of Flash Photolysis Resonance Fluorescence Apparatus for Measuring Reactivity of Compound with OH Radicals. [2]

The apparatus consisted of a stainless steel or glass cell surrounded by an outer wall between which fluid was circulated to a temperature regulator to maintain a fixed temperature, measured by means of a thermocouple. The cell had four window ports at 90° positions around the cell, and one additional window port on the base of the cell. The entire cell was mounted within a vacuum housing. Gases were admitted to the cell through inlets connected to a gas handling system. A hydroxyl radical resonance lamp, consisting of a microwave powered discharge in 130 Pa of a mixture of He saturated with water vapor, and a pulsed N_2 discharge flash lamp, which was powered by discharge capacitors and a power supply, were located at right angles to each other and to a photomultiplier detector.

Hydroxyl radicals were produced by the flash photolysis of H_2O. The OH radical resonance lamp was used in cw mode to excite a small fraction of the hydroxyl radicals which then emitted resonance radiation at 308 nm which was detected by the photomultiplier. The signal output was then fed to pulse counting electronics, and ultimately to a computer for signal averaging and subsequent statistical analysis and graphical display. The measurement process was initiated by a photomultiplier (PM) which was triggered by the visible light from the flash lamp. A delay gate introduced a delay time of 100 μs to 300 μs to eliminate any scattered light interference from the flash lamp. Fluorescence signal from 50 to 500 flashes were typically averaged to generate a suitable decay curve.

In a typical experiment, reaction mixtures containing the test compound, argon, and water vapor (prepared manometrically in a 5 L bulb before admission to the reaction cell) were flowed slowly (at about 100 $cm^3\ s^{-1}$) through the cell. The quantity measured in this test was the rate of loss of OH radicals in the presence of a great excess of the test compound. Under these conditions, the rate expression can be written as:

$$\frac{-d(OH)}{dt} = k(OH)(S), \tag{6-19}$$

where OH is the concentration of OH radicals, S is the concentration of the test substance, k is the rate constant, and t is the reaction time. Under conditions where (OH) << (S), S is essentially constant, and the OH decay is first order, and the rate expression becomes:

$$\frac{-d(OH)}{(OH)} = k(S)\,dt = k'\,dt, \tag{6-20}$$

where k', the apparent first-order rate constant, is obtained directly from a measurement of the exponential rate of decay of OH. The true rate constant is then:

$$k = \frac{k'}{(S)}. \tag{6-21}$$

However, since there are OH diffusional losses from the reaction zone, in practice the first order decay was measured as a function of the concentration of the test compound, and from a plot of first order rate constant against concentration, the second order rate constant was obtained from the slope.

Tests for impurity effects must be included as part of the screening protocol. The effect of reactive impurities on test results can be illustrated by considering a test compound which has a rate constant for reaction with OH radicals of about 1 x 10^{-15} cm^3 $molec^{-1}$ s^{-1}, corresponding to an atmospheric lifetime of 30 years. If the test sample contained a 1 % impurity in the form of an alkene, which typically may have a rate constant for reaction with OH of about 1 x 10^{-12} cm^3 $molec^{-1}$ s^{-1}, then the apparent OH rate constant would be about 1 x 10^{-14} cm^3 $molec^{-1}$ s^{-1}, corresponding to a lifetime of 3 years. Purity was thus of great importance in carrying out these tests, and it was desirable for the test compounds to have impurity levels for alkenes and other unsaturated compounds of less than about 0.1 %. If the purity was not known, then the following test procedure was followed:

- Measure the rate constant.

- If $k < 3 \times 10^{-15}$ cm^3 molec^{-1} s^{-1}, the test results were acceptable.
- If $k > 3 \times 10^{-15}$ cm^3 molec^{-1} s^{-1}, check the test sample for impurities. This was done initially by carrying out a trap-to-trap distillation and then remeasuring the rate constant. If the rate constant decreased, the sample was impure, and an analysis was necessary. Only after analysis and, if necessary, purification, were additional measurements be undertaken.

6.5.5 Measurement of Photolysis Rates

Photolysis is the process whereby a molecule is chemically transformed following the absorption of light. For photolysis to be important in the troposphere, the molecule must be able to absorb photons in the VIS-UV region of the solar spectrum (between about 290 nm and 700 nm), and the resultant energy-rich molecule must be chemically transformed rather than being physically quenched back to the original state. The rate of photolysis depends upon the flux of solar photons in the VIS-UV region, the absorption cross section of the substance over the same region, and the quantum yield for dissociation as a function of wavelength. The rate of photolysis is:

$$-\frac{dX}{dt} = k_p(X) = f\sigma\phi(X), \tag{6-22}$$

where f is the flux of solar photons in cm^{-2} s^{-1}, σ is the cross section in cm^2, ϕ is the quantum yield for dissociation, k_p is the effective first order rate constant in s^{-1}, and (X) is the concentration of substance X in molec cm^{-3}. Thus:

$$k_p = f\sigma\phi. \tag{6-23}$$

The rate constant must actually be determined as the integral of this quantity over the whole range of atmospherically-accessible solar radiation. The process is considerably simplified by carrying out the calculation for discrete intervals of the solar spectrum of interest and summing to obtain the total rate constant. Other factors including solar zenith angle, season, latitude, altitude, and surface albedo also enter into the calculation.

The lifetime with respect to photolysis is defined as,

$$t_p(trop) = \frac{1}{k_p}, \tag{6-24}$$

or, numerically,

$$t_p(trop) = 3 \times 10^{-8} k_p^{-1} \tag{6-25}$$

where the units of t_p(trop) are years and the units of k_p are s^{-1}.

To determine k_p, it is necessary to know the atmospheric flux of solar photons and their wavelength distribution, the absorption cross section of the compound over the same spectral range, and the quantum yield for dissociation, also as a function of wavelength. The first quantity is tabulated and available.[54] The second quantity is readily measured in the laboratory. The third quantity, however, is not easily

obtained. For the purpose of developing a screening test, the quantum yield was conservatively taken to be unity at all wavelengths, and the screening test was based on measurement of the absorption cross section.

Then,

$$k_p \leq f\sigma \text{ and } t_p(trop) \geq k_p^{-1}. \tag{6-26}$$

and since f is a tabulated quantity, the test measurement involved measurement of the absorption cross section in the VIS-UV region of the spectrum.

The measurement can be undertaken using a variety of spectrometer configurations. Design options include single pass or multipass for the absorption train, and also single beam or double beam for the detection system. Double beam instruments consist of true double beam configurations employing two identical monochrometers and two detection systems, virtual double beam configurations employing a beam splitter at the exit of the monochrometer followed by two detection systems, and broad-band referencing, where the wavelength dispersed signal is referenced to the non-dispersed incident light source. Any of these experimental configurations are acceptable. Of particular relevance are the measurements of Molina and coworkers[74], using a double-beam instrument to measure absorption cross sections for several brominated methanes and ethanes, and those of Gillotay and coworkers[75] who measured absorption cross sections for some bromine-containing compounds using both multiple reflection and single pass single-beam instruments.

The choice of instrument is dictated by the requirement that it be able to measure absorption cross sections as low as 10 cm^2 to 24 cm^2. Absorption cross section is defined in terms of the fractional absorption of light passing through a defined path length of a given concentration of absorber.

One can define a figure of merit for the measurement system based on the quantity σpP (the optical depth), where σ is the absorption cross section (wavelength dependent), p the pressure (or concentration) of the test compound, and P the path length. Highest precision cross section measurements are made with an optical depth of about one (30 % to 40 % absorption). For weak absorbers, σpP will be much smaller. In addition, for a fixed path length, absorption depends on the pressure (or concentration) of the test substance in the optical path. Under nominal conditions of "room" temperature (298 K), absorption may be limited by the available vapor pressure of the test substance.

To measure the cross section for a weak absorber requires high pressure, and/or long path length, and/or high accuracy in measuring very small amounts of absorption. For screening purposes, the accuracy or reproducibility of the measurements should be about 25 %, and this should define the smallest possible value of σpP suitable for making the measurements.

The measurement method described here was based on the use of a single beam monochrometer.[76] The absorption cross section is defined as:

$$\sigma(\lambda) = \left(\frac{1}{c} ln\left(\frac{I_\lambda}{I_O} \right) \right), \tag{6-27}$$

where σ_λ is the cross section at a given wavelength, (c) the concentration of absorbing test substance in molec cm^{-3}, ℓ the path length in cm, I_λ the intensity of light passing through the cell containing the absorber, and I_0 the intensity of light passing through the empty cell, both in arbitrary units. The test measurement thus involved measuring and taking the ratio of the quantities I_λ and I_0.

A schematic of a suitable apparatus is shown in Figure 6–33**.**

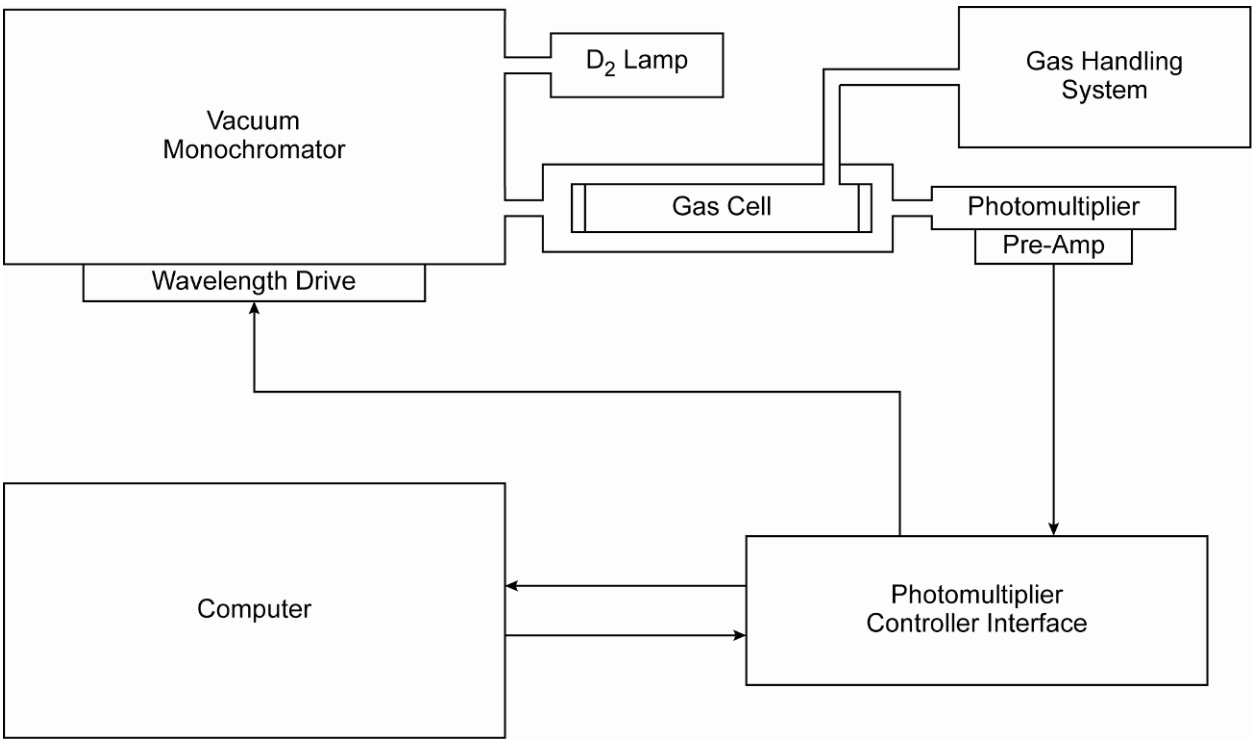

Figure 6–33. Apparatus for Measuring the Absorption Cross Section of Candidate Fire Suppressants. [1]

The apparatus consisted of a 1 m incidence McPherson vacuum monochrometer employing a 600 lines/mm grating blazed at 150 nm. The lamp shown in the figure was a Hamamatsu deuterium lamp with a highly stabilized power supply. This provided a convenient source of radiation over the 290 nm to 400 nm range. For measurements further into the red region of the spectrum, a tungsten lamp was used. The detector was a Hamamatsu solar blind side-on multiplier tube. Five absorption cells having a range of path lengths ranging from 0.2 cm to 20 cm were chosen by use of the turret assembly. The monochrometer wavelength drive was controlled by a stepping motor with 800 steps per revolution. The gear train used was such that 16 pulses were equivalent to 0.1 nm wavelength change. Gas pressure in the cell was monitored with a diaphragm type gauge.

The signal from the photomultiplier tube, which was observed in real time during a measurement, was processed and fed to a controller interface module which was part of an IBM compatible personal

computer system. A spectrum was first measured with no gas in the cell, then with an appropriate amount of gas in the cell, and finally with the cell again empty. The deuterium lamp was very stable, and this procedure led to a very reliable measurement of the adsorption cross section down to about 10^{-23} cm^2.

The procedure was to measure the absorption cross section from 290 nm to 700 nm using the definition of absorption cross section given above. The absorption cross section as a function of wavelength was then related to photolysis rate constant using procedures outlined by Finlayson-Pitts and Pitts. [54]

The experimentally measured absorption cross section was averaged over discrete wavelength intervals. Over the same intervals, Table A7 in Reference 1 provided values of the solar flux, corresponding to a cloudless day, zenith angle of 0°, surface albedo zero, uncorrected for latitude or season. For each discrete spectral region the rate of absorption was calculated as the product of columns 2 and 3 or that table, and the result entered into column 4. The summation of column 4 then gave the total rate of absorption. This was an upper limit to the number of photons absorbed. Following Molina and coworkers[74], it was recommended that the maximum rate of absorption be divided by 3 to provide a more realistic estimate of the average atmospheric absorption rate. This absorption rate constant was an upper limit to the true rate constant for photolysis:

$$k_p \leq k_a . \tag{6-28}$$

The problem of test sample purity was of concern here as well as with respect to OH reactivity. Low levels of a strongly absorbing impurity will give an incorrect set of cross section results. Therefore, when the purity was not known, the following test procedure was followed:

- Measure the absorption cross section as a function of wavelength, and calculate k_p.
- If $k_p < 3 \times 10^{-9}$ s^{-1}, the test results were acceptable.
- If $k_p > 3 \times 10^{-9}$ s^{-1}, check the test sample for impurities by carrying out a trap-to-trap distillation and then re-measuring the absorption cross section. If the absorption cross section changed significantly, the sample was impure, and an analysis was necessary. Only after analysis and if necessary, purification, were additional measurements undertaken.

The test value derived for lifetime with respect to photolysis provided only a lower limit to the true lifetime, and if the quantum yield were low, the test compound could have a much longer lifetime.

6.5.6 Estimation of Reactivity

The estimation method was based on an analysis of the structure of the molecule and its breakdown into component structural sub-units. The reactivity was expressed in terms of (a) abstraction of H atoms, (b) addition at double or triple C-C bonds, and (c) addition to aromatic structures. The total rate constant was obtained by summing the contributions of the different groups. In some cases, the reactivity and hence lifetimes of certain classes of compounds were estimated without going through a detailed estimation calculation or making laboratory measurements. For instance, the completely halogenated (with F, Cl, Br, or I) alkanes are essentially inert with respect to reaction with OH radicals. On the other hand, reactions of OH radicals at unsaturated sites (aliphatic or aromatic in character) are always very much faster than abstraction[77], and therefore, unsaturated substances have short atmospheric lifetimes. Thus, the estimation methods were presented only with reference to saturated compounds containing at least one abstractable hydrogen atom.

The reactions of OH radicals have been the most studied of all classes of gas-phase reactions, and, as a result, there was a very large body of reliable kinetic data. Atkinson[78] used this database to develop a group method for estimating OH radical rate constants for hydrogen atom abstraction. He also provided a basis for estimating rate constants for attack at double and triple C-C bonds, and attack at unsaturated aromatic sites. Examination of his database showed that the rate constants for the latter classes of reactions were all very fast compared to those for abstraction reactions.

The basis for the Atkinson method was the separation of the molecule into defined structural units. The rate constants for $-CH_3$, $-CH_2-$, and >CH- groups are dependent on the nature of the substituents alpha and beta to the group. In general, rate constants for the groups can be written as:

$$k(CH_3 - X) = k_{p'} F(X),$$
$$k(Y - CH_2 - X) = k_{s'} F(X) F(Y),$$
$$k(X - CH(Z) - Y) = k_{t'} F(X) F(Y) F(Z), \text{ and}$$
$$k(X - OH) = k_{OH} F(X),$$

where $k_{p'}$, $k_{s'}$, $k_{t'}$, and $k_{OH'}$ refer to the rate constant for abstraction from nominal primary, secondary, tertiary, and hydroxyl groups, respectively, and the factors F(X), F(Y), and F(Z) are correction factors to account for the effects of substituent groups. Using values for group rate constants and correction factors tabulated by Atkinson, rate constants for test compounds were derived.

Nimitz and Skaggs also estimated ODP values and atmospheric lifetimes of one- and two-carbon hydrofluorocarbons and hydrochlorofluorocarbons on the basis of quantitative structure activity relationships.[79] Their values were based on estimates of the OH reactivity with the hydrogen atoms(s). They were able to predict the results one- and two-dimensional atmospheric calculations within about a factor of two for compounds with atmospheric lifetimes under 30 years.

However, experimental studies had demonstrated that the reactivity of the hydroxyl radical with many, more complex types of halogenated organic compounds was not adequately correlated by simple structure-activity relationships. In particular, when an ether linkage was introduced, even the relative order of reactivity among the various ethers could not be predicted correctly.[80] This implied that it would be necessary to measure rate constants for a large number of members of any new class of reactants. A better method of screening candidate molecules was clearly needed.

Under the NGP, Huie and coworkers developed a refined method to predict atmospheric lifetimes for new classes of halogenated compounds.[81,82,83] At the heart of the method was a computational scheme for OH reaction rate constants for those compounds for which hydrogen abstraction would be expected to be the dominant reaction mechanism. They established accuracy of this approach utilizing a set of compounds for which reliable experimental data were available. Combining calculations with new measurements of ultraviolet absorption spectra, they then estimated atmospheric lifetimes of a set of bromine-containing compounds for which no data had been reported.

At the core of the method was the establishment of a level of theory that would predict the reactivity of the hydroxyl radical with a series of simple molecules, seeking the lowest possible degree of computational difficulty. This level would then be applied to more complex molecules and, ultimately,

applied to the new families of candidate fire suppressants. The results would be validated by a limited number of experimental determinations, but extensive experimentation and synthesis could be avoided.

In the initial study, several levels of theory were explored for the reaction of OH with CH_2Br_2. [81] This molecule was chosen both because of the importance of bromine as a fire suppressant and because the relatively large electron system of the molecule made this reaction a serious test of the various levels of theory. This study included the treatment of tunneling, making use of three different methods of approximating this correction. A low level of *ab initio* structure calculations was found to be more than adequate for screening purposes. Building on the results of this study, the reactions of OH with the other halogen-substituted methanes, up to bromine, were also calculated[82, 83] and compared with experimental results where available. Huie and coworkers also performed measurements on some bromopropanes[84] and bromofluoroalkenes.[85] Table 6–3 summarizes the results of these calculations and measurements.

Table 6–3. Atmospheric Lifetimes (years), from Theory and from OH Reactivity Measurements, for Selected Molecules.

	Atmospheric Lifetime (theory)	Atmospheric Lifetime (from meas.)	Theory/Meas.
CH_2Br_2	0.1	0.25	0.5
CH_3F	6.4	2.9	2.2
CH_3Cl	1.5	1.5	1.0
CH_3Br	2.5	2.0	1.3
CH_2F_2	3.6	5.6	0.6
CH_2FCl	1.7	1.4	1.2
CH_2Cl_2	0.43	0.46	0.9
CH_2ClBr	0.54	0.49	1.1
CH_2Br_2	0.57	0.42	1.4
CHF_3	400	263	1.5
CHF_2Cl	13.2	12.7	1.0
CHF_2Br	6.0	5.6	1.1
$CHFCl_2$	1.2	2.1	0.6
$CHCl_3$	0.15	0.51	0.3
CH_2FBr	1.9	Unknown	
$CHFBr_2$	0.49	Unknown	
$CHFClBr$	0.73	Unknown	
$CHCl_2Br$	0.16	Unknown	
$CHClBr_2$	0.12	Unknown	
$CH_2BrCH_2CH_3$		14 days	
$CH_3CHBrCH_3$		19 days	
$CF_2=CF_2$		1.1 days	
$CFBr=CF_2$		1.4 days	
$CHBr=CF_2$		2.4 days	
$CH_2=CBr-CF_3$		2.8 days	
$CH_2=CBr-CF_2-CF_3$		3.2 days	
$CH_2=CH-CF_2-CF_2Br$		7.0 days	

In summary, the calculated rate constants for the reaction of OH with halomethanes were in good agreement with their experimental counterparts, establishing the viability of *ab initio* calculations as the basis of a screening tool. Calculations for the reactions of OH with several fluoroethanes and the ethers derived from them have reproduced the experimental trends, with predictions in absolute reactivity within a factor of three. Calculations are being extended to ethers with several carbons and containing fluorine along with one or more bromine atoms.

6.5.7 Solution of Fluoroalkylamines

Fluorinated alkylamines were considered as possible alternate fire suppressants. In this case, a possible atmospheric loss mechanism was solution into atmospheric droplets and subsequent rainout. To investigate the likelihood of this process, Huie and coworkers calculated Henry's Law constants (K_h) for a series of fluoroalkylamines, using the SM5.42 solvation model at the PM3 level of theory. Based on comparisons of the results of calculations for similar alkylamines with experiment, they estimated that these results were valid to within a factor of three. Based on these results, rainout is likely not to be a very effective removal mechanism for the more highly fluorinated species.

6.5.8 Reactivity of Alkyl Phosphates towards Radicals in Water

Some suggested fire suppressants are not volatile but their environmental fate is still of concern. Alkyl phosphates are a class of chemicals that have been extensively investigated as fire suppression agents. They have very low volatility and are unlikely to be degraded in the atmosphere. They are, however, soluble in water and their environmental fate is likely to involve reactions in this medium. As part of this project, Huie and coworkers measured the rate constants for their reactions with the radicals important in aqueous phase degradation processes: the carbonate radical, CO_3^-, and the dichloride radical, Cl_2^-. The reactivity towards the sulfate radical, SO_4^-, was also measured for comparison. The procedure used was pulse radiolysis, in which a high-energy electron pulse is utilized to generate the radicals, whose temporal history is monitored by the use of optical absorption. The results of this study are presented in Table 6–4 (in units of L mol^{1} s^{1}).

Table 6–4. Reactions of Phosphates.

Compound	SO_4^-	Cl_2^-	CO_3^-
Triethyl phosphate	$1.6. \times 10^6$	$< 7 \times 10^4$	$< 1 \times 10^4$
Diethyl Phosphate	8.7×10^6		$< 1 \times 10^4$
Trimethyl Phosphate	1.3×10^5	$< 4 \times 10^4$	$< 3 \times 10^3$
Dimethyl Phosphate	7×10^4		

Although the sulfate radical reacted at a measurable rate with all the compounds, only upper limits could be obtained for the reactions of the two other radicals. The results indicated that both hydrogen abstraction and electron transfer reactions took place for the very strong oxidant SO_4^-, but that the reduction potentials of CO_3^- and Cl_2^- were not high enough to react with these phosphates and neither of these radicals had a strong propensity for hydrogen abstraction. The reactions of the two radicals, CO_3^- and Cl_2^-, were too slow for this degradation mechanism to be of importance in the environment.

6.6 VOLATILITY SCREEN

6.6.1 Extinguishant Volatility

For a chemical to be successful as a total flooding agent, it must evaporate and fill a space to the desired concentration within the time available for extinguishment. As determined by Pitts et al.[86], and noted earlier in this chapter, if the boiling point of the fluid is below the ambient temperature, the dispensed fluid will flash and disperse rapidly. For fluids of higher boiling point, estimation of the capability to flood a volume entailed two determinations: (1) the equilibrium vapor pressure at the ambient temperature in the fire compartment and (2) the rate of evaporation to achieve that vapor pressure.

6.6.2 Extinguishant Evaporation Equilibrium

Estimation of whether a given compound can achieve the required extinguishment concentration upon discharge entailed a thermodynamic analysis.[87] The logarithm of the ratio of the vapor pressure (p) at two different temperatures, T_2 and T_1 (in Kelvins), can be estimated from Equation 6-29, the Clausius-Clapeyron equation, where R is the ideal gas constant and ΔH_{vap} is the heat of vaporization. This equation is based on the assumptions that (1) ΔH_{vap} is temperature independent and (2) the vapor is an ideal gas. The ratio of $\Delta H_{vap}/T_b$, where T_b is the boiling point temperature, is equal to the molar entropy of vaporization ΔS_{vap} at the boiling point. For closely related compounds, ΔS_{vap} at the boiling point is nearly constant (Equation 6-30). Thus, by selecting T_1 as the boiling point (T_b) at p_1 = 101 kPa (1 atm), one can estimate the vapor pressure at other temperatures.

$$\log_{10}(p_2/p_1) = (\Delta H_{vap} (T_2-T_1)/2.303\ RT_2T_1) \tag{6-29}$$

$$\Delta H_{vap}/T_b = \Delta S_{vap} \approx t_c \tag{6-30}$$

Combining the two equations for a boiling point, T_b (K), at a pressure, P_b, Equation 6-31 is obtained. Trouton's constant, t_c (J/K-mol), is a variable to be determined for a particular family of compounds.

$$p_2 = P_b 10^{**}(0.052)\ t_c\ [1-(T_b/T_2)] \tag{6-31}$$

For example, if t_c were equal to 88 J/K-mol, which holds for many compounds, then the estimated vapor pressure at 25 °C for a compound with a boiling point of T_b = 50 °C at 101 kPa (1 atm) is 42 kPa. From vapor pressure values, the maximum possible volume % were estimated. These values are listed in Table 6–5. Similar tables can be prepared for other pressures.

The maximum allowable boiling point (T_b) able to achieve a desired volume % of a chemical in air at a given ambient temperature, T_2, was then estimated. Equation 6-32 calculates values of T_b for temperatures in K, P_b in kPa, and t_c in J/K-mol. The calculated estimates in Table 6−6 are for a Trouton's constant of 88 J/K-mol. The results are shown graphically in Figure 6–34.

$$T_b = [1-(\log(101^{*}\ C/0.13\ P_b)/0.052\ t_c)]T_2 \tag{6-32}$$

Table 6–5. Estimated Equilibrium Vapor Pressure (Volume %) as a Function of Boiling Point and Ambient Temperature.[87] [Trouton's Constant = 88 J/K-mol; P = 101 kPa]

	Ambient Temperature, °C												
T_b, °C	-60	-50	-40	-30	-20	-10	0	10	20	25	30	40	50
-60	100												
-50	61	100											
-40	37	62	100										
-30	23	39	64	100									
-20	14	24	40	65	100								
-10	8	15	26	42	66	100							
0	5	9	16	27	43	67	100						
10	3	6	10	18	29	45	68	100					
20	2	4	7	11	19	30	46	69	100				
30	1	2	4	7	12	20	31	47	70	84	100		
40	1	1	3	5	8	13	21	33	s49	59	71	100	
50	0	1	2	3	5	9	14	22	34	41	50	71	100

Table 6–6. Estimated Maximum Boiling Point That Can Achieve a Given Volume Percent of Chemical in Air.[87]

	Ambient Temperature, °C											
Volume %	-60	-50	-40	-30	-20	-10	0	10	20	30	40	50
1	33	47	61	76	90	105	119	133	148	162	176	191
2	19	33	46	60	74	87	101	115	128	142	156	169
3	11	24	37	51	64	77	91	104	117	130	144	157
4	5	18	31	44	57	70	83	96	109	122	135	148
5	0	13	26	39	52	65	77	90	103	116	129	142

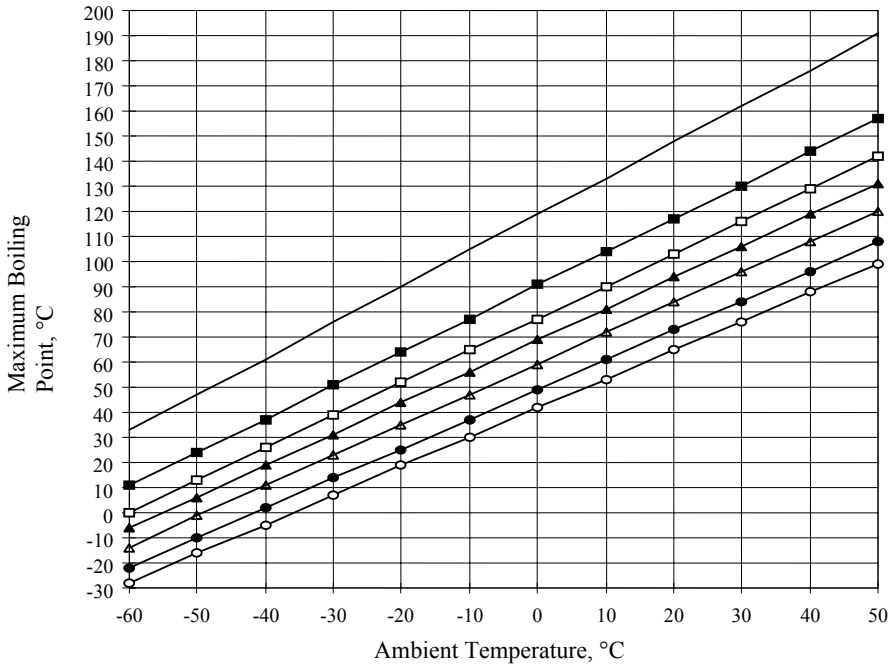

Figure 6–34. Estimated Maximum Boiling Points That Can Achieve Selected Values of Volume % in Air as a Function of Ambient Temperature.[87] Top to Bottom: 1 %, 3 %, 5 %, 7 %, 10 %, 15 %, 20 %

6.6.3 Extinguishant Evaporation Rate

Estimation of evaporation rates is much more difficult than the calculation of equilibrium agent concentrations. The following is an overview of some of the factors that must be considered. [87]

In the simplest case, a spherical droplet of fire suppressant agent of radius, r, is ejected into stagnant, completely unsaturated air at a velocity, U_0. The rate of evaporation as a function of the droplet radius and the time for complete evaporation was of interest. It was assumed that the temperature of the droplet was the same as its surroundings, and that the temperature at the surface of the droplet did not change as the droplet evaporated. While neither of these conditions is generally true, considering temperature changes was too complex for a simple analysis. The following uses cgs units.

Fick's first law for one-dimensional diffusion relates the flux (J in g/s-cm^2) of a vapor through a gaseous medium to the concentration gradient dc/dx, where c is the agent concentration (g/cm^3) and x is the direction of diffusion (Equation 6-33).

$$J = -D\frac{dc}{dr} \tag{6-33}$$

D, the diffusion coefficient of the vapor in cm^2/sec, is a function of the agent and the ambient conditions. Kinetic theory shows that for ideal gases of density, ρ, of rigid spherical molecules having a molecular mass, m, and a diameter, σ, the diffusion coefficient is given by Equation 6-34, where k is the Boltzmann constant and T is the absolute temperature.[88]

$$D = \frac{3}{8}\frac{(\pi mkT)^{1/2}}{\pi\sigma^2\rho} \tag{6-34}$$

Setting the density ρ = Pm/kT, one obtains Equation 6-35, which shows that the diffusion coefficient is proportional to $T^{3/2}$ and inversely proportional to the pressure P for this idealized gas composed of hard-spheres. It is also inversely proportional to the square root of the molecular mass and to the square of the molecular diameter. Real gases, of course, show significant deviations from this relationship, which may be modified to take into account actual molecular interactions.

$$D = \frac{3}{8}\frac{(kT)^{3/2}}{\pi^{1/2}\sigma^2 Pm^{1/2}} \tag{6-35}$$

Continuing to use the hard-sphere model, one can relate the diffusion coefficient to the coefficient of viscosity (η, g/cm-s), the heat capacity per molecule (c_v, g-cm^2/s^2-°C, = C_v/N_o, where N_o is Avogadro's number), and the coefficient of thermal conductivity (λ, g-cm/s^3-°C) (Equations 6-36 and 6-37).

$$D = \frac{12\lambda m}{25\rho c_v} \tag{6-36}$$

$$D = \frac{6\eta}{5\rho} \tag{6-37}$$

Equation 6-33 was rewritten to give the diffusion mass transport through a spherical surface of radius r (Equation 6-38).

$$\frac{dm}{dt} = -4\pi r^2 \frac{dc}{dr} D \tag{6-38}$$

Equation 6-38 was used to determine the mass transport from the liquid/gas interface surrounding a spherical drop of radius r_o with a concentration of c_o to a region far from the drop (r_∞) with a vapor concentration c_∞. Since dm/dt, the mass transport, is independent of r, integration of Equation 6-38 gives Equation 6-39. If r_∞ is very large and if c_∞ is taken as zero, Equation 6-40 results.

$$\frac{dm}{dt} \int_{r_o}^{r_\infty} \frac{dr}{r^2} = -4\pi D \int_{c_o}^{c_\infty} dc \tag{6-39}$$

$$\frac{dm}{dt} = 4\pi D \frac{c_o - c_\infty}{(1/r_o - 1/r_\infty)} \tag{6-40}$$

If r_4 is taken as sufficiently large, Equation 6-40 can be rewritten to give Equation 6-41. Note that as c_∞ approaches c_o (the air becomes saturated), the rate of evaporation approaches zero.

$$\frac{dm}{dt} = 4\pi D r_o (c_o - c_\infty) \tag{6-41}$$

Equation 6-41 can be rewritten to give Equation 6-42.

$$\frac{dm}{dt} = \frac{4\pi r D M (p_o - p_\infty)}{RT} \tag{6-42}$$

where M = molecular weight of the vapor, and p_o and p_4 are the partial pressures of the vapor at the surface of the droplet and at a distance infinitely far from the droplet. In the case of a fire suppressant agent, it was assumed that p_∞ is initially zero, since no agent has yet been released into the compartment. If c_∞ is zero, one obtains Equation 6-43.

$$\frac{dm}{dt} = 4\pi D r_o c_o \tag{6-43}$$

Equation 6-43 shows that the transport rate increases with drop size and with the concentration of agent at the liquid/vapor interface.

Performing estimates using this equation posed two problems. First, one must determine D for a real gas (rather than for the hard-sphere idealized gas discussed earlier). Second, and more difficult, one must determine the concentration of agent at the interface.

Since measured values of diffusivity were often not available, the only way to obtain values was to perform estimates based on available equations. Reference 89 lists several correlations for diffusivity. The lowest error was estimated to be from the Fuller-Chapman-Giddings equation, Equation 6-44.

$$D = \frac{0.1013 T^{1.75} \left(\frac{1}{M_1} + \frac{1}{M_2}\right)^{0.5}}{P\left[\left(\sum v_1\right)^{1/3} + \left(\sum v_2\right)^{1/3}\right]^2} \tag{6-44}$$

Here, T is the temperature of gases in K, M_1 is the molecular weight of the gas diffusing into the air, M_2 is the molecular weight of the air, P is the pressure of the gases, and v_1 and v_2 are atomic diffusion volumes

which are given in tables. Unfortunately, atomic diffusion volumes are not available for the majority of compounds and must be estimated for many of the compounds of interest in fire suppression.

The question of motionless droplets is academic at best. Droplets of fire suppressant chemicals will be rapidly expelled through the nozzle to ensure complete coverage of the protected area or the fire as well as providing mechanical breakup to smaller droplet sizes. Any realistic evaluation of evaporation must include inertia, gravity, and other forces acting on the droplets. The rapid acceleration of the droplets also distorts the droplets; however, one usually assumes spherical droplets.

The problem quickly escalates from a simple diffusion mechanism to a heat and mass transfer mechanism; it reduces to the calculation of the rate of evaporation or heat transfer from a spherical body in a moving gas stream (in the case of interest, the droplet is in motion within stagnant air, but the mathematics are the same). Solutions to such problems rely on the use of dimensionless numbers such as Reynolds, Nusselt, Prandtl, and Schmidt numbers. The problem is complicated by the fact that flow may be either laminar or turbulent, depending on the value of the Reynolds number; heat and mass transfer are radically different in laminar and turbulent flow.

A simple correction to Equation 6-43 to allow for the increase in evaporation rate due to motion through air is where dm/dt equals the evaporation rate with flow around the droplet is equal to 0.276, Equation 6-45.

$$\frac{dm}{dt} = 4r\pi D(c_o - c_\infty)(1 + \beta Sc^{1/3}\ Re^{1/2}) = I_o f \qquad (6\text{-}45)$$

(measured for a sphere), Re is the Reynolds number characterizing the flow of the air around the drop, and Sc is the Schmidt number. The term f is usually called the wind or ventilation factor. It is reported that Equation 6-45 accurately represents the evaporation rate of droplets in moving air.[90] For very small droplets falling in air, f is small, approaching 1; for larger droplets in moving streams, f can be rather large, reflecting the higher heat and mass transfer rates at higher velocity.

6.6.4 Boiling Temperature

From this analysis, it became clear that the estimation of evaporation rates was far beyond the capability for screening candidate fire suppressants. Thus, the NGP utilized a compound's boiling point as the screen for volatility.

A chemical's boiling temperature is one of the most fundamental properties, and literature values were available for many of the compounds under consideration by the NGP. Yang and coworkers reported on the use of a software package to estimate boiling points.[91]

For those compounds that were custom synthesized for the NGP (see Chapter 7), frequently the supplier measured the boiling point.

For those instances where a measurement was needed, it was generally necessary that the measurement use very little sample. Available techniques for determinations involving higher boiling compounds include a microscale method[92], based on determination of the temperature at which the pressure above the boiling liquid is large enough to overcome its vapor pressure in an inverted capillary tube. This method

typically employs a melting point apparatus and melting point capillary tubes. Boiling point determination methods applicable to low boiling compounds include the vapor pressure based isoteniscope method.[93] Both methods are applicable to very small samples.

6.7 TOXICITY SCREEN

6.7.1 Hazards and Regulation

There are a variety of acute toxic effects that can result from exposure to a fire suppressant chemical. These include sensory irritation, incapacitation, or even death. The NGP was concerned with the full range of such effects.

It has been recognized for decades that a principal toxic effect of halocarbon agents is cardiac sensitization.[94,vii] This is the sudden onset of cardiac arrhythmia caused by a chemical sensitization of the heart to epinephrine (adrenaline). Cardiac sensitization is a particularly important concern in fires because under the stress of the fire event, or even an accidental discharge of a fire suppressant, higher levels of epinephrine are secreted in the body, increasing the possibility of sensitization. Since the current firefighting halons and most replacement chemicals were halocarbons, most (but not all) of the NGP screening effort focused on this toxic effect.

Under the EPA SNAP Program,[4] cardiac sensitization values helped define the use restrictions placed on a replacement chemical. For example, when using halon substitutes as total flooding agents, the following conditions, which were adopted from an OSHA safety and health standard (29 CFR 1910 Subpart L), generally applied:

- Where egress from a normally occupied area cannot be accomplished within 1 min, the employer shall not use the agent in concentrations exceeding its NOAEL.[viii]
- Where egress from a normally occupied area takes longer than 30 s but less than 1 min, the employer shall not use the agent in a concentration greater than its LOAEL.[ix]
- Agent concentrations greater than the LOAEL are only permitted in areas not normally occupied by employees provided that any employee in the area can escape within 30 s. The employer shall assure that no unprotected employees enter the area during agent discharge.

There were no regulatory guidelines for conducting a cardiac sensitization study. However, the procedure most often followed for evaluating exposure to agents that might potentially evoke a cardiac sensitization response was the test performed using beagle dogs.[95] In this procedure, an intravenous dose of epinephrine was administered to each dog to establish its cardiac response to an epinephrine challenge alone. The dogs were monitored continually for electrocardiographic changes indicative of the appearance of ventricular fibrillation. The doses were increased from 1 μg per kg of body weight toward 12 μg/kg in steps of 0.1 ml/kg. After a recovery period, the dog was exposed to a selected concentration of the candidate suppressant. At 5 min into the exposure, the dog was injected with an epinephrine dose

[vii] See section 6.7.8 for screening for other acute toxic effects.

[viii] NOAEL, the "no observed acute exposure level," is the highest concentration at which no adverse toxicological or physiological effect was observed.

[ix] LOAEL, the "lowest observed acute exposure level, is the lowest concentration at which an adverse toxicological or physiological effect was observed.

just below the value that caused cardiac arrhythmia by itself. It was noted whether the dog experiences a response or not. Exposures at different suppressant concentrations were performed until the onset of an effect was bracketed to the desired precision. The results of this test are expressed in terms of the LOAEL and the NOAEL. The separation of these values was a function of the step size in suppressant concentration used for the cardiac sensitization test. The expense of the test often prevented a small increment from being used.

LOAEL data obtained from the dog-based cardiac sensitization testing are very conservative and, perhaps as a direct result, very rarely have people died as a result of exposure to the halons. The dog-based standard seems to be achieving exactly what it was designed to achieve – ensuring a wide margin of safety to a broad spectrum of end users.

6.7.2 Screening Process

The 1997 NGP Workshop on Fire Suppressant Compatibility with People, Materials, and the Environment developed a preferred protocol for obtaining indicative data regarding the various toxic possible effects of candidate agents. [2] The participants noted that there was no checklist to be used in a "cookbook" fashion. Expert judgment was needed to interpret the results of each test and decide what, if any, additional testing was necessary to evaluate the health effects of new agents. The progression of steps they endorsed was:

1. use published values,
2. derive values from quantitative structure-activity relationships (QSARs),
3. conduct non-animal biological tests, and
4. conduct live animal tests.

The steps involve successively more time, cost, and agent. The report on the Workshop contains extensive references to resources for performing the steps.

A protocol containing an even more comprehensive set of toxicity tests was developed by Dodd and co-workers.[96] This included tests for genotoxicity, subchronic toxicity, carcinogenicity, development and reproductive toxicity, among others. However, the NGP identified no compounds that progressed to that level of testing.

With regard to cardiotoxicity, performing the dog exposure tests was not feasible for the large number of chemicals under consideration by the NGP. Only a few laboratories in the world have the equipment and the expertise. Completing the testing takes about two months. The testing cost per chemical is currently approaching $100 k. The test requires about 30 moles of the test chemical, which generally would have needed to be custom-synthesized. Nonetheless, for the safety of personnel and for obtaining regulatory approval, estimating the cardiac sensitization LOAEL for a candidate fire suppressant was important.

Hence, the NGP conducted an extensive review to identify methods to aid in the selection of compounds with a higher probability of acceptable LOAEL and NOAEL values when actually tested. While any estimation method enabling a ranking of compounds would facilitate compound acquisition efforts, it was felt that the accuracy of the absolute LOAEL values needed to be within 2 volume % for the method to be of much use in final compound selection.

Halogenated compounds have found a variety of uses beyond fire suppression. Cardiac sensitization has surfaced as a consideration in the development of propellants for medical inhalers, it has been observed as a cause of cardiac arrest in substance abuse by inhalation of solvents used in spray paints and hairsprays, and it has occurred in the use of some pharmaceuticals and surgical anesthetics. Thus, there was significant background material to be searched for the current purpose.

At the time of the completion of the NGP, no accurate screening procedure existed to obviate the need for the standard dog exposure test. In fact, such testing of two otherwise promising chemicals generated negative results (Chapter 7). Sections 6.7.3 through 6.7.6 summarize the NGP investigation process.

6.7.3 Literature Values

A useful starting place for assessing the toxic properties of a candidate fire suppressant was a compendium of health and safety or toxicological data on chemicals, such as Reference 97. A number of databases also existed, both computerized and non-computerized, which were helpful in determining known toxic properties of a chemical, a set of chemicals, or even a chemical class:

- The Chemical Abstract Services (CAS) ONLINE (http://info.cas.org/) database was a pay-for-services, informational compendium of thousands of substances, which included information on chemical and physical properties, structures, synonyms, and in some cases, toxicity values.
- The National Library of Medicine site called MEDLARS (http://toxnet.nlm.nih.gov). MEDLARS contained a number of specific databanks including the Registry of Toxic Effects of Chemical Substances (RTECS), Hazardous Substance Databank (HSDB), the Integrated Risk Information System (IRIS), the Genetic Toxicology (Mutagenicity) Database (GENE-TOX), and the Chemical Carcinogenesis Research Information System (CCRIS).
- The National Library of Medicine (NLM) also had a number of other citation databases such as TOXLINE, MEDLINE, or CANCERLIT containing abstracted literature information on various aspects of toxicology. The NLM databases could be accessed free via the Internet (http://igm-01.nlm.nih.gov/index.html).
- RTECS was a comprehensive online database developed by the National Institute of Occupational Safety and Health (NIOSH) for the purpose of collecting, collating, and disseminating toxic effects information for "all known toxic substances," which were considered to be potentially all known chemicals that can elicit abnormal biological effects.
- The Merck Index (http://www.dupontmerck.com) contained physical and toxicity data from published literature sources. The Index was free, but limited to only a select few single substances.
- The Environmental Protection Agency's Office of Pollution Prevention and Toxics holds the Toxic Release Inventory (http://www.epa.gov/opptintr/tri/), which was a valuable free source of information about toxic chemicals that were being used, manufactured, treated, transported, or released into the environment.
- The EPA's GENE-TOX data bank compiled information on mutagenicity and carcinogenicity for several thousand chemicals (found through the MEDLARS online site) and the International Agency for Research on Cancer (IARC) (http://www.iarc.fr/pub/publist.htm) published for-fee monographs reviewing the carcinogenic potential of certain chemicals.

- The National Technical Information Service (NTIS) covered government-sponsored research and development efforts and some work may contain toxicological information. Searches for reports could be performed free of charge, but the actual documents could only be obtained for a fee (http://www.ntis.gov/search.htm).

For screening purposes, the literature examination was directed at finding any severe toxic effects that occurred at exposures of up to concentrations of the order of 5 volume % for several minutes. If there was insufficient information regarding the specific chemical under consideration, chemically similar compounds were examined.

Table 6–7, Table 6–8, and Table 6–9 list published NOAEL and LOAEL values for members of different families of halocarbons. These data enabled some preliminary insights:

- There were a wide range of values among and within the chemical families.
- The limited data for partially fluorinated methanes (Table 6–7, compounds 6 and 7) demonstrated a relatively low tendency to induce cardiac sensitization.
- The three hydrofluoropropanes (Table 6–7, compounds 3 through 5) showed a wide range of LOAEL values with no obvious correlation with the degree of fluorination. There may be a relationship with the location of the hydrogen atoms, both with this family and the hydrofluoroethanes (compounds 8 through 11).
- In Table 6–8, an iodine atom appeared to lead to a low LOAEL value.
- Many CFCs and HCFCs, which are closely related to the halons, were cardiotoxins.[98] Table 6–9 gives little or no indication of relationships between degree of fluorination or chlorination (or hydrogenation) and LOAEL values. While the highly fluorinated compound, CF_3CF_2Cl, was notable for its unusually high LOAEL of 15 volume % most values ranged from a low of 0.5 volume % to a more nominal high of 5 volume %.

Table 6–7. Cardiac Sensitization Values for Fluorocarbons and Hydrofluorocarbons.

#	Chemical Formula	NOAEL (vol. %)	LOAEL (vol. %)	Reference
1	$CF_3CF_2CF_2CF_3$	40	>40	99
2	$CF_3CF_2CF_3$	30	>30	62
3	$CF_3CHFCHF_2$	2.5	3.5	100
4	CF_3CHFCF_3	9	10.5	99
5	$CF_3CH_2CF_3$	10	15	99
6	CH_2F_2	20	25	61
7	CHF_3	30	>50	99
8	CH_2FCF_3	4	8	61
9	CH_3CF_3	4	8	62
10	CHF_2CF_3	7.5	10	99
11	CH_3CF_2H	5	15	95

Table 6–8. Cardiac Sensitization Values for Br-, Cl-, and I-containing Alkanes.

#	Chemical Formula	NOAEL (vol. %)	LOAEL (vol. %)	Reference
1	CF_3I	0.2	0.4	101
2	CF_3Br	5.0	7.5	99
3	CF_2HBr	2	3.9	99
4	CF_2BrCl	0.5	1.0	102
5	CF_2BrCF_2Br	-	0.1	103
6	$CBrClFCBrF_2$		0.5	103
7	$CF_3CF_2CF_2I$	-	0.1	104

Table 6–9. Cardiac Sensitization Values for CFCs and HFCs.

#	Chemical Formula	NOAEL (vol. %)	LOAEL (vol. %)	Reference
1	CF_2ClH	2.5	5	61
2	CF_2Cl_2	2.5	5	95
3	$CFCl_3$	-	0.5	105
4	$CH_2=CClH$	2.5	5	95
5	CCl_3CH_3	0.25	0.5	95
6	CF_2ClCH_3	2.5	5	95
7	$CFCl_2CH_3$	-	0.5	106
8	CF_3CF_2Cl	-	15	95
9	CF_3CCl_2H	1	2	61
10	$CFCl_2CH_3$	-	1	106
11	CF_2ClCF_2Cl	-	2.5	95
12	$CClF_2CFCl_2$	0.25	0.5	95
13	CF_2ClCF_2CFHCl	-	2.0	107

6.7.4 Quantitative Structure Activity Relationships

Quantitative structure-activity relationships (QSARs), based on scientific judgment by experienced scientists, may be used as an integral part of health hazard characterization. This approach relies on the toxicologist or chemist being able to fit the new chemical into a category of existing chemicals because of similarities in molecular structure or chemical functionality. In order for this approach to be of value, the existing chemicals category or close structural analog must have its own robust toxicology database and the uncertainty of read-across from the close structural analogs or the category to the new chemical must be recognized and, if possible, defined.

Skaggs et al. performed an extensive review of toxicity prediction and screening approaches, identifying chemical attributes employed in the development of QSARs, predictors of relationships between biological activity and chemical properties.[108] The descriptor types included:

- Hydrophobicity, a measure of water insolubility. Neutral, unreactive chemicals exhibit a strong relationship between the hydrophobicity of the compound and its LC_{50}. Hydrophobicity is equated to the octanol-water partition coefficient and reflects the ability of a chemical to cross a biological membrane and correlates with toxicity because diffusion through cell walls allows chemicals to influence internal cellular processes and biochemistry. Both the Hammett Constant and the Taft Polar Substituent Constants are measures of

substituent polarity. Steric properties relate to molecular structure and affect the binding of molecules to biological sites.

- Molecular connectivity descriptors describe the number of atoms in a compound and their formally-bonded and spatial relationships. Molecular Connectivity Indices (MCI) associate numerical values with structure of the molecule. Many properties are directly related to the number and connections of atoms in molecules.[109] Molecular connectivity describes structural information and relates to physical properties.
- Linear Solvation Energy Relationship (LSER) analysis is based on the correlation of diverse chemical properties, including toxicity and solvent-solute interactions. The analysis is based on four molecular parameters: intrinsic molecular volume, polarity, and two measures of ability to hydrogen bond as an acceptor or donor. While this measure provides the most accurate QSARs covering the widest range of chemical classes, the parameters are available on only a finite amount of chemicals.[110]
- Molecular connectivity QSARs require that indices based on structure be determined, and generally the amount of data needed is less than that for quantitative property-activity relationships (QPAR). In both cases, sufficient toxicity data must be available with which to develop correlations capable of providing toxicity estimates of unknown substances. These data are not available in the required abundance to perform highly reliable assessments across a broad range of compounds.

Skaggs et al. reported that the key to using any of these techniques was to determine a family of chemicals for which biological indices (for example, LD_{50}), as well as physical/chemical properties, molecular structure, or both, are known. [108] In actual QSAR modeling, these sets of data are referred to as "training sets." By the use of statistical techniques such as multiple regression analysis (MRA), a relationship between the biological indices and property/molecular structure is determined based on the "training set" data. The better or more extensive the training set the more the predictions are apt to be accurate.[111]

Vinegar[112] has extracted some general, but not universal, toxicity trends that have been used to provide a relative toxicity ranking for the candidate compounds and compound groups:

- Toxicity Ranking Criteria
  - Aromatics are more toxic than aliphatics.
  - Asymmetric molecules are more toxic than symmetric molecules.
  - Straight (carbon) chains are more toxic than branched.
  - Ethers are more toxic than alkanes.
  - Short chain ethers are more toxic than long chain ethers.
  - Vinyl ethers are more toxic than saturated ethers.
  - Polyoxyethers are more toxic than monoethers.
- Cardiac Sensitization Ranking Criteria
  - Halogen presence is more potent than hydrogen.
  - Bromine presence is more potent than fluorine presence.
  - Iodine presence is more potent than bromine presence.

QSAR analysis has been formalized and computerized for some health endpoints (e.g., cancer, mutagenicity, and teratogenicity) and may be useful with appropriate recognition of the limitations of these programs. Evaluation of the computerized QSAR programs available commercially has been the subject of a review.[113] The U.S. EPA has grouped chemical substances with similar physical-chemical, structural and toxicological properties into working categories. These groupings enable the user of the NCP Chemical Categories guidance document to benefit from the accumulated data and decisional precedents within EPA's new chemicals review process since 1987, in order to identify areas of health hazard concern. There were 51 chemical categories listed in the table of contents of the EPA document, the detailed summaries of which may be found at: http://www.epa.gov/opptintr/newchms/chemcat.htm.

Multiple investigators have developed numerous QSARs to predict the toxicity of chemicals, as indicated in Table 6–10, taken from Reference 2.

Table 6–10. Availability of QSARs for Various Chemical Classes and Toxic Endpoints. [2]

Chemical Class	Functional Group	Possible Toxicity Endpoints	References
Alcohols	-C-OH	Irritation	114, 115, 116, 117
Aldehydes and Acetals	> C = O	Irritation, Sensitization, Anesthesia, Mutagencity and Carcinogenicity	114, 118
Allyl compounds	H_2C=CH-R	Liver Toxicity, Kidney Toxicity, Neurotoxicity, Sensitization, Carcinogencity	119
Amides	-$CONH_2$	Irritation, and liver, kidney and brain toxicity	120, 121, 122, 123, 124, 125, 126, 127, 128
Amines		Cholinesterase Inhibition, Carcinogenicity	114, 129, 130, 131, 132, 133, 134, 135, 136
Azides	-N_3	Cardiovascular actions and enzyme inhibition	137
Bromides	Inorganic and organic bromides	Neurotoxicity, Irritation, Hepatotoxicity, Cardiotoxicity	138, 139, 142
Chlorinated Hydrocarbons	Cl-C-R	Carcinogencity, Anesthesia, Hepatotoxicity	140, 141, 142, 143, 144, 145, 146, 147, 148
Epoxy Compounds		Irritation, Mutagenicity, Neurotoxicity, Hepatotoxicity, Kidney Toxicity, Embryotoxicity	119, 149, 150, 151, 152,
Esters	RCOOR'	Asphyxiants, Narcotics, Irritants	138, 153, 154, 155, 156
Ethers	R-C-O-R'	Anesthesia, Cardiotoxicity, Irritation, Carcinogenicity	157, 139, 158, 159, 160, 161
Ketones	RCOR'	Anesthesia	114, 118, 123, 155, 162, 163, 164
Nitro, Nitrate, and Nitrite	-NOx	Irritation, Neuromuscular Dysfuction, Hepatotoxicity, Cardiotoxicity, Mutagenicity, Carcinogenicity	139, 165, 166
Nitroso compounds	C-N=O or N-N=O	Carcinogenicity, Mutagenicity, Teratogenicity	167
Phosphorus compounds		Anesthesia, Cholinesterase Inhibition, GI Dysfunction, Irritation, Neurotoxicity, Kidney Toxicity, Hepatotoxicity, Teratogenicity, Reproductive Toxicity	129, 153, 168
Sulfur Compounds		Irritation, Corrosivity, Cardiotoxicity, Neurotoxicity	138, 124, 126, 139, 128

Because the predictive capabilities of QSARs are based on the quality of the data used in their development and an understanding of the mechanisms of toxicity, these techniques can sometimes be unreliable and should not be the sole criterion for screening decisions. The basic principles behind QSAR technology are well documented and can apply to any class of chemical and any measurable end point.[169]

Several texts describe the basics of QSAR techniques,[170] but briefly, QSARs involve taking a sufficiently large, consistent data set and correlating it with known descriptors of the chemicals within the data set. The correlation techniques are principally multivariate regression and discriminant analysis for weighting descriptors.[171] This leads to a mathematical expression, whereby endpoint data can be predicted for chemicals with known descriptors. For example, one can use a data set of lethal concentration values (e.g., LC_{50})[x] for halogenated hydrocarbons and correlate these values with certain physico-chemical descriptors such as numbers or type of halogens, vapor pressures, and/or octanol-water partition coefficients. The resulting mathematical equation would allow one to calculate the lethal concentration for a new halogenated hydrocarbon knowing only the physico-chemical descriptors for that particular chemical. Several of these approaches have been employed in the search for clean fire suppressants.[172,173]

6.7.5 Non-animal Laboratory Testing

The Case for Octanol-Water Partition Coefficients

There is some evidence to support a relationship between the tendency of a chemical toward cardiac sensitization and its relative solubility in polar and non-polar liquids.[174] However, the actual mechanism is not yet fully understood.

Frazier reported that some researchers had concluded that cardiac sensitization is a direct result of a physical-chemical interaction of the sensitizing agent with heart cell membrane structures.[175] This mechanistic hypothesis was derived from the observation that a critical blood concentration of agent is needed to elicit a cardiac sensitization response and the effects are immediately reversible, if they are not sufficiently severe to cause death, when the sensitizing agent is removed. Below that critical concentration, the effect does not occur.

Clark and Tinston had reported a possible correlation of cardiac sensitizing potentials of halogenated and some non-halogenated chemicals with selected physiochemical properties.[176] Based on the data in Table 6–11, they suggested that the effect was not a chemical (reactivity based) toxicity but instead a generalized physical property effect that just happened to cause cardiac arrhythmia when sufficient chemical "occupied a constant fraction of he critical biophase," i.e., was absorbed into heart nerve and muscle cells membranes. For the tested chemicals in the table, the EC_{50} (volume % of chemical that has an effect, E, on half of the test animals) and vapor pressure at 37 °C data appear to correlate. This hypothesis suggested that if a chemical were preferentially soluble in a barely polar liquid, such as octanol, and less soluble in a polar fluid, such as water, it would be less likely to be flushed from the tissue environment.

[x] LC_{50} (or similar terms indicating various toxicological endpoints) denotes the concentration of a toxic gas statistically calculated from concentration-response data to produce lethality in 50 % of the test animals within a specified exposure and post-exposure time

Tanner et al.[177] provided support for this polarity effect. Using differential scanning calorimetry, they showed that the inhalation anesthetic agent halothane ($CF_3CHClBr$) destabilized some proteins in aqueous solution with respect to thermal unfolding, presumably due to halothane binding to the native folded state. Low (millimolar) concentrations of halothane produced significant destabilization of proteins, and they concluded that destabilization of proteins by halothane could be attributed to mainly hydrophobic interactions of halothane with the proteins.

There was further information on the phenomenon of cardiac sensitization from the fields of surgical anesthesia agents and pharmaceutical development. While the published literature was abundant in the former area, not surprisingly, little was found describing the approaches and methods employed by major pharmaceutical companies in their drug development research related to avoiding cardiac sensitizing or arrhythmia inducing drugs.

Anesthesia was an active area of research, with considerable published data on the influence of various compounds on human systems.[178] These studies included data on the relative tendencies of a wide range of current and former anesthesia agents to induce cardiac arrhythmia as well as comparison molecular property data, toxicity information, and models for agent uptake to target tissues. Reviews covering cell membrane ion gate channel effects and the effects of molecular structure were found in studies of pharmacokinetics and molecular physiology.[179, 180] The data presented relate uptake of anesthesia agents and physical properties, such as blood gas ratios (partitioning) of the anesthesia agent based on relative solubility in the two media.

Table 6–11. Air Concentration Inducing Cardiac Sensitization in 50 % of Animals. [176]

Compound	Volume % at EC_{50}	Partial Pressure at EC_{50}, kPa	Vapor Pressure at 37 °C, kPa	Relative Saturation for Cardiac Sensitization
CCl_4	0.53	0.53	25	0.02
CH_3CCl_3	0.75	0.76	28	0.03
CCl_2FCF_2Cl	1.0	1.0	70	0.02
$CFCl_3$	1.3	1.3	158	0.02
$CF_3CHClBr$	2.0	2.0	64	0.01
CH_2Cl_2	2.4	2.4	88	0.03
$CHFCl_2$	2.5	2.5	273	0.03
CH_2=$CHCl$	5.1	5.1	560	0.01
CF_2Cl_2	8.1	8.2	900	0.01
CF_2ClCF_2Cl	10.0	10.1	307	0.01
$CH_3CH_2CH_3$	20	20	1270	0.03
CF_3Br	20	20	2030	0.01
CF_3Cl	80	81	5410	0.01

Evidence for some of the effects of general (volatile) anesthetics on membranes and membrane ion channels were described in terms of a protein binding mechanism.[181] However, this interpretation did not account for the lack of demonstrated differential anesthetic effects of the two sterioisomers (R and S) of isoflurane. The R and S sterioisomers of isoflurane would be predicted to bind quite differently to stereospecific protein sites, yielding marked differences in the relative abilities of the R and S forms of

isoflurane to induce anesthesia. Investigation of the effects of volatile anesthesia agent on voltage gated ion channels was also ongoing and provided evidence for their inhibition of voltage-gated ion channels and to a greater extent on ligand-gated ion channels. [181] These same researchers reported that "we can summarize these findings with the generalization that volatile anesthetics had high-efficacy on ligand-gated ion channels, whereas they had relatively low potency and high efficacy effects on voltage-gated ion channels." While these observations did not conclusively or perhaps significantly further the identification of one particular mode of interaction they related to the search for cardiac sensitization screening methods, they did provide insight to both the status of current investigations into the interaction of volatile halocarbons and cell membranes.

Anesthesia agents are not unlike halons in elemental composition. Anesthesia agents are represented by lower molecular weight brominated and chlorinated hydrofluoroalkanes and ethers. Some are chlorinated fluorocarbons. Of potential use were studies of the minimum alveolar concentration (MAC) values determined for anesthesia agents[181,182] and clinical observations of the tendency of volatile anesthetics to induce cardiac arrhythmia or premature ventricular contractions (PVCs).[183]

Table 6–12 combines these physiological effects with the hypothesis of Clark and Tinston. These data indicated a potential correlation between the tendency of a compound to induce PVCs and its log(K_{OW}) value.

Octanol-water partition coefficients have also been used in QSAR analysis and rational drug design as a measure of molecular hydrophobicity and are key parameters in studies of the environmental fate of chemicals. This was because the degree of hydrophobicity of a compound was known to affect its drug absorption, bioavailability, hydrophobic drug-receptor interactions, metabolism of a compound, and toxicity.

Given the compositional and molecular similarities between anesthesia agents and many of the current halon replacement compounds of interest as well as the reports reviewed above linking a compounds hydrophobicity to toxicity, cardiac arrhythmia, protein interaction effects measures of hydrophobicity seemed a clear strong choice for further evaluation and study as potential screening methods for cardiac sensitization. The possibility of a near term screening method based on the comparative hydrophobicities of the candidate compounds seemed worthy of further investigation.

Table 6–12. Partitioning (K_{OW}) and Arrhythmia Properties of Selected Anesthetics.[184,185]

Property	Halothane	Enflurane	Isoflurane	Desflurane	Sevoflurane
Blood-gas Ratio[a]	2.5	1.9	1.4	0.42	0.6
Oil-water Ratio[b]	220	120	170	19	55
Arrhythmia[c]	+++	+	+	~	~
MAC[d]	0.74 %	1.68 %	1.15 %	6.3 %	2.0 %

a Ratio of the anesthesia agent concentration in the blood over the anesthesia agent concentration in the gas phase. High values indicate more effective transport of the chemical throughout the body and thus to cardiac tissue.

b The "oil" phase is commonly, but not exclusively, octanol.

c The symbols "+++," "+," and "~" reflect, in order, a decreasing tendency of the anesthetic to induce PVCs in human patients during anesthesia. The last of these indicates only a slight tendency. Halothane is notable for its greater tendency to induce PVCs than the other anesthesia agents listed.

d Minimum Alveolar (air) Concentration (MAC) for an anesthesia agent is a measure of the anesthetic potency of the compound, i.e., the air concentration required to immobilize 50 % of patients such that they don't give a motor response to a pain stimulus.

Measurement of K_{OW}

Experimental determination of the octanol-water partition coefficient, K_{OW}, using reverse phase high pressure liquid chromatography, is rapid and requires only a few mg of the compound. [174] The measured property is the equilibrium constant for the concentrations of the chemical in the two liquids. Referencing the retention times on the chromatographic column of compounds for which K_{OW} values are known establishes a basis for obtaining partition coefficients for candidate fire suppressants.

Calculation of K_{OW}

Values of K_{OW} were estimated from the contributions of molecular fragment-based terms plus correction factors.[186] Different algorithms can give different results, so experience was needed to select or develop an appropriate version for the particular chemicals under consideration. Two of the most commonly used algorithms were from Molinspiration Cheminformatics (http://www.molinspiration.com) and Syracuse Research Corporation (http://esc.syrres.com).

Octanol-water partition coefficients were calculated for the difluorinated bromopropenes using these two molecular fragment contribution-based methods and plotted in Figure 6−35. For this family of compounds, the two methods were in good agreement. Interestingly, the highest log(K_{OW}) value calculated for this series was for CH_2=$CHCF_2Br$, which proved highly toxic in inhalation toxicity tests.[187]

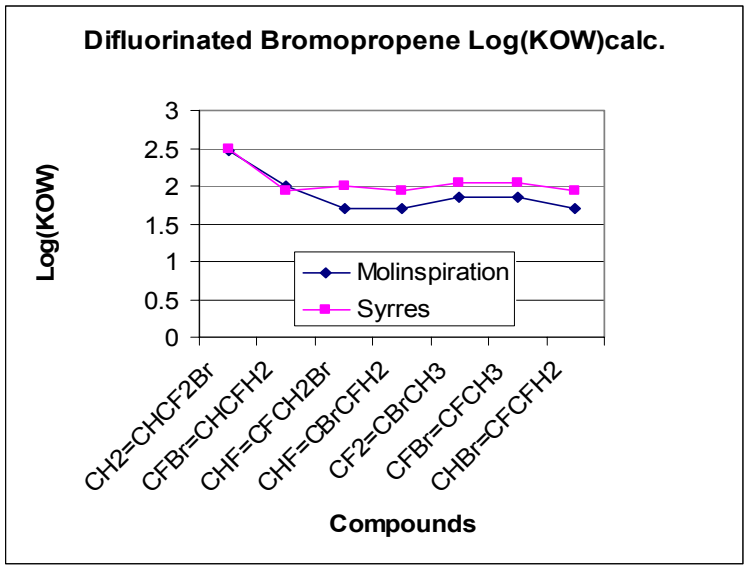

Figure 6–35. Comparison of Two Difluorobromopropene Log(K_{OW}) Calculation Methods. [174]

Octanol-water partition coefficients were also calculated for the trifluorinated bromopropenes using the two methods (Figure 6–36). The plotted data points (line connecting data points from same method calculation) were also roughly comparable.

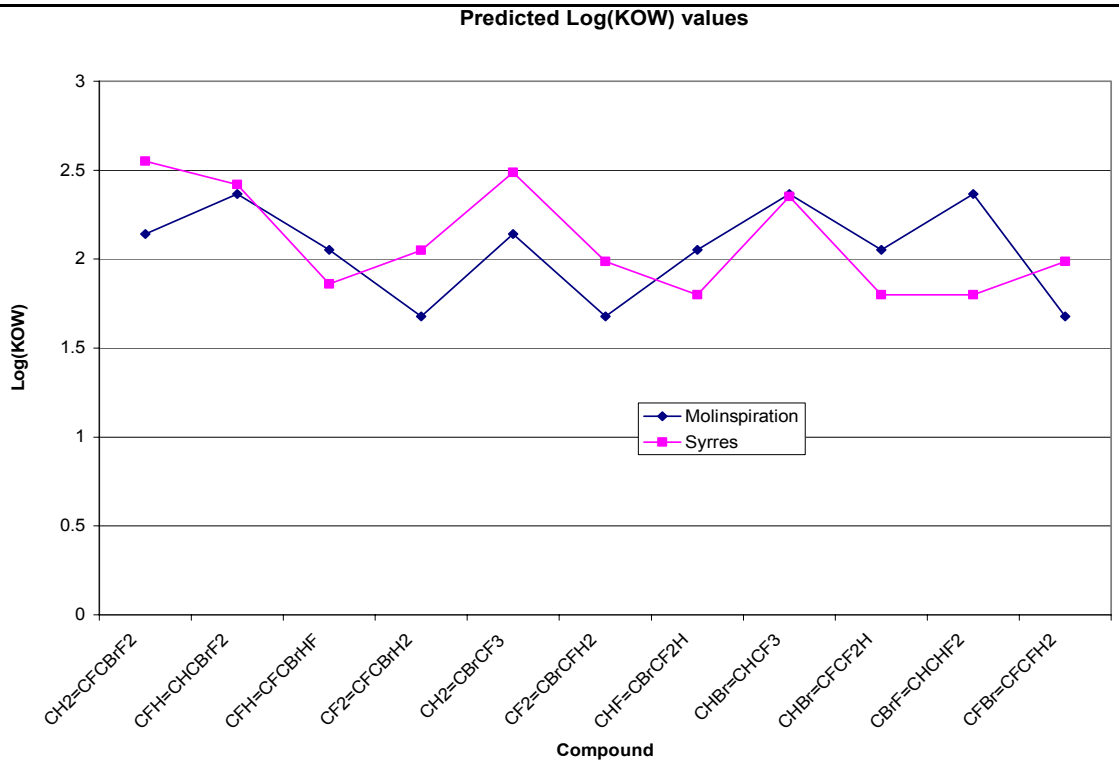

Figure 6–36. Comparison of Two Trifluorobromopropene Log(K_{OW}) Calculation Methods. [174]

An indication of the disparity as well as trends in the predicted values for the two calculation methods can be seen in Table 6–13.

Table 6–13. Comparison of Calculated and Measured Values of Log K_{OW} of Selected Halocarbons. [174]

Compound	Log K_{OW} * (calculated)	Log K_{OW} ** (calculated)	Log K_{OW} (measured)	LOAEL (volume %)
CF_3Br (halon 1301)	1.83	1.59	1.86	7.4
$CHBrF_2$	1.85	0.98	NA	3.9
CH_2=$CBrCF_3$	2.14	2.49	NA	1.0
CF_2ClBr (halon 1211)	2.17	1.90	2.1	1.0
CF_3I	2.22	2.01	NA	0.4
C_3HF_7	2.35			10.5

* Molinspiration Cheminformatics algorithm
** Syracuse Research Corporation algorithm

It is probable that the use of calculated partition coefficient values to develop predictions of trends in LOAEL performance works best when only applied to narrowly defined groups of compounds (for instance, bromofluoroalkenes) and even then only used as a tentative predictor of LOAEL value. This limitation is demonstrated by the last line of Table 6–13. The calculated log K_{OW} value for C_3HF_7 suggests a LOAEL lower than that any of the other compounds, which is clearly not the case.

Another potential shortcoming of the available calculations is that they do not recognize or differentiate between the cis and trans structural isomers of compounds, such as the 1-bromo-3,3,3-trifluoropropenes

and the 3-bromo-1,3,3-trifluoropropenes. There were no experimental data to establish the actual differences between such isomers.

6.7.6 *In Vitro* Tests

A wide range of *in vitro* methods has been developed for specific toxic endpoints, including acute lethality, mutagenicity, anesthesia, kidney toxicity, hepatotoxicity, and teratogenicity.[2] These methods commonly use perfused organ preparations, isolated tissue preparations, single cell suspensions, or tissue culture systems. Upon exposure to the test chemical, the specific response can vary from one species to the next. Thus, preparations should be derived from species that respond to the chemical challenge in ways which are similar to humans. Furthermore, caution should always be exercised when utilizing *in vitro* techniques during the screening process because many factors, such as absorption and transport processes, influence the toxicity of a chemical. Thus, it was not deemed wise to rule out further consideration of a candidate based exclusively on the results of a single *in vitro* test.

The development of an *in vitro* cardiac sensitization screening method requires the development and validation of a system that retains the essential components of the process of cardiac sensitization. Identified requirements[175] for an in vitro system include a cardiomyocyte system that:

1. exhibits synchronized and spontaneous contraction,
2. is responsive to exogenous epinephrine,
3. exhibits sensitivity to known cardiac sensitizers, and
4. allows exposure of sensitizing agents to system in a controlled atmosphere.

To this list must be added the ability to accurately rank compounds whose LOAELs differ by as little as a few percent.

Frazier has reviewed a number of studies involving cardiac cell systems.[175] Most of these were performed to assess the effects of certain drugs on cardiac functions or to determine specific of cardiac function itself. These are categorized in Table 6–14.

Table 6–14. *In Vitro* Cardiac Cell Systems.

Model	Life stage	Species	Reference
Myocardial cells	Fetal	Human	188
Cardiomyocytes	Neonatal	Rat	189
Ventricular Cardiomyocytes	Neonatal	Rat	190
Ventricular Cardiomyocytes	Neonatal	Dog	191
Cardiomyocytes	Adult	Rat	192
Cardiomyocytes	Adult	Rabbit	193
Cardiomyocytes	Adult	Dog	194
Cardiomyocytes	Adult	Feline	195
Ventricular Cardiomyocytes	Adult	Guinea Pig	196
Ventricular Cardiomyocytes	Adult	Rat	197

Skaggs et al. [108] concluded that, despite the variety of *in vitro* systems available to assess the cardiac toxicity of certain agents, any model selected would have to be characterized with respect to the

expression and response of adrenergic receptors and the ion fluxes (sodium and calcium) before cardiac sensitization validation studies could be initiated. At the time of completion of the NGP, there was no *in vitro* method that was established as predictive of the standard dog exposure test for cardiac sensitization.

6.7.7 PBPK Modeling of Cardiotoxic Effects

The Time-dependence of Toxic Hazard

Should a suppression system discharge into an area that is either occupied intentionally (such as a ground vehicle crew compartment) or unintentionally (such as during maintenance of an engine nacelle), people could be exposed to a high concentration of the agent for a relatively short time. The methods presented above involve a steady exposure for a long enough time period to see an effect. This masks the kinetic effects of a short exposure.

Figure 6–37 shows a hypothetical time dependence of a toxic response to a short exposure to a discharged fire suppressant. The concentration in the local atmosphere rises sharply following the discharge. Depending on the airtightness of the surroundings, the agent can dissipate quickly (as in the engine nacelle) or moderately (as in the crew compartment). There is a time lag in the concentration of the agent at the body site where the toxic effect will occur. This is due to transport time to that site, a process that could involve multiple steps. As the suppressant dissipates, the occupant breathes a lower concentration. Thus, the eventual dose (the integral of local agent concentration and time) reaching the sensitive site can be far lower than the exposure (the integral of the environmental concentration overt the exposure time).

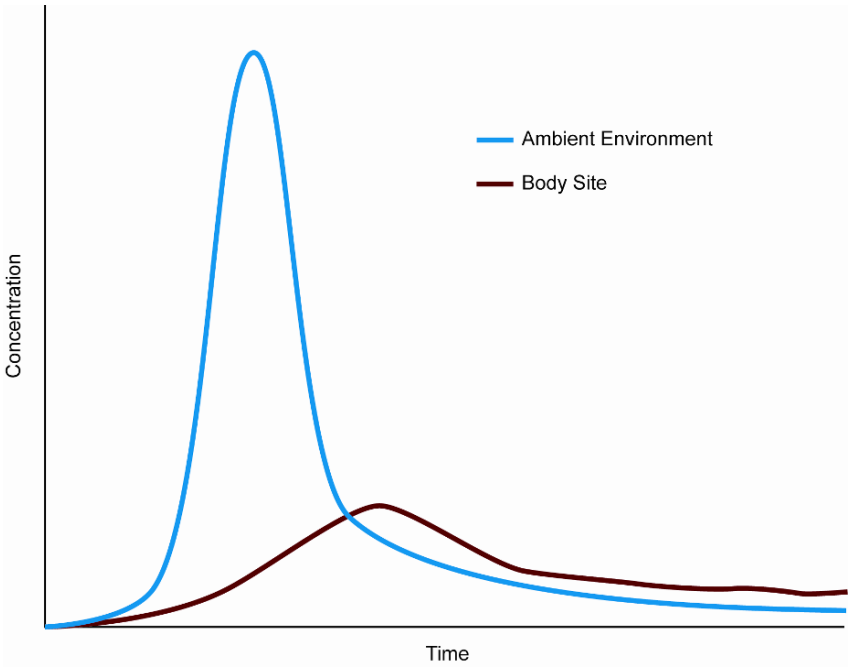

Figure 6–37. Hypothetical Time Dependence of a Toxic Response to Exposure to a Fire Suppressant. (NIST drawing)

The PBPK Model

Under sponsorship of the EPA and the NGP, a team of toxicologists at the Air Force Research Laboratory (AFRL) modified a physiologically-based pharmacokinetic (PBPK) model of a human to include time-

dependent representation of the cardiovascular system and lungs that will allow simulation of the outcome of short-term exposures to fire suppressant chemicals.[xi] This was an important improvement over commonly used PBPK models that used steady-state descriptions to describe uptake of chemical via the lung and subsequent transfer of chemical to arterial blood. The principal features of the model[198,199,200,201] are summarized here.

A PBPK model provides the quantitative link between a (possibly time-varying) exposure concentration and the blood levels of the chemical achieved following inhalation. The PBPK model is a mathematical description of the uptake, distribution, metabolism, and elimination of a chemical in the species of interest. The time required for an arterial concentration to reach the LOAEL target arterial concentration is considered the safe (i.e., protective) exposure duration. The physiological compartments that compose the model are based on appropriate physiological and anatomical properties for the species of interest as well as the chemical specific properties of the test compound. The use of PBPK models for kinetic description of chemical interaction with biological systems has been well represented in the scientific literature and is widely accepted by the scientific community as a tool for risk assessment.

The human PBPK model used in this work[198] differed from the more traditional PBPK model in that it included a respiratory-tract compartment containing a dead-space region and a pulmonary exchange area. It was used successfully to simulate the pharmacokinetics of halothane, isoflurane, and desflurane which are structurally similar to many of the chemicals being considered as halon replacements. The pulmonary exchange area had its own air space, tissue, and capillary subregions. Respiration was described on a breath-by-breath basis. This more detailed lung description was necessary to successfully simulate pharmacokinetic data in the 0 min to 1 min range. [198] Additional physiological compartments described in this model were liver, fat, lung, gut, and slowly perfused and rapidly perfused tissues. All model compartments were perfusion limited and metabolism, if present, was assumed to occur in the liver.

The model required a considerable amount of input data:

- Cardiac sensitization LOAEL. This was determined using beagle dogs, as described above. The LOAEL thus determined was conservative in that the epinephrine challenge was well above physiological levels, and the LOAEL value was used without any correction factors. That the effect was due to the peak concentration of chemical rather than the area under the curve has been established by Reinhardt et al. [95]
- Arterial concentration measured after five minutes of exposure of beagles to the LOAEL concentration. Obtaining this information required that studies be done with beagles that have been cannulated for the sampling of arterial blood. At least six beagles should be exposed, without epinephrine challenge, at three exposure concentrations for 10 min at each exposure. The concentrations should be the LOAEL, approximately 25 % above the LOAEL, and approximately 25 % below the LOAEL. Blood samples should be taken at least at (1, 2, 5, 7, and 10) min to check the reliability of the data obtained at 5 min.
- Partition coefficients of the chemical in blood, liver, fat, and muscle. The most sensitive parameter for determination of the correct blood concentration was the blood partition coefficient, and there could be as much as a two-fold difference between human and rat blood. Therefore, since the model was being used to simulate human exposures, AFRL measured human blood partition coefficients. For the other partition coefficients, where much

[xi] This model addresses accidental exposure to the suppressant itself, such as might occur following an accidental discharge. It does not include the contribution of any decomposition products that are formed during and following flame extinguishment.

less difference was expected, rat tissue partition coefficient data were used when human data were not available. Details on obtaining these data are presented in reference 201.

- Metabolic constants. These were obtained using a gas uptake method using rats, as described by Gargas et al.[202] Fortunately, most of the proposed halon replacements were relatively inert and had extremely low to no measurable metabolism. Furthermore, even with moderate metabolism, there was no noticeable effect on the outcome of short-term simulations required for modeling of cardiac sensitization.
- Human blood flows and tissue volumes. There is significant variation in these variables among people. Therefore, Monte Carlo simulations were performed as part of the simulation of the concentration of an inhaled fire suppressant in the bloodstream. The ranges of the variables were compiled in Tables 1 and 2 of Reference 201. The Monte Carlo simulations were performed using ACSL TOX simulation software (Pharsight Corp., Mountain View, CA) operating under Windows 95 and Windows NT (Microsoft Corp., Redmond, WA).

Simulations of Exposure to Constant Concentration Environments

The combined application of cardiac sensitization data and physiologically based modeling provided a quantitative approach, which could facilitate the selection and effective use of halon replacement candidates. The AFRL team exercised the model, performing the first simulations of short term (0 min to 5 min) effects. They used these results to determine short-term safe exposure times for halon 1301 and four potential replacement chemicals CF_3I (trifluoroiodomethane), HFC-125 (pentafluoroethane), HFC-227ea (1,1,1,2,3,3,3-heptafluoropropane), and HFC-236fa (1,1,1,3,3,3-hexafluoropropane). [201]

Figure 6–38 and Figure 6–39 show the result of Monte Carlo simulations of the concentration of halon 1301 and HFC-125, respectively, in human blood during exposure to six different constant concentrations of the suppressant in air. The simulation lines represent the results of 1000 Monte Carlo simulations. The horizontal line at 25.7 mg/L represents the lowest arterial blood concentration measured at 5 min in a group of 6 dogs exposed to halon 1301 at the cardiac sensitization LOAEL of 7.5 %. For the six concentrations, Table 6–15 shows the safe exposure times, the time at which the blood concentration of halon 1301 reached the LOAEL for the most sensitive dog. Table 6–15 show such estimates for HFC-125. Similar curves and tables were generated for the other four fire suppressants.

Table 6–15. Time for Safe Human Exposure at Stated Concentrations for Halon 1301 and HFC-125. [199]

Halon 1301 Concentration (mole %)	Time (min)	HFC-125 Concentration (mole %))	Time (min)
5.5	5.00	11.5	5.00
6.0	5.00	12.0	1.13
6.5	1.33	12.5	0.73
7.0	0.59	13.0	0.59
7.5	0.42	13.5	0.50
8.0	0.35	11.5	5.00

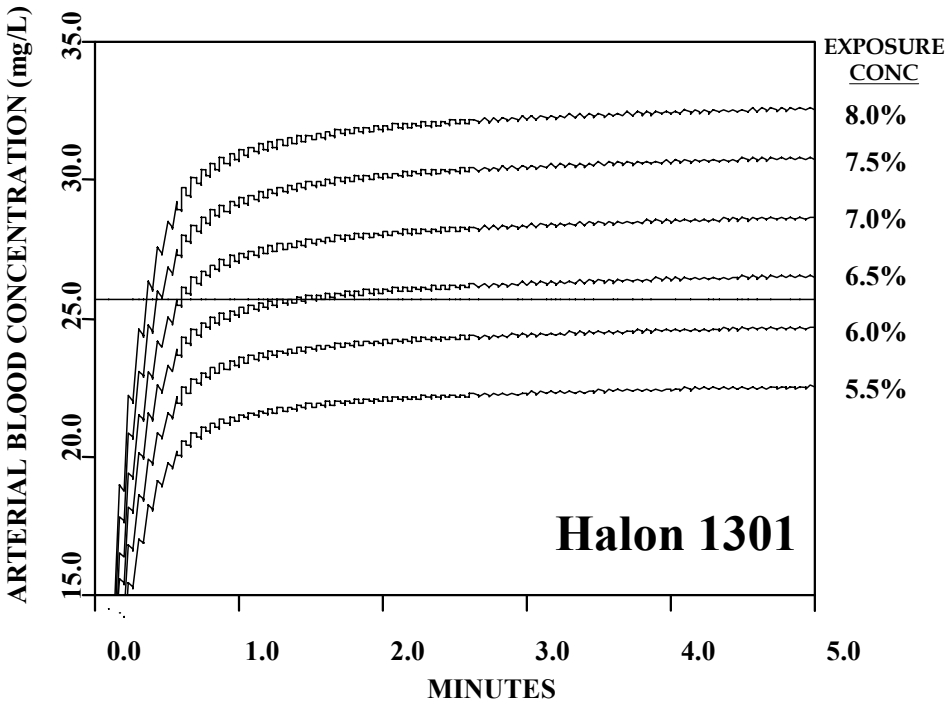

Figure 6–38. Monte Carlo Simulations of Humans Exposed to Halon 1301. [199]

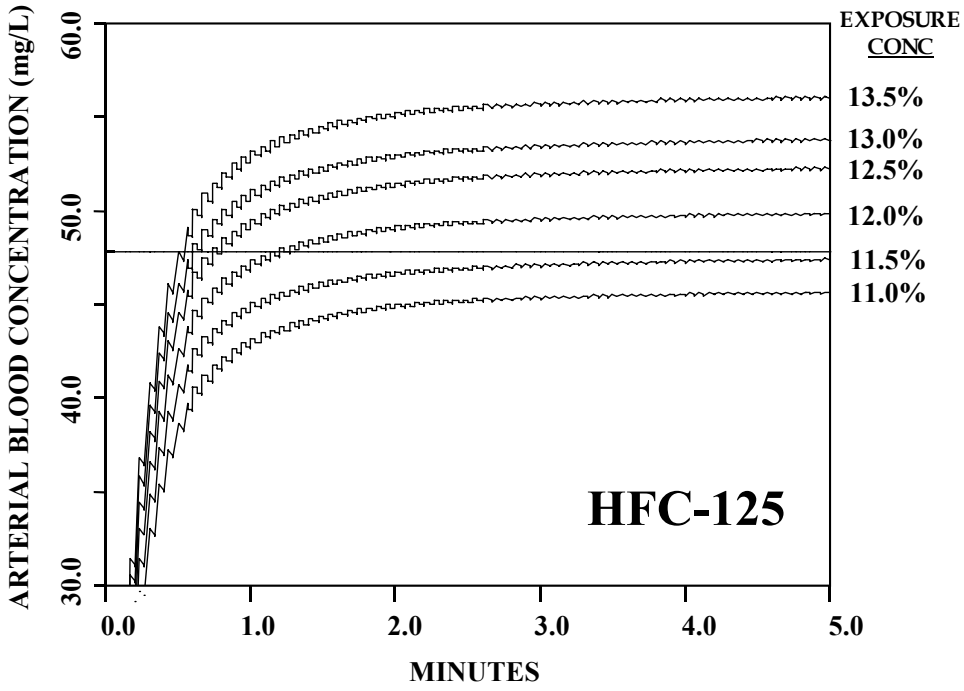

Figure 6–39. Monte Carlo Simulations of Humans Exposed to HFC-125. [199]

The importance of this to approval of a fire suppressant is significant. The specifications for safe exposure design of halon 1301 and potential replacement chemicals for use as total flooding agents in a fire-fighting scenario (section 6.7.1) do not take into consideration the pharmacokinetics of the agents and the relationship between the exposure concentration and the internal concentration actually associated with a cardiac event.

The critical issue in applying any standard for safe exposure is the relationship between the effective concentration of agent necessary to extinguish a fire and the concentration that poses a potential threat for cardiac sensitization. Where the extinguishing concentration approaches the cardiac sensitization concentration, the agent may still be approved for use as a fire extinguishant but only in areas that are normally unoccupied. For candidate agents where the extinguishing concentration is above the cardiac sensitization concentration, there is reluctance by some to risk using the agent because of perceived potential for accidental exposure. An additional consideration is that many of these agents release halogen acids upon contact with heat. The toxicity of these acids is of concern. Levels of release can be reduced if the fire can be put out quickly, which can be done if higher concentrations of extinguishing agent are used.

A comparison was made between the concentration for safe 5 min exposure and the recommended design concentration of agent for extinguishing a fire. As can be seen in Table 6–15, exposure to HFC-125 can occur safely for at least 5 min at an exposure concentration of 11.5 volume %, which is above the LOAEL by 1.5 volume %. The recommended design concentration for fire extinguishment is 10.4 volume % to 11.3 volume %.[99] Thus, the PBPK simulation suggested that it was safe to stay for 5 min in an HFC-125 environment that would put out a fire. From Table 6–15, the safe 5 min exposure for halon 1301 occurred at 5.5 volume % which was below the LOAEL by 2.0 volume %. The design concentration for fire extinguishment was 5 volume %.[203] Thus, the PBPK simulation suggested that it is not safe to stay for 5 min in a halon 1301 environment that would put out a fire. Halon 1301 has a long history of safe use, which points to the conservative nature of the cardiac sensitization endpoint, which ultimately determines the target arterial concentration, which in turn is used for determining safe exposure time.

After a range of chemical concentrations has been evaluated using the cardiac sensitization protocol, the dose-response data can be used to establish the NOAEL and LOAEL. Utilization of the animal testing data for assessing potential risks to humans requires development of appropriate risk assessment methods. These methods must address the unusual exposure circumstances involved in the use of chemicals as fire suppressants. In particular, potential exposures would be for relatively brief, but varying, periods of time at concentrations high enough to effectively extinguish fires. Egress times need to be established for people occupying a facility at the time of chemical agent discharge. The LOAEL determined in dogs has been applied directly by the EPA in evaluating acceptable use and allowable exposure limits for humans. Establishing egress times from the 5 min exposure LOAEL requires careful consideration of the relationship between exposure concentration, duration, and the temporal aspects of the biological response. Under steady state conditions, the concentration in blood and tissues would be constant regardless of the exposure duration.

Simulations of Exposure to Time-varying Concentration Environments

AFRL demonstrated how to use the method to evaluate the potential for the occurrence of a cardiac-sensitizing event for time-varying concentrations. [199] The examples chosen were exposures to halon 1301 and halon 1211 in three aircraft for which concentration measurements had been reported. These data were used with the PBPK model to see if any of the described scenarios could put passengers or crew at potential risk for cardiac sensitization.

1. A fleet-configured Navy E-2B "Hawkeye" airplane.[204] Using a Statham Laboratories Model GA-2A gas recorder, concentrations of halon 1301 were measured at head level in areas occupied by flight crewmembers and in airplane locations where fire hazard potential posed the greatest threat. Under these conditions at floor level in the equipment area, the concentrations of halon 1301 in arterial blood exceeded the target concentration at about 40 s into the exposure and remained above the target for the duration of the measurements. Arterial concentration simulations remained below target at the other measured sites.
2. A Cessna Model C-421B, a small pressurized aircraft.[205] Halon 1211 and halon 1301 were measured using factory field-modified Beckman Model 865 infrared gas analyzers. Measurements were made at three locations:
   - The actual fire extinguisher discharge location.
   - Knee area – 0.50 m above the floor at the area of discharge. The discharge area for pilot's and copilot's seat tests was at knee level where the seat cushion meets the seat back.
   - Nose area – 0.94 m above the floor at the area of discharge.

   The releases of halon 1301 resulted in simulated arterial concentrations well below the target concentration. Releases of halon 1211 resulted in simulated arterial concentrations that surpassed the target concentration of 21.0 mg/L in well under a minute.
3. A Cessna Model 210C, a small non-pressurized aircraft.[206] Halon 1211 and halon 1301 were measured using modified Beckman Model 865 infrared gas analyzers. Measurements were made at the point of release and at two other selected sites during each test. Halon 1301 arterial concentrations remained below the target concentration, while halon 1211 arterial concentrations exceeded the target level at all measured locations when the extinguisher was directed under the instrument panel on the pilot's side with overhead vents open or closed.

The use of halon 1301 for several decades has occurred with an excellent safety record. Retrospective modeling of scenarios such as those illustrated here showed that generally under normal use there has been little to no opportunity for the occurrence of exposure situations where individuals have been put at potential risk of having blood levels of halon 1301 ever reach a target concentration that might predispose for the onset of a cardiac sensitization response. Halon 1211, when used as a streaming agent under open conditions, likewise has posed little risk. However, when used under more confined situations, the potential for cardiac sensitization exists. Several scenarios illustrated above showed situations where arterial concentrations of halon 1211 exceeded the target associated with a potential for cardiac sensitization. The report of an incident by Lerman et al.[207] demonstrated that the risk is real if halon 1211 were used under confined situations where the exposure concentration got high enough to result in highly elevated blood concentrations.

The PBPK model has been used both retrospectively to evaluate previous actual exposure scenarios and prospectively to evaluate potential exposure scenarios. An example of a retrospective evaluation was given in Vinegar et al., where they evaluated an accidental exposure to halon 1211 that had occurred during an Israeli military exercise.[198] In this instance, model predictions were consistent with the outcome where the gunner, having only brief exposure, successfully escaped without incident but the driver, with prolonged exposure, reached levels adequate for cardiac sensitization. The driver, in fact, was observed to be in ventricular fibrillation, never regained consciousness, and died as a result of the incident.

A prospective application of the model was demonstrated by Vinegar et al.[208] In order to evaluate the potential hazard to ground crews of an accidental release of CF_3I, a discharge test was conducted on an F-15 aircraft to record CF_3I concentration time histories at various locations near the aircraft. These exposure data were used with the PBPK model to simulate the potential blood levels of workers at various locations around the aircraft during the release. The blood levels were compared to the target arterial blood concentration associated with cardiac sensitization. Results showed that at some locations the target was not reached, but at the open nacelle the blood concentrations could potentially reach double the target. This information was put in perspective with a further retrospective simulation of individuals who had actually inhaled CF_3I and whose blood concentrations were simulated and estimated to be 100 times the target. These individuals experienced no apparent effect of their exposures.

The code for the PBPK model has been listed in a report by Vinegar and Jepson.[209] It can provide a defensible approach and appropriate tools for decision makers, who are tasked with balancing performance and personnel safety issues, to evaluate the acute toxicity potential of inhaled fire suppressants.

6.7.8 Limit Tests

An acute toxicity test is an essential component of a screening protocol, since the EPA's SNAP program requires acute toxicity of a substitute chemical as part of its submission package. However, under DoD Directive #3216.1, stringent polices dictate that the most conservative approaches must be taken with regard to the use of laboratory animals in research programs. The need to spend time and resources to obtain a once traditional "LC_{50} value" for a halon replacement candidate is discouraged in favor of a single limit test.

The purpose of the limit test is to evaluate mammalian toxicity following a single dose or exposure of the halon replacement candidate. A traditional limit test involves exposing several rats to a single, conservative dose of chemical for a fixed period of time and determining whether this dose is lethal.[210] For gaseous chemicals, inhalation is the most important route of exposure, whereas for liquids, skin contact may be more important than inhalation. For volatile candidate fire suppressants, a typical exposure is to a concentration of 10 volume % for 15 min, both of which are likely in excess of the exposure of people were the chemical eventually used as a fire suppressant. Following the limit test, the (surviving and dead) animals are typically examined for other adverse effects.

For liquid and solid candidate suppressants, an acute irritancy test could be used to evaluate the potential of a chemical to cause irritation in test animals after a single dose or exposure. These tests are usually performed in rabbits' eyes and skin since rabbits have a well-characterized response to irritants. Standard

protocols for irritation testing are described in the EPA's Office of Prevention, Pesticides, and Toxic Substances Health Effects Test Guidelines. The guidelines for acute eye and skin irritation are 870.2400 and 870.2500, respectively (OPPTS Series 870). The URL is:

http://www.epa.gov/docs/OPPTS_Harmonized/870_Health_Effects_Test_Guidelines.

6.8 APPLICATION OF SCREEN TESTS

Table 6–16 summarizes the screening tests as described above, along with the quantities of chemicals needed for their use. In practice, as will be seen in Chapter 7, it was generally easy to eliminate candidate chemicals from further consideration based on the most basic screening procedures.

- The NGP relied most heavily on cup burner data and the presence of one or more chemically active atoms for estimating a chemical's fire suppression efficiency. Only compounds whose extinguishment concentration was measured or estimated to be below 5 volume % were considered further.
- Next, compounds whose boiling points were above 20 °C were eliminated from further consideration. For fluids with slightly higher boiling points, similar fluids were considered to see if there might be a lower boiling member of the chemical family.
- Third, a chemical continued under consideration if it had a feature that rendered it tropodegradable, i.e., likely to have a short atmospheric lifetime.
- Most of the compounds considered were of unknown toxicity, so in relatively few cases could a confident safe exposure value be assigned. For compounds that were successful in the first three properties, a limit test would be performed. Success there would lead to a dog exposure test. In practice, no animal tests were performed for agents for in-flight fire suppression.

Table 6–16. Nominal Quantities of Chemicals Needed for Screening Tests.

Property Screened	Method	Total Mass/Volume of Chemical Required
Fire Suppression Efficiency	Cup burner	750 mL (gas)
	DLAFSS	10 mL (liquid)
	TARPF	10 g
Volatility	Boiling point	0.2 mL
Atmospheric lifetime	OH reactivity	5 L (gas)
	Absorption spectrum	10 mL (gas)
Toxicity	Literature	0 g
	Dog test	5 kg

6.9 REFERENCES

1. Gann, R.G., Barnes, J.D., Davis, S., Harris, J.S., Harris, R.H., Herron, J.T., Levin, B.C., Mopsik, F.I., Notarianni, K.A., Nyden, M.R., Paabo, M., and Ricker, R.E., *Preliminary Screening Procedures and Criteria for Replacements for Halons 1211 and 1301*, NIST Technical Note 1278, National Institute of Standards and Technology, 1990.

2. Nyden, M.R., and Skaggs, S.R., *Screening Methods for Agent Compatibility with People, Materials, and the Environment*, NISTIR 6323, National Institute of Standards and Technology, Gaithersburg, MD, 1999.

3. Hamins, A., Gmurczyk, G., Grosshandler, W., Rehwoldt, R.P., Vazquez, I., and Cleary, T., "Flame Suppression Effectiveness," in Grosshandler, W.L., Pitts, W.M., and Gann, R.G., eds., *Evaluation of Alternative In-Flight Fire Suppressants for Full-Scale Testing in Simulated Aircraft Engine Nacelles and Dry Bays,* NIST Special Publication 861, National Institute of Standards and Techno, Gaithersburg, MD, 1994.

4. Significant New Alternative Policy (SNAP) Program Final Rule, *Federal Register* **59**, 13044, March 18, 1994.

5. *Climate Change 1995, The Science of Climate Change*, Intergovernmental Panel on Climate Change (IPCC), 1995.

6. Pitts, W.M., Yang, J.C., Bryant, R.A., Blevins, L.G., and Huber, M.L., *Characteristics and Identification of Super-Effective Thermal Fire-extinguishing Agents*, NIST Technical Note 1440, National Institute of Standards and Technology, Gaithersburg, MD, 2006.

7. Creitz, E.C., "Inhibition of Diffusion Flames by Methyl Bromide and Trifluoromethyl Bromide Applied to the Fuel and Oxygen Sides of the Reaction Zone," *Journal of Research of the National Bureau of Standards (U.S.)* **65 (4)**, 389, (1961).

8. Hirst, R., and Booth, K., "Measurement of Flame-extinguishing Concentrations," *Fire Technology* **13(4)**, 296-315 (1977).

9. Bajpai, S.N., *Inerting Characteristics of Halons 1301 and 1211*, Report 22391.3, Factory Mutual Research, Norwood, MA, 1974.

10. Mather, J.D., and Tapscott, R.E., *Tropodegradable Bromocarbon Extinguishants II, Final report to the Strategic Environmental Research and Development Program (SERDP)*, 1994, available on the NGP web site: www.bfrl.nist.gov/866/NGP.

11. Yang, J.C., Donnelly, M.K., Prive, N.C., and Grosshandler, W.L., "An Apparatus for Screening Fire Suppression Efficiency of Dispersed Liquid Agents," *Fire Safety Journal* **36**, 55-72 (2001).

12. Yang, J.C., Donnelly, M.K., Prive, N.C., and Grosshandler, W.L., *Dispersed Liquid Agent Fire Suppression Screen*, NISTIR 6319, National Institute of Standards and Technology, Gaithersburg, MD, 1999.

13. Tsuji, H. and Yamaoka, I., "The Counterflow Diffusion Flame in the Forward Stagnation Region of a Porous Cylinder," *Proceedings of the Combustion Institute* **11**, 979-984 (1967).

14. Tsuji, H. and Yamaoka, I., "The Structure of Counterflow Diffusion Flames in the Forward Stagnation Region of a Porous Cylinder," *Proceedings of the Combustion Institute* **12**, 997-1005, (1969).

15. Tsuji, H. and Yamaoka, I., "Structure Analysis of Counterflow Diffusion Flames in the Forward Stagnation Region of a Porous Cylinder," *Proceedings of the Combustion Institute* **12,** 723-731 (1971).

16. Tsuji, H., "Counterflow Diffusion Flames," *Progress in Energy and Combustion Science* **8**, 93 (1982).

17. Ishizuka, S. and Tsuji, H., "An Experimental Study of Effect of Inert Gases on Extinction of Laminar Diffusion Flames," *Proceedings of the Combustion Institute* **18**, 695-703 (1981).

18. Milne, T.A., Green, C.L., and Benson, D.K., "The Use of the Counterflow Diffusion Flame in Studies of Inhibition Effectiveness of Gaseous and Powdered Agents," *Combustion and Flame* **15**, 255 (1970).

19. Dixon-Lewis, G., David, T., Gaskell, P.H., Fukutani, S., Jinno, H., Miller, J.A., Kee, R.J., Smooke, M.D., Peters, N., Effelsberg, E., Warnatz, J., and Behrendt, F., "Calculation of the Structure and Extinction Limit of a Methane-Air Counterflow Diffusion Flame in the Forward Stagnation Region of a Porous Cylinder," *Proceedings of the Combustion Institute* **20**, 1893-1904, (1984).

20. Dreier, T., Lange, B., Wolfrum, J., Zahn, M., Behrendt, F., and Warnatz, J., "CARS Measurements and Computations of the Structure of Laminar Stagnation-Point Methane-Air Counterflow Diffusion Flames," *Proceedings of the Combustion Institute* **21**, 1729-1736 (1986).

21. Peters, N. and Kee, R.J., "The Computation of Stretched Laminar Methane-Air Diffusion Flames Using a Reduced Four-Step Mechanism," *Combustion and. Flame*, **68**, 17 (1987).

22. Olson, S.L. and T'ien, J.S., "A Theoretical Analysis of the Extinction Limits of a Methane-Air Opposed-Jet Diffusion Flame," *Combustion and Flame*, **70**, 161 (1987).

23. Dixon-Lewis, G. and Missaghi, M., "Structure and Extinction Limits of Counterflow Diffusion Flames of Hydrogen-Nitrogen Mixtures in Air," *Proceedings of the Combustion Institute* **22**, 1461-1470 (1988).

24. Chen, C.H. and Weng, F.B., "Flame Stabilization and Blowoff Over a Porous Cylinder," *Combustion. Science and Technology*, **73**, 427 (1990).

25. Sick, V., Arnold, A., Diesel, E., Dreier, T., Ketterle, W., Lange, B., Wolfrum, J., Thiele, K.U., Behrendt, F., and Warnatz, J., "Two-Dimensional Laser Diagnostics and Modeling of Counterflow Diffusion Flames," *Proceedings of the Combustion Institute* **23**, 495-501 (1990).

26. Yang, J.C., Chien, W., King, M., and Grosshandler, W.L., "A Simple Piezoelectric Droplet Generator," *Experiments in Fluids*, **23**, 445 (1997).

27. Yang, J.C., Donnelly, M.K., Privé, N.C., and Grosshandler, W.L., "Fire Suppression Efficiency Screening Using a Counterflow Cylindrical Burner," *Proceedings of the 5th ASME/JSME Joint Thermal Engineering Conference*, San Diego, California, March 1999.

28. Hamins, A., Gmurczyk, G, Grosshandler, W., Rehwoldt, R.G., Vazquez, I., Cleary, T., Presser, C., and Seshadri, K., Flame Suppression Effectiveness," Chapter 4 in Grosshandler, W., Gann, R.G., , and Pitts, W.M., eds., *Evaluation of Alternative In-flight Fire Suppressants for Full-scale Testing in Simulated Engine Nacelles and Dry Bays*, NIST SP 861, National Institute of Standards and Technology, Gaithersburg, MD, 1994.

29. Yang, J.C., Prive, N.C., Donnelly, M.K., Grosshandler, W.L., "Recent Results from the Dispersed Liquid Agent Fire Suppression Screen," in Gann, R.G., Burgess, S.R., Whisner, K.C., and Reneke, P.A., eds., *Papers from 1991-2006 Halon Options Technical Working Conferences (HOTWC)*, CD-ROM, NIST SP 984-4, National Institute of Standards and Technology, Gaithersburg, MD, 2006.

30. Rossotti, H., *Fire*, Oxford University Press, Oxford, UK, 1993.

31. Finnerty, A.E., McGrill, R.L., and Slack, W.A., *Water-Based Halon Replacement Sprays*, ARL-TR-1138, U.S. Army Research Laboratory, Aberdeen Proving Ground, MD, July 1996.

32. Lentati, A.M. and Chelliah, H.K., "Physical, Thermal, and Chemical Effects of Fine-Water Droplets in Extinguishing Counterflow Diffusion Flames," *Proceedings of the Combustion Institute* **27**, 2839-2846 (1998).

33. Grosshandler, W., Hamins, A., McGrattan, K, Charagundla, S.R., and Presser, C., "Suppression of a Non-Premixed Flame Behind a Step," *Proceedings of the Combustion Institute* **28**, 2957-2964 (2001).

34. Hirst, R. and Sutton, D., "The Effect of reduced pressure and Airflow on Liquid Surface Diffusion flames," *Combustion and Flame* **5***,* 319-330 (1961).

35. Hirst, R., Farenden, P.J., and Simmons, R.F., "The Extinction of Fires in Aircraft Jet Engines – Part 1, Small-scale Simulation of Fires," *Fire Technology* **12***,* 266-275 (1976).

36. Hirst, R., Farenden, P.J., and Simmons, R.F., "The Extinction of Fires in Aircraft Jet Engines – Part II, Full-scale Fire Tests," *Fire Technology* **13***,* 59-68 (1977).

37. Hamins, A., Cleary, T., Borthwick, P., Gorchov, N., McGrattan, K., Forney, G., Grosshandler, W., Presser, C., and Melton, L., "Suppression of Engine Nacelle Fires," Chapter 9 in *Fire Suppression System Performance of Alternative Agents in Aircraft Engine and Dry Bay Lab. Simulations*, NIST SP 890: Vol. II, Gann, R.G. (ed.), National Institute of Standards and Technology, Gaithersburg, MD, 1995.

38. Takahashi, F., Schmoll, W.J., Strader, E.A., and Belovich, V.M., "Suppression of a Nonpremixed Flame Stabilized by a Backward-Facing Step," *Combustion and Flame* **122**, 105-116 (2000).

39. Hamins, A, Gmurczyk, G., Grosshandler, W., Rehwoldt, R., Vazquez, I., Cleary, T., Presser, C., and Seshadri, K., "Flame Suppression Effectiveness," Chapter 4 in *Evaluation of Alternative In-flight Fire Suppressants for Full-scale Simulated Aircraft Engine Nacelles and Dry Bays*, (Grosshandler, W.L., Gann, R.G., and Pitts, W.M., eds.) NIST SP 861, National Institute of Standards and Technology, Gaithersburg, MD, 1994.

40. W. Leach, Naval Air Systems Command, personal correspondence to W. Grosshandler, National Institute of Standards and Technology, 1998.

41. Hamins, A., Cleary, T., and Yang, J., "An Analysis of the Wright-Patterson Full-Scale Engine Nacelle Fire Suppression Experiments," NISTIR 6193, National Institute of Standards and Technology, Gaithersburg, MD, 1997.

42. Mitchell, M., "Hybrid Fire Extinguisher for Occupied and Unoccupied Spaces," in Gann, R.G., Burgess, S.R., Whisner, K.C., and Reneke, P.A., eds., *Papers from 1991-2005 Halon Options Technical Working Conferences (HOTWC)*, CD-ROM, NIST SP 984-3, National Institute of Standards and Technology, Gaithersburg, MD, (2005).

43. Wierenga, P .H., and Holland, G. F., "Developments in and Implementation of Gas Generators for Fire Suppression," in Gann, R.G., Burgess, S.R., Whisner, K.C., and Reneke, P.A., eds., *Papers from 1991-2006 Halon Options Technical Working Conferences (HOTWC)*, CD-ROM, NIST SP 984-4, National Institute of Standards and Technology, Gaithersburg, MD, 2006.

44. Grosshandler, W., Hamins, A., McGrattan, K., and Presser, C., *Transient Application, Recirculating Pool Fire, Agent Effectiveness Screen: Final Report, NGP Project 3A/2/890,* NISTIR 6733, National Institute of Standards and Technology, Gaithersburg, MD, 2001.

45. Taylor, B.N. and Kuyatt, C.E., *Guidelines for Evaluating and Expressing the Uncertainty of NIST Measurement Results*, NIST Technical Note 1297, National Institute of Standards and Technology, Gaithersburg, MD, (1993).

46. J. Neidert, Atlantic Research Corporation, personal communication to W. Grosshandler, National Institute of Standards and Technology, 2000.

47. McGrattan, K.B., Baum, H.R., Rehm, R.G., Hamins, A., and Forney, G.P., *Fire Dynamics Simulator, Technical Reference Guide*, NISTIR 6467, National Institute of Standards and Technology, Gaithersburg, MD, 2000.

48. Reid, R.C., Prausnitz, J.M. and Poling, B.E., *Properties of Gases and Liquids*, McGraw-Hill, Inc., New York, 4th edition, 1987.

49. Satcunanathan, S., and Zaczek, B.J., "The Spontaneous Ignition and Ignition Delay of Liquid Fuel Droplets Impinging on a Hot Surface," Thermodynamics and Fluid Mechanics Convention, Institution of Mechanical Engineers, London, 27-29 March, 1968.

50. Jomaas, G., Roberts, B.T., DuBois, J., and Torero, J.L.,*A Study of the Mechanisms Leading to Re-ignition in a 'Worst Case' Fire Scenario*, Final Report, Cooperative Agreement No. 70NANB8H0043, Department of Fire Protection Engineering, University of Maryland College Park, MD20742-3031, June, 2000. (Also NIST GCR 01-806, National Institute of Standards and Technology, Gaithersburg, MD, 2001.)

51. Grosshandler, W.L., Hamins, A., Charagundla, R., and Presser, C., "Suppression Effectiveness Screening for Impulsively Discharged Agents," in Gann, R.G., Burgess, S.R., Whisner, K.C., and Reneke, P.A., eds., *Papers from 1991-2006 Halon Options Technical Working Conferences (HOTWC)*, CD-ROM, NIST SP 984-4, National Institute of Standards and Technology, Gaithersburg, MD, 2006.

52. Trees, D., Seshadri, K., and Hamins, A.M., "Exp. Studies of Diffusion Flame Extinction with Halogenated and Inert Fire Suppressants," in *Halon Replacements - Technology and Science*, Miziolek, A.W., and Tsang, W. (eds.), ACS Symposium Series 611, American Chemical Society, Washington, DC, 1995.

53. Sheinson, R. S., Penner-Hahn, J. E., and Indritz, D., "The Physical and Chemical Action of Fire Suppressants," *Fire Safety Journal* **15**, pp 437-450 (1989).

54. Finlayson-Pitts, B.J., and Pitts, Jr., J.N., *Chemistry of the Upper and Lower Atmosphere*, Academic Press, New York, 2000.

55. Tapscott, R.E. and Olivares-Sooley, M.G., "Decision Tree for Global Environmental Impact Screening," in Gann, R.G., Burgess, S.R., Whisner, K.C., and Reneke, P.A., eds., *Papers from 1991-2006 Halon Options Technical Working Conferences (HOTWC)*, CD-ROM, NIST SP 984-4, National Institute of Standards and Technology, Gaithersburg, MD, 2006.

56. Fischer, D.A., Hales, C.H., Filkin, D.L., Ko, M.K.W., Sze, N.D., Connell, P.S., Wuebbles, D.J., Isaksen, I.S.A., and Stordal, F., "Relative Effects on Stratospheric Ozone of Halogenated Methanes and Ethanes of Social and Industrial Interest," in World Meteorological Organization, Global Ozone Research and Monitoring Project - Report No. 20, *Scientific Assessment of Stratospheric Ozone: 1989*, Vol. II, Appendix: AFEAS Report, pp. 301-377. (Available from Upper Atmosphere Research Program, NASA Headquarters, Washington, D.C., 20546).

57. Skaggs, S. R., and Nimitz, J. S., "Estimating Tropospheric Lifetimes and Ozone-Depletion Potentials of One- and Two-Carbon Hydrofluorocarbons and Hydrochlorofluorocarbons," *Environmental Science and Technology* **26**, 739-744 (1992).

58. Iikubo, Y., and Robin, M. L., "Fire Extinguishing Methods and Blends Utilizing Hydrofluorocarbons," USA, Patent Number 5,124,053, 23 June 1992. Assigned to Great Lakes Chemical Corporation.

59. *Scientific Assessment of Ozone Depletion: 1994*, Report No. 37, National Oceanic and Atmospheric Administration, National Aeronautics and Space Administration, United Nations Environment Programme, and World Meteorological Organization, February 1995.

60. Connell, P. S., and Wuebbles, D. J., "Ozone Depletion Potential, Halons, and Halon Alternatives," NMERI Halon Alternatives Program Review, Albuquerque, NM, 23-24 Jan 1991.

61. *Risk Screen on the Use of Substitutes for Class I Ozone-Depleting Substances: Fire Suppression and Explosion Protection (Halon Substitutes)*, SNAP Technical Background Document, U.S. Environmental Protection Agency, Washington, DC, March 1994.

62. "Protection of Stratospheric Ozone: Final Rule," *Federal Register*, **60 (113)**, 31092-31107, 13 June 1995.

63. Prinn, R., Weiss, R. F., Miller, B. R., Huang, J., Alyea, F. N., Cunnold, D. M., Fraser, P. J., Hartley, D. E., and Simmonds, P. G., "Atmospheric Trends and Lifetime of CH_3CCl_3 and Global OH Concentrations," *Science* **269**, No. 5221, 187-192 (1995).

64. Wuebbles, D. J., and Connell, P. S., *A Screening Methodology for Assessing the Potential Impact of Surface Releases of Chlorinated Halocarbons on Stratospheric Ozone*, UCID-19233, Lawrence Livermore Laboratory, Livermore, California, November 1981.

65. Prather, M. J., and Spivakovsky, C. M., "Tropospheric OH and the Lifetimes of Hydrochlorofluorocarbons," *Journal of Geophysical Research*, **95**, 18723-18729 (1990).

66. Imasu, R., Suga, A., and Matsuno, T., "Radiative Effects and Halocarbon Global Warming Potentials of Replacement Compounds for Chlorofluorocarbons," *Journal of the Meteorological Society of Japan* **73**, No. 6, 1123-1136 (1995).

67. Zhang, Z., Saini, R. D., Kurylo, M. J., and Huie, R. E., "Rate Constants for the Reactions of the Hydroxyl Radical with Several Partially Fluorinated Ethers," *Journal of Physical Chemistry*, **96**, 9301-9304 (1992).

68. Atkinson, R., "Kinetics and Mechanisms of the Gas-Phase Reactions of the Hydroxyl Radical with Organic Compounds," *Journal of Physical and Chemical Reference Data, Monograph No. 1*, American Chemical Society, Washington, DC, and American Institute of Physics, Woodbury, New York, 1989.

69. Cooper, D. L., Cunningham, T. P., Allan, N. L., and McCulloch, A., "Potential CFC Replacements: Tropospheric Lifetimes of C3 Hydrofluorocarbons and Hydrofluoroethers," *Atmospheric Environment* **27A**, No. 1, 117-119 (1993).

70. Prather, M.C., "Tropospheric Hydroxyl Concentrations and the Lifetimes of Hydrochlorofluorocarbons (HCFCs)," in World Meteorological Organization, *op. cit.*, 147-158.

71. Kurylo, M.J., and Braun, W., "Flash Photolysis Resonance Fluorescence Study of the Reaction Cl + O3 6 ClO + O2 Over the Temperature Range 213-298 K," *Chemical Physics Letters* **37**, 232 (1976).

72. Kurylo, M.J., Cornett, K.D., and Murphy, J.L., "The Temperature Dependence of the Rate Constant for the Reaction of Hydroxyl Radicals with Nitric Acid," *Journal of Geophysical Research* **87**, 3081-3085 (1982).

73. Ravishankara, A.R., Wine, P.H., and Nicovich, J.M., "Pulsed Laser Photolysis Study of the Reaction between $O(^3P)$ and HO_2," *Journal of Chemical Physics* **78**, 6629 (1983).

74. Molina, L.T., Molina, M.J., and Rowland, F.S., "Ultraviolet Absorption Cross Sections of Several Brominated Methanes and Ethanes of Atmospheric Interest," *Journal of Physical Chemistry* **86**, 2672-2676 (1982).

75. Gillotay, D., and Simon, P.C., "Ultraviolet Absorption Spectrum of Trifluoro-bromomethane, Difluoro-dibromomethane, and Difluoro-bromo-chloromethane in the Vapor Phase," *Journal of Atmospheric Chemistry* **8**, 41 (1989).

76. Klein, R., Braun, W., Fahr, A., Mele, A., and Okabe, H., "Scattered Light and Other Corrections in Absorption Cross Section Measurements in the Vacuum Ultraviolet: A Systems Approach," *Journal of Research of the National Institute of Standards and Technology* **95**, 337-344 (1990).

77. Kaufman. F., "Kinetics of Elementary Radical Reactions in the Gas Phase," *Journal of Physical Chemistry* **86**, 69 (1984).

78. Atkinson, R., "Kinetics and Mechanisms of the Gas-Phase Reactions of the Hydroxyl Radical with Organic Compounds under Atmospheric Conditions," *Chemical Reviews* **86**, 69-201 (1986).

79. Nimitz, J.S., and Skaggs, S.R., "Estimating Tropospheric Lifetimes and Ozone-depleting Potentials of One- and Two-carbon Hydrofluorocarbons," *Environmental Science and Technology* **26**, 739-744, (1992).

80. Orkin, V. L., Villenave, E., Huie, R. E., and Kurylo, M. J., "Atmospheric Lifetimes and Global Warming Potentials of Hydrofluoroethers: Reactivity Toward OH, UV Spectra, and IR Absorption Cross Sections", *Journal of Physical Chemistry A*, **103**, 9770-9779 (1999).

81. Louis, F., Gonzalez, C., Huie, R. E., and Kurylo, M. J., "An *ab Initio* Study of the Reaction of Halomethanes with the Hydroxyl Radical. Part 1: CH_2Br_2", *Journal of Physical Chemistry A*, **104**, 2931-2938 (2000).

82. Louis, F., Gonzalez, C., Huie, R. E., and Kurylo, M. J., "An *Ab Initio* Study of the Kinetics of the Reactions of Halomethanes with the Hydroxyl Radical. Part 2: A Comparison between Theoretical and Experimental Values of the Kinetic Parameters for 12 Partially Halogenated Substituted Methanes," *Journal of Physical Chemistry A*, **104**, 8773-8778 (2000).

83. Louis, F., Gonzalez, C., Huie, R. E., and Kurylo, M. J., "An *Ab Initio* Study of the Kinetics of the Reactions of Halomethanes with the Hydroxyl Radical. Part 3. Reactivity Trends and Kinetics Parameter Predictions for the Potential Halon Replacements CH_2FBr, $CHFBr_2$, CHFClBr, $CHCl_2Br$, and $CHClBr_2$," *J. Phys. Chem. A*, **105**, 1599-1604 (2001).

84. Kozlov, S. N., Orkin, V. L., Huie, R. E., and Kurylo, M. J., "OH Reactivity and UV Spectra of Propane, n-Propyl Bromide, and Isopropyl Bromide," *Journal of Physical Chemistry A.* **107**, 1333-1338 (2003).

85. Orkin, V. L., Louis, F., Huie, R. E., and Kurylo, M. J., "Photochemistry of Bromine-Containing Fluorinated Alkenes: Reactivity toward OH and UV Spectra," *Journal of Physical Chemistry A*, **106**, 10195-10199 (2002).

86. Pitts, W.M., Yang, J.C., Gmurczyk, G., Cooper, L.Y., Grosshandler, W.L., Cleveland, W.G., and Presser, C., "Fluid Dynamics of Agent Discharge," in Grosshandler, W.L., Pitts, W.M., and Gann, R.G., eds., *Evaluation of Alternative In-Flight Fire Suppressants for Full-Scale Testing in Simulated Aircraft Engine Nacelles and Dry Bays,* NIST Special Publication 861, National Institute of Standards and Technology, Gaithersburg, MD, 1994.

87. Brabson, G.D., Garcia, M.M., Heinonen, E.W., Juarez, G., Mather, J.D., and Tapscott, R.E., *Main Group Compounds as Extinguishants*, Report No. 98/8/33380, New Mexico Engineering Research Institute, Albuquerque, NM, 2001, available on the NGP web site: www.bfrl.nist.gov/866/NGP.

88. Hirschfelder, J. O., Curtiss, C. F., and Bird, R. B., *The Molecular Theory of Gases and Liquids*, John Wiley & Sons, New York, 1954.

89. Perry, R. H., and Green, D. W., editors, *Perry's Chemical Engineering Handbook*, Seventh Edition, McGraw-Hill, New York, 1997.

90. Green, H. L., and Lane, W. R., *Particulate Clouds: Dusts, Smokes, and Mists*, E. & F. N. Spon Ltd., London, 1964.

91. *NIST Structures and Properties, Version 2.0*, NIST Standard Reference Database 25, National Institute of Standards and Technology, Gaithersburg, MD, January 1994.

92. Pavia, D.L., Lampman, G.M., Kriz, G.S., and Engel, R.G., *Introduction to Organic Laboratory Techniques - A Small Scale Approach*, Brooks/Cole Publishing, 2005.

93. The isoteniscope procedure and equipment are a modification of ASTM D 2879-86, ASTM International, West Conshohocken, PA.

94. *An Appraisal of Halogenated Fire Extinguishing Agents,* National Academy of Sciences, Washington, DC, 1972.

95. Reinhardt, C.F., Azar, A., Maxfield, M.E., Smith, P.E., and Mullin, L.S, "Cardiac Arrhythmias and Aerosol Sniffing," *Archives of Environmental Health* **22**, 265-279 (1971).

96. Dodd, D.E., Jepson, G.W., and Macko, Jr., J.A., *Human Health Safety Evaluation of Halon Replacement Candidates*, Section II" Final Report to the U.S. Department of Defense, Strategic Environmental Research and Development Program, 2000.

97. Lewis, R. J., Sr., *Sax's Dangerous Properties of Industrial Materials*, Ninth Edition, Van Nostrand Reinhold, New York, 1996.

98. Harris, W. S., "Cardiac Effects of Halogenated Hydrocarbons," in *An Appraisal of Halogenated Fire Extinguishing Agents*, National Academy of Sciences, Washington, DC, pp. 114-126, 1972.

99. NFPA 2001, Standard on Clean Agent Fire Extinguishing Systems, NFPA, Quincy, MA, 2004.

100. Gage, C. L., Hendriks, R. V., Smith, N. D., Brna, T. G., *New Chemical Alternative for Ozone-Depleting Substances: HFC-236ea*, EPA-600/R-97-117, NTIS PB98-127384, 1997.

101. *Acute Inhalation Toxicity Study of Iodotrifluoromethane in Rats*, Armstrong Laboratory, Air Force Systems Command, Wright-Patterson Air Force Base, Ohio, March 1994

102. Beck, P. S., Clark, D. G., Tinston, D. J., "The Pharmacologic Actions of Bromochlorodifluoromethane (BCF)," *Toxicology and Applied Pharmacology*, (1973).

103. *Registry of Toxic Effects of Chemical Substances, 1985-86 Edition*, National Institute of Occupational Safety and Health, U.S. Department of Health and Human Services, Washington, DC.

104. Skaggs, S. R., Dierdorf, D. S., and Tapscott, R. E., "Update on Iodides as Fire Extinguishing Agents," *Proceedings of the 1993 CFC and Halon Alternatives Conference,* Washington, DC, pp. 800-809, 1993.

105. Calm, J.M., "Refrigerant Safety," *ASHRAE Journal*, 17-26, (1974).

106. Bogdan, M., "Blowing Agents: Producer and User Perspective," International Chemical Congress of Pacific Basin Societies, 17-22 December, 1996.

107. Davies, R. H.,Bagnall, R. D.,Bell, W., Jones, W. G. M., "The Hydrogen Bond Proton Donor Properties of Volatile Halogenated Hydrocarbons and Ethers and Their Mode of Action in Anaesthesia," *International Journal of Quantum Chemistry*, Quantum Biology Symposium No. 3, 171-185, (1976).

108. Skaggs, S. R., Tapscott, R. E., Heinonen, E.W., "Advanced Agent Program: Toxicological Screening Methods," NMERI 95/48/31882, Wright Laboratories (WL/FIVCF), Tyndall Air Force Base, Florida, December 1996.

109. Kier, L. B., and Hall, L. H., "The Nature of Structure-Activity Relationships and Their Relation to Molecular Connectivity," *European Journal of Medicinal Chemistry* **12**, 307-312 (1977).

110. Blum, D., and Speece, R., "Determining Chemical Toxicity to Aquatic Species," *Environmental Science and Technology* **24**, 284-294 (1990).

111. Kier, L. B., and Hall, L. H., *Molecular Connectivity in Structure-Activity Analysis*, John Wiley & Sons, Inc., New York, 1986.

112. Vinegar, A., ManTech Environmental Technology Inc., Dayton, Ohio, personal correspondence to R. E. Tapscott, New Mexico Engineering Research Institute, The University of New Mexico, May 1997.

113. Dearden, J.C., Barratt, M.D., Benigni, R., Bristol, D.W., Combes, R.D., Cronin, M.T.D., Judson, P.N., Payne, M.P., Richard, A.M., Tichy, M., Worth, A.P., and Yourick, J.J., "The Development and Validation of Expert Systems for Predicting Toxicity," The Report and Recommendations of ECVAM Workshop 24, Atlanta, pp. 25:223-252, 1997.

114. Alarie, Y., Abraham, M.H., Nielsen, G.D., and Schaper, M., "Structure-activity Relationships of Volatile Organic Chemicals as Sensory Irritants," *Archives of Toxicology* **72(3)**,125-40, (1998).

115. Wang, G., and Bai, N., "Structure-activity Relationships for Rat and Mouse LD_{50} of Miscellaneous Alcohols," *Chemosphere* **36(7)**,1475-83 (1998).

116. Rucki, M., Tichy, M., "Acute Toxicity of Alcohols: Prediction by QSAR Analysis and by Molecular Similarity," *Central European Journal of Public Health* **5(4)**,183-187 (1997).

117. Debord, J, et al., "Inhibition of Arylesterase by Aliphatic Alcohols," *Chemical and Biological Interactions* **113(2)**, 105-115 (1998).

118. Cronin, M. T., Schultz, T.W., "Structure-toxicity Relationships for Three Mechanisms of Action of Toxicity to Vibrio Fischeri," *Ecotoxicological Environmental Safety* **39(1)**, 65-69, (1998).

119. Politzer, P, et al., "Molecular Properties of the Chlorinated Ethylenes and their Epoxide Metabolites," *Annals of the New York Academy of Sciences* **367**, 478-492, (1981).

120. Boyes, R. N., "A review of the Metabolism of Amide Local Anesthetic Agents," *British Journal of Anaesthiology* **47 suppl**, 225-230 (1975).

121. Huang, Y., et al., "Synthesis and Quantitative Structure-activity Relationships of N-(1-benzylpiperidin-4-yl) phenylacetamides and Related Analogues as Potent and Selective Sigma1 Receptor Ligands," *Journal of Medicinal Chemistry* **41(13)**, 2361-2370 (1998).

122. Hadjipavlou-Litina, D., "Review, Reevaluation, and New Results in Quantitative Structure-activity Studies of Anticonvulsants," *Medical Research Review* **18(2)**, 91-119 (1998).

123. Nilsson, J., et al. "GRID/GOLPE 3D Quantitative Structure-activity Relationship Study on a Set of Benzamides and Naphthamides, with Affinity for the Dopamine D3 Receptor Subtype," *Journal of Medicinal Chemistry* **40(6)**, 833-840 (1997).

124. Krystek, S.R., Jr., et al., "Three-dimensional Quantitative Structure-activity Relationships of Sulfonamide Endothelin Inhibitors," *Journal of Medicinal Chemistry* **38(4)**, 659-668, (1995).

125. Mager, P.P., "QSAR, Diagnostic Statistics, and Molecular Modelling of Antiallergic Acrylamide Derivatives," *Drug Des. Discov.* **9(2)**, 107-18 (1992).

126. Kaul, S., et al., "Quantitative Structure--pharmacokinetic Relationship of a Series of Sulfonamides in the Rat," *European Journal of Drug Metabolism and Pharmacokinetics* **15(3)**, 211-217 (1990).

127. Lisciani, R., et al., "Structure-analgesic Activity Relationships in a Set of 2-aminobenzamide Derivatives," *Farmaco [Sci]*. **41(2)**, 89-102 (1986).

128. Seydel J.K., et al., "Quantitative Structure-pharmacokinetic Relationships Derived on Antibacterial Sulfonamides in Rats and its Comparison to Quantitative Structure-activity Relationships," *Journal of Medicinal Chemistry* **23(6)**, 607-613 (1980).

129. Recanatini, M., Hansch, C., and Cavalli, A., "A Comparative QSAR Analysis of Acetylcholinesterase Inhibitors Currently Studied for the Treatment of Alzheimer's Disease," *Chemical and Biological Interactions* **105(3)**, 199-228 (1997).

130. Debord, J., et al., "Cholinesterase Inhibition by Derivatives of 2-amino-4,6-dimethylpyridine," Journal of Enzyme Inhibition **12(1)**, 13-26 (1997).

131. Akamatsu, M., et al., "Quantitative Analyses of the Structure-hydrophobicity Relationship for N-acetyl di- and tripeptide Amides," *Journal of Pharmaceutical Science* **83(7)**, 1026-1033 (1994).

132. McGuire, E.J., et al., "Peroxisome Induction Potential and Lipid-regulating Activity in Rats. Quantitative Microscopy and Chemical Structure-activity Relationships," *American Journal of Pathology* **139(1)**, 217-229 (1991).

133. Dai, Q.H., et al., "Quantitative Explanation on Structure-carcinogenic Activity Relationship of Aromatic Amines by Di-region Theory," *Sci. China B* **34(5)**, 547-559 (1991).

134. Trieff, N.M., et al., "Aromatic Amines and Acetamides in Salmonella Typhimurium TA98 and TA100: a Quantitative Structure-activity Relation Study," *Molecular Toxicology* **2(1)**, 53-65 (1989).

135. Purdy, R., "The Utility of Computed Superdelocalizability for Predicting the LC_{50} Values of Epoxides to Guppies," *Sci Total Environ.* **109-110**, 553-6 (1991).

136. Hatch, F.T., et al., "Quantitative Structure-activity (QSAR) Relationships of Mutagenic Aromatic and Heterocyclic Amines," *Mutation Research* **376(1-2)**, 87-96 (1997).

137. Sabbioni, G., et al., "Quantitative Structure-activity Relationships of Mutagenic Aromatic and Heteroaromatic Azides and Amines," *Carcinogenesis* **13(4)**, 709-73 (1992).

138. Roberts, D. W., Basketter, D. A., "Further Evaluation of the Quantitative Structure-activity Relationship for Skin-sensitizing Alkyl Transfer Agents," *Contact Dermatitis* **37(3)**, 107-112 (1997).

139. Ehring, G.R., et al., "Quantitative Structure Activity Studies of Antiarrhythmic Properties in a Series of Lidocaine and Procainamide Serivatives," *J. Pharmacol. Exp. Ther.* **244(2)**, 479-492 (1988).

140. Chaisuksant Y., et al., "Effects of Halobenzenes on Growth Rate of Fish (Gambusia Affinis)," *Ecotoxicology and Environmental Safety* **39(2)**, 120-130 (1998).

141. Waller, C.L., et al., "Modeling the Cytochrome P450-mediated Metabolism of Chlorinated Volatile Organic Compounds," *Drug Metab Dispos.* **24(2)**, 203-210 (1996).

142. Roldan-Arjona, T., et al., "Mutagenic and Lethal Effects of Halogenated Methanes in the Ara Test of Salmonella Typhimurium: Quantitative Relationship with Chemical Reactivity," *Mutagenesis* **8(2)**,127-131 (1993).

143. Mumtaz, M.M., et al., "A Weight-of-evidence Approach for Assessing Interactions in Chemical Mixtures," *Toxicology and Industrial Health* **,** 377-406 (1992).

144. Crebelli, R., et al., The Induction of Mitotic Chromosome Malsegregation in Aspergillus Nidulans. Quantitative Structure Activity Relationship (OSAR) Analysis with Chlorinated Aliphatic Hydrocarbons," *Mutation Research* **266(2)**, 117-34 (1992).

145. Benigni, R., et al., "Relationship between Chlorofluorocarbon Chemical Structure and Their Salmonella Mutagenicity," *Journal of Toxicology and Environmental Health* **34(3)**, 397-407 (1991).

146. Devillers, J., et al., "Quantitative Structure-activity Relations of the Lethal Effects of 38 Halogenated Compounds against Lepomis Macrochirus," *C. R. Acad. Sci. III*, **303(14)**, 613-616 (1986) French.

147. Weinstein, H., et al., "Determinants of Molecular Reactivity as Criteria for Predicting Toxicity: Problems and Approaches," *Environ. Health Perspective* **61**, 147-162 (1985).

148. Sabljic, A., "Quantitative Structure-Toxicity Relationship of Chlorinated Compounds: A Molecular Connectivity Investigation," *Bulletin of Environmental Contamination Toxicology* **30(1)**, 80-83 (1983).

149. Politzer, P., Trefonas, P., Politzer, I., and R., Elfman, B., "Molecular Properties of the Chlorinated Ethylenes and their Epoxide Metabolites," *Annals of the New York Academy of Sciences* **367**, 478-492 (1981).

150. Hooberman, B.H., et al., "Quantitative Structure-activity Relationships for the Mutagenicity of Propylene Oxides with Salmonella," *Mutation Research* **299(2)**, 85-93 (1993).

151. Purdy, R., "The Utility of Computed Superdelocalizability for Predicting the LC_{50} Values of Epoxides to Guppies," *Sci. Total Environ.***109-110**, 553-556 (1991).

152. Lutz, W.K., "Structural Characteristics of Compounds that can be Activated to Chemically Reactive Metabolites: Use for a Prediction of a Carcinogenic Potential," *Arch Toxicol. Suppl.* **7**, 194-207 (1984).

153. Johnson, M.K. "The mechanism of delayed neuropathy caused by some organophosphorus esters: using the understanding to improve safety," *Journal of Environmental Science and Health [B]* **16(6)**, 823-841 (1980).

154. Jones, S.L., et al., "Quantitative Structure-activity Relationships for Estimating the No-observable-effects Concentration in Fathead Minnows (Pimephales promelas)," *Quality Assurance* **4(3)**, 187-203 (1995).

155. Jaworska, J.S., et al., "Quantitative Structure-toxicity Relationships and Volume Fraction Analyses for Selected Esters," *Archives of Environmental Contamination Toxicology* **29(1)**, 86-93 (1995).

156. Kluwe, W.M., "Carcinogenic Potential of Phthalic Acid Esters and Related Compounds: Structure-activity Relationships," *Environmental Health Perspectives* **65**, 271-278 (1986).

157. Nielsen, G. D., et al., "Sensory Irritation Mechanisms Investigated from Model Compounds: Trifluoroethanol, Hexafluoroisopropanol and Methyl Hexafluoroisopropyl Ether," *Archives of Toxicology* **70(6)**, 319-28 (1996).

158. Ren, S., et al., "QSAR Analysis of Membrane Permeability to Organic Compounds," *J Drug Target.* **4(2)**, 103-107 (1996).

159. Hamerton, I., et al., "Development of Quantitative Structure Property Relationships for Poly(arylene Ethers)," *Journal of Molecular Graphics* **13(1)**, 14-17, 51 (1995).

160. Hooberman, B.H., et al., "Quantitative Structure-activity Relationships for the Mutagenicity of Propylene Oxides with Salmonella," *Mutation Research* **299(2)**, 85-93 (1993).

161. Di Paolo, T., "Structure-activity Relationships of Anesthetic Ethers Using Molecular Connectivity," *Journal of Pharmacological Science* **67(4)**, 564-566 (1978).

162. Di Paolo, T., "Molecular Connectivity in Quantitative Structure--activity Relationship Study of Anesthetic and Toxic Activity of Aliphatic Hydrocarbons, Ethers, and Ketones," *Journal of Pharmacological Science* **67(4)**, 566-568 (1978).

163. Cronin, M.T., et al., "Structure-toxicity Relationships for Three Mechanisms of Action of Toxicity to Vibrio Fischeri," *Ecotoxicological Environmental Safety* **39(1)**, 65-69 (1998).

164. Wieland, T., "The Use of Structure Generators in Predictive Pharmacology and Toxicology," *Arzneimittelforschung* **46(2)**, 223-227 (1996).

165. Dai, Q.H., et al., "Quantitative Pattern Recognition for Structure-carcinogenic Activity Relationship of N-nitroso Compounds Based upon Di-region Theory," *Sci. China [B]* **32(7)**, 776-790 (1989).

166. Purdy, R.," A Mechanism-mediated Model for Carcinogenicity: Model Content and Prediction of the Outcome of Rodent Carcinogenicity Bioassays Currently Being Conducted on 25 Organic Chemicals," *Environmental Health Perspectives* **104 Supplement 5**, 1085-1094 (1996).

167. Lewis, D.F., Parke, D.V., Walker, R., Ioannides, C., and Brantom, P.G., "Nitrosamine Carcinogenesis: Rodent Assays, Quantitative Structure-activity Relationships, and Human Risk Assessment," *Drug Metabolism Reviews* **29(4)**, 1055-78 (1997).

168. Johnson, M.K., "The Mechanism of Delayed Neuropathy Caused by Some Organophosphorus Esters: Using the Understanding to Improve Safety," *Journal of Environmental Science and Health [B]* **15(6)**, 823-41 (1980).

169. Martin, Yvonne C., "Studies of Relationships between Structural Properties and Biological Activity by Hansch Analysis," in Golberg, Leon, editor, *Structure-Activity Correlation as a Predictive Tool in Toxicology*, Hemisphere Publishing, Washington, DC, 1983, pp. 77.

170. Golberg, Leon, editor, *Structure-Activity Correlation as a Predictive Tool in Toxicology*, Hemisphere Publishing, Washington, DC, 1983.

171. Chan, P. and Hayes, A. W., "Acute Toxicity and Eye Irritancy," in Hayes, A.W., ed., *Principles and Methods of Toxicology*, Third Edition, Raven Press, Ltd., New York, 1994.

172. Grzyll, L. R. and Back, D. D., *Development of Quantitative Structure-Property Relationships for Tropodegradable Halocarbon Fire Suppression Agents*" Final Report, Mainstream Engineering, Inc., Rockledge, FL, March 1997.

173. Grzyll, L. R., Back, D. D., Ramos, C., and Samad, N. A., "Screening and Characterization of Second-Generation Halon Replacements," in Gann, R.G., Burgess, S.R., Whisner, K.C., and Reneke, P.A., eds., *Papers from 1991-2006 Halon Options Technical Working Conferences (HOTWC)*, CD-ROM, NIST SP 984-4, National Institute of Standards and Technology, Gaithersburg, MD, 2006.

174. Mather, J.D., and Tapscott, R.E., *Environmentally Acceptable Extinguishants*, Final Report, NIST GCR 06-901, National Institute of Standards and Technology, Gaithersburg, MD, 2006.

175. Frazier, J. M., Evaluation of *In vitro* Alternatives to the Dog Cardiac Sensitization Assay, ManTech Environmental Technologies, Inc., Toxic Hazards Research Unit, Dayton Ohio, April 1994.

176. Clark, D.G., Tinston, D.J., "Correlation of the Cardiac Sensitization Potential of Halogenated Hydrocarbons with their Physiochemical Properties," Imperial Chemical Industries Limited - Short Communications, May 25, 1973.

177. Tanner, Liebman & Eckenhoff, *Toxicology Letters* **100-101**, 387-391 (1998).

178. Hemmings, Jr., H.C., and Hopkins, P.M., "*Foundations of Anesthesia - Basic and Clinical Science,*" Harcourt, 2000.

179. *Ibid*., Chapter 5, "Molecular Physiology."

180. *Ibid.*, Chapter 8, "Pharmacokinetics of Inhalation Anesthetics."

181. *Ibid.*, Chapter 22, "Mechanisms of Anesthesia."

182. *Ibid.*, Chapter 24, "Inhalation of Anesthetic Agents."

183. www.virtual-anaesthesia-textbook.com/vat/volatile.htm. A tutorial website with a wide variety of anesthesia agents' clinical human exposure and cardiac effects information, as well as further reference citations.

184. Hemmings, Jr., H.C., and Hopkins, P.M., *op cit*., Chapter 41 "Cardiac Anesthesia."

185. www.virtual-anaesthesia-textbook.com/vat/volatile.htm. This is an excellent tutorial website with detailed discussions of a wide variety of anesthesia agents including clinical human exposure and cardiac effects information as well as further reference citations.

186. Molinspiration Cheminformatics web site: http://www.molinspiration.com and Syracuse Research Corporation web site: http://esc.syrres.com.

187. Finch, G.L., Barr, E., Nikula, K., Krone, J., and Mather, J.D., "Acute Inhalation Toxicity of Candidate Halon Replacement Compounds in Rats," Final Report, Lovelace Respiratory Research Institute, Albuquerque, NM, April 22, 1999.

188. Goldman, B. I., and Wurzel, J., "Effects of Subcultivation and Culture Medium on Differentiation of Human Fetal Cardiac Myocytes," *In Vitro Cell Development Biology* **28A**, 109-119 (1992).

189. Mark, G. E. and Strasser, F. F., "Pacemaker Activity and Mitosis in Culture of Newborn Rat Heart Ventricle Cells," *Experimental Cell Research* **44**, 217-233 (1966).

190. Schanne, O.F., Ruiz-Ceretti, E., Rivard, C., and Chartier, D., "Determinants of Electrical Activity in Clusters of Cultured Cardiac Cells From Neonatal Rats," *Journal of Molecular and Cellular Cardiology* **9**, 269-283 (1977).

191. Liu, W., Clarkson, C. W., Yamasaki, S., Chang, C., Stolfi, A., and Pickoff, A. S., "Characterization of the Rate-Dependent Effects of Ethmozine on Conduction, In Vivo, and on the Sodium Current, *In vitro*, in the Newborn Heart," *Journal of Pharmacological Experiments and Theory* **263**, 608-616 (1992).

192. Vahouny, G. V., Wei, R., Starkweather, R., and Davis, C., "Preparation of Beating Heart Cells from Adult Rats," *Science* **167**, 1616-1618 (1970).

193. Dani, A. M., Cittadini, A., and Inesi, G., "Calcium Transport and Contractile Activity in Dissociated Mammalian Heart Cells," *American Journal of Physiology* **6**, C147-C155 (1979).

194. Youker, K., Smith, C. W., Anderson, D. C., Miller, D., Michael, H., Rossen, R. D., Entman, M. L., "Neutrophil Adherence to Isolated Adult Cardiac Myocytes. Induction by Cardiac Lymph collected During Ischemia and Reperfusion," *Journal of Clinical Investigation* **89**, 602-609 (1992).

195. Woosley, R. L., Chen, Y., Freiman, J. P., Gillis, R. A., "Mechanism of the Cardiotoxic Actions of Terfenadine," *Journal of American Medical Association* **269**, 1532-1536 (1993).

196. Failli, P., Fazzini, A., Franconi, F., Stendardi, I., Giotti, A., "Taurine Antagonizes the Increase in Intracellular Calcium Concentration Induced by Alpha-Adrenergic Stimulation in Freshly Isolated Guinea-Pig Cardiomyocytes," *Journal of Molecular and Cellular Cardiology* **24**, 1253-1265 (1992).

197. Eid, H., Larson, D. M., Springhorn, J. P., Attawia, M. A., Nayak, R. C., Smith, T. W., Kelly, R. A., "Role of Epicardial Mesothelial Cells in the Modification of Phenotype and Function of Adult Rat Ventricular myocytes in Primary Coculture," *Circulation Research* **7**, 40-50 (1992).

198. Vinegar, A., G.W. Jepson, and J.H. Overton. "PBPK Modeling of Short-term (0 to 5 min) Human Inhalation Exposures to Halogenated Hydrocarbons," *Inhalation Toxicology* **10,** 411-429 (1998).

199. Vinegar, A., "Modeling Cardiac Sensitization Potential of Humans Exposed to Halon 1301 or Halon 1211 aboard Aircraft," *Aviation, Space, and Environmental Medicine* **72(10)**, 928-936 (2001).

200. Vinegar, A., (PBPK Modeling of Canine Inhalation Exposures to Halogenated Hydrocarbons," *Toxicological Sciences* **60**, 20-27 (2001).

201. Vinegar, A., Jepson, G.W., Cisneros, M., Rubenstein, R., and Brock, W.J., "Setting Safe Acute Exposure Limits for Halon replacement Chemicals using Physiologically Based Pharmacokinetic Modeling," *Inhalation Toxicology* **12**, 751-762 (2000).

202. Gargas, M.L., Andersen, M.E., and Clewell, III, H.J., "A Physiologically-based Simulation Approach for Determining Metabolic Constants from Gas Uptake Data," *Toxicology and Applied Pharmacology* **86,** 341-352 (1986).

203. NFPA 12A, *Standard on Halon 1301 Fire Extinguishing Systems*, NFPA , Quincy, MA, 2004.

204. Smith, D.G. and Harris, D.J., "Human Exposure to Halon 1301 ($CBrF_3$) During Simulated Aircraft Cabin Fires," *Aerospace Medicine* **44**, 198-201 (1973).

205. Abramowitz, A., Neese, W., and Slusher, G., "Smoke and Extinguisher Agent Dissipation in a Small Pressurized Fuselage," Federal Aviation Administration report DOT/FAA/CT-89/31, 1990.

206. Slusher, G.R., Wright, J., and Demaree, J., "Halon Extinguisher Agent Behavior in a Ventilated Small Aircraft," Federal Aviation Administration report DOT/FAA/CT-86/5, 1986.

207. Lerman, Y., Winkler, E., Tirosh, M.S., Danon, Y., and Almog, S., "Fatal Accidental Inhalation of Bromochlorodifluoromethane (Halon 1211), *Human Experiments in Toxicology* **10**, 125-128 (1991).

208. Vinegar, A., Jepson, G.W., Hammann, S.J., Harper, G., Dierdorf, D.S., and Overton, J.J., "Simulated Blood Levels of CF_3I in Personnel Exposed During its Release from an F-15 Jet Engine Nacelle and During intentional inhalation," *Journal of the American Industrial Hygiene Association* **60**, 403-408 (1999).

209. Vinegar, A., and Jepson, G., *Toxicological Assessment of Human Health Consequences Associated with Inhalation of Halon Replacement Chemicals; Section I: Physiologically-based Modeling of Halon Replacements for Human Safety Evaluations*, Final Report to the Strategic Environmental Research and Development Program, (2000).

210. "Acute Inhalation Toxicity," Guideline 403, Organization of Economic and Commercial Development (OECD), Paris, France, adopted 12 May 1981.